NOTICE

The quality of this microform is heavily dependent upon the quality of the original thesis submitted for microfilming. Every effort has been made to ensure the highest quality of reproduction possible.

If pages are missing, contact the university which granted the degree.

Some pages may have indistinct print especially if the original pages were typed with a poor typewriter ribbon or if the university sent us an inferior photocopy.

Reproduction in full or in part of this microform is governed by the Canadian Copyright Act, R.S.C. 1970, c. C-30, and subsequent amendments.

AVIS

La qualité de cette microforme dépend grandement de la qualité de la thèse soumise au microfilmage. Nous avons tout fait pour assurer une qualité supérieure de reproduction.

S'il manque des pages, veuillez communiquer avec l'université qui a conféré le grade.

La qualité d'impression de certaines pages peut laisser à désirer, surtout si les pages originales ont été dactylographiées à l'aide d'un ruban usé ou si l'université nous a fait parvenir une photocopie de qualité inférieure.

La reproduction, même partielle, de cette microforme est soumise à la Loi canadienne sur le droit d'auteur, SRC 1970, c. C-30, et ses amendements subséquents.

ASPECTS OF ELECTROMAGNETIC INTERFERENCE ON PRINTED CIRCUIT BOARDS

By

Marko Radojičić, B.A.Sc.

A Thesis submitted to the

School of Graduate Studies and Research

in partial fulfillment of the requirements

for the degree of

Master of Applied Science

Ottawa-Carleton Institute for Electrical Engineering

Department of Electrical Engineering

Faculty of Engineering

University of Ottawa

ISBN 0-315-60055-1

UNIVERSITÉ D'OTTAWA
UNIVERSITY OF OTTAWA

I hereby declare that I am the sole author of this document. I authorize the University of Ottawa to lend this document to other individuals or institutions for the purpose of scholarly research.

I further authorize the University of Ottawa to reproduce this document by photocopying or by other means, in total or in part, at the request of other institutions or individuals for the purpose of scholarly research.

Abstract

General guidelines for the design of printed circuit boards have been developed for two important aspects of electromagnetic compatibility: *cross-talk* and *radiated emissions.*

Numerical methods were used to study the cross-talk between tracks of several common printed circuit board technologies. Design recommendations are suggested that minimize the cross-talk on printed circuits boards.

A simple model was developed to predict radiated emissions from complicated circuits on printed circuit boards. The concepts of *ground impedance* and *common-mode currents* were used to build a model which gives fast and accurate predictions. The technique was tested using a method of moments program.

Acknowledgements

First and foremost, I would like to warmly thank Dr. George Costache for his help and encouragement throughout the entire Master's program.

The aid of everyone at BNR's Product Integrity group is also gratefully acknowledged, especially Mr. R.R. Goulette and Mr. Stan Xavier. The skills learned during the co-op portion of the graduate program proved invaluable.

Thanks also goes out to Dr. S.S. Stuchly who got me started with this program and to all the members, students and staff, of the electromagnetics group at the University of Ottawa without whom I could never have completed this program. I gratefully acknowledge the help of Darcy Ladd, Karu Esselle and Chris Sibbald who read this document and gave their thoughtful suggestions.

Finally, my deepest gratitude is reserved for my parents and Dragana Antić. Their encouragement and understanding was a constant source of strength throughout this endeavor.

Contents

Abstract ii

Acknowledgements iii

1 Introduction 1

1.1 Motivation 1

1.2 Objectives 6

1.3 Contributions 7

2 Prediction of Crosstalk on Different Printed Circuit Boards 8

2.1 Introduction 8

2.2 Problem Definition 8

2.3 Results 14

2.4 Observations and Discussions 21

3 Calculation of Partial Inductance 27

3.1 Introduction 27

3.2 Problem Formulation 31

3.3 Results 37

3.4 Verification of Results 38

3.5 Discussion 39

4 Models to Determine Radiated Emission for Printed Circuit Boards 40

4.1 Introduction 40

4.2 Synthesis of Problem 45

4.3 Determining Impedance of Ground Track 48

4.4 Calculation of Ground Current 54

4.5 Prediction of Radiated Emissions 56

5 Conclusions 64

5.1 Cross-Talk 64

5.2 Partial Inductance 67

5.3 Predicting Radiated Emissions 68

A Verification of Equation (4.14) 69

A.1 Introduction 69

A.2 Calculation of Internal Inductance for a Rectangular Conductor . . . 71

A.3 Verification of Results 74

A.4 Conclusion 74

B A Model to Predict Radiated Emissions From Simple Electronic Circuits 75

B.1 Introduction 75

B.2 The Model 75

B.3 Results 83

B.4 Summary and Conclusions 86

C Program Listings **87**

C.1 Program Created to Calculate Partial Inductance in Chapter 3 87

C.2 Program Used to Create Finite Element Mesh for Chapter 3 94

C.3 Sample of Input File for NEC 100

C.4 Program Created to Calculate the Radiated Emissions From Fig. B.1 101

Bibliography **105**

List of Tables

3.1 Comparison of the partial inductance for different structures 37

4.1 Segementation data of the wire grid model shown in Fig. 4.4 45

4.2 Comparison between CPU times of the two methods on a DEC VAX-station II 57

B.1 Comparison between CPU times of the two methods on a DEC VAX-station II 83

List of Figures

1.1 Graphic Representation of EMI Product Development Costs and Techniques 3

1.2 CISPR and FCC Radiated Emission Requirements 4

2.1 Configuration 1 9

2.2 Configuration 2 10

2.3 Configuration 3 11

2.4 Configuration 4 12

2.5 Cross-talk on Configuration 1 15

2.6 Cross-talk on Configuration 2 16

2.7 Cross-talk on Configuration 3 17

2.8 Near-End Cross-talk on Configuration 4 18

2.9 Far-End Cross-talk on Configuration 4 19

2.10 Cross-talk on Modified Configuration 2 20

2.11 Comparison of Cross-talk between Configuration 1 and 2 22

2.12 Comparison of Cross-talk Between Configuration 2 and 3 23

2.13 Comparison:Config. 2 and Modified Config. 2 24

2.14 Comparison:Config. 3 and Modified Config. 2 25

3.1 Rectangular loop supporting a current 28
3.2 Partial inductances present on a rectangular loop 29
3.3 Different Rectangular Cross-Section Conductor Configurations 32
3.4 Finite Element Mesh 33
3.5 Contour of integration used to find partial inductance 34
3.6 Equipotential lines of A from Configuration F 36

4.1 Differential and common mode currents on transmission lines 41
4.2 Comparison of radiated emissions from a typical circuit with and without attached cables 43
4.3 Seven track printed circuit board to be studied 46
4.4 NEC wire grid model for the circuit to be analyzed 47
4.5 Schematic representation of ground track conductor 49
4.6 Determining equivalent impedance of printed circuit track 50
4.7 Equivalent circuit of parallel plates 51
4.8 Seven track circuit with lumped impedances 54
4.9 Simplified model of circuit shown in Fig. 4.4 used to predict radiated emissions 56
4.10 Comparison of 30m radiated electric field from seven track circuit . . 58
4.11 Comparison of 3m radiated electric field from seven track circuit . . . 59
4.12 Three track printed circuit board 61
4.13 Comparison of 30m radiated electric field from three track circuit . . 62
4.14 Comparison of 3m radiated electric field from three track circuit . . . 63

A.1 Conductor with rectangular cross-section 70

B.1 Printed circuit board model 76
B.2 Comparison of 30m radiated electric field 78
B.3 Determination of ground current 79
B.4 Determination of input current 80
B.5 Comparison of input currents 81
B.6 Determination of radiated field 82
B.7 Comparison of 30m radiated electric field 84
B.8 Comparison of 3m radiated electric field 85

Chapter 1

Introduction

1.1 Motivation

Electromagnetic interference (EMI) is increasingly becoming a problem in electronics operation. In order to minimize this problem, various governments around the world have legislated regulations which impose strict limits on the amount of radiated and conducted emissions from equipment to ensure the electromagnetic compatibility of electronic systems. A random sample of new electronic products must be tested after production. If this device fails to pass the necessary EMI regulations, it is then very expensive to make modifications. Hence, the cost of a product will be minimized if the manufacturers concern themselves with all the possible EMI problems during the design phase.

A major problem is that the analysis of an entire electronic system is very difficult. Many systems being sold today comprise thousands of components, dozens of printed circuit boards (PCBs) and hundreds of metres of connections. Only a limited number of strategies applied at the system level are effective in limiting the electromagnetic interference. For example, a product can be enclosed in a metal box in order to lessen

the electromagnetic radiation and to provide a degree of shielding from electro-static discharge (ESD). Another system level strategy is to place transient line filters on the power cables in order to protect against lightning or nuclear electromagnetic pulse (NEMP) transients.

A far better time to consider EMI problems is when the product's printed circuit boards are being designed. Consider Fig. 1.1 where the number of available EMC techniques and their relative cost are plotted versus time. As the equipment development prodeeds, fewer EMC techniques are available to the designer and the cost of these techniques becomes increasingly higher. It is therefore necessary to have an understanding of the electromagnetic interactions on the PCB and it's inter-relating components, such as the connecting cables, so that the maximum number of potential problems are dealt with during the design phase.

The two most important aspects of electromagnetic compatibility (EMC) at the printed circuit board level are the radiated emissions and the cross-talk. New regulations published and enforced by the FCC in the United States [1], the Department of Communications in Canada [2] and other organizations around the world (such as CISPR[3]) now strictly regulate the maximum amount of radiated emissions that may be produced by any device which has components operating at frequencies greater than 10 KHz (virtually all electronic devices). Figure 1.1 shows the maximum allowable radiated emissions which may be produced by electronic equipment.

Besides the radiated emissions, the other key EMI problem in printed circuit board design is the amount of coupling which occurs between printed circuit tracks. This phenomena, commonly known as *cross-talk*, can cause problems in electronic circuits. The effects range from noise on a speaker to a complete system crash. Again, the

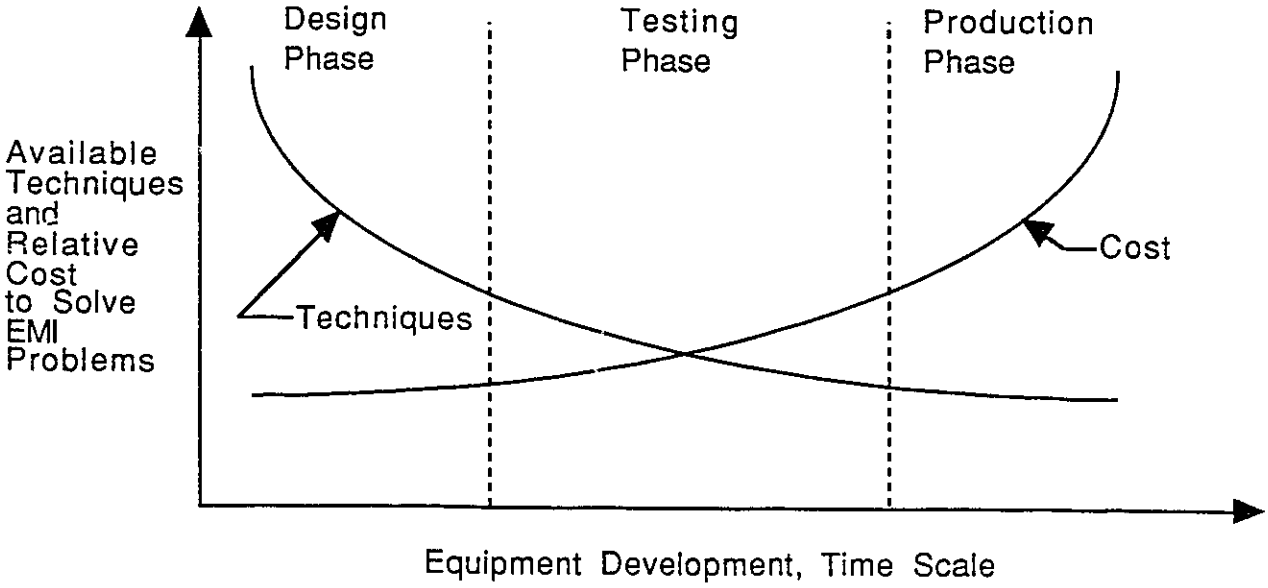

Figure 1.1: Graphic Representation of EMI Product Development Costs and Techniques

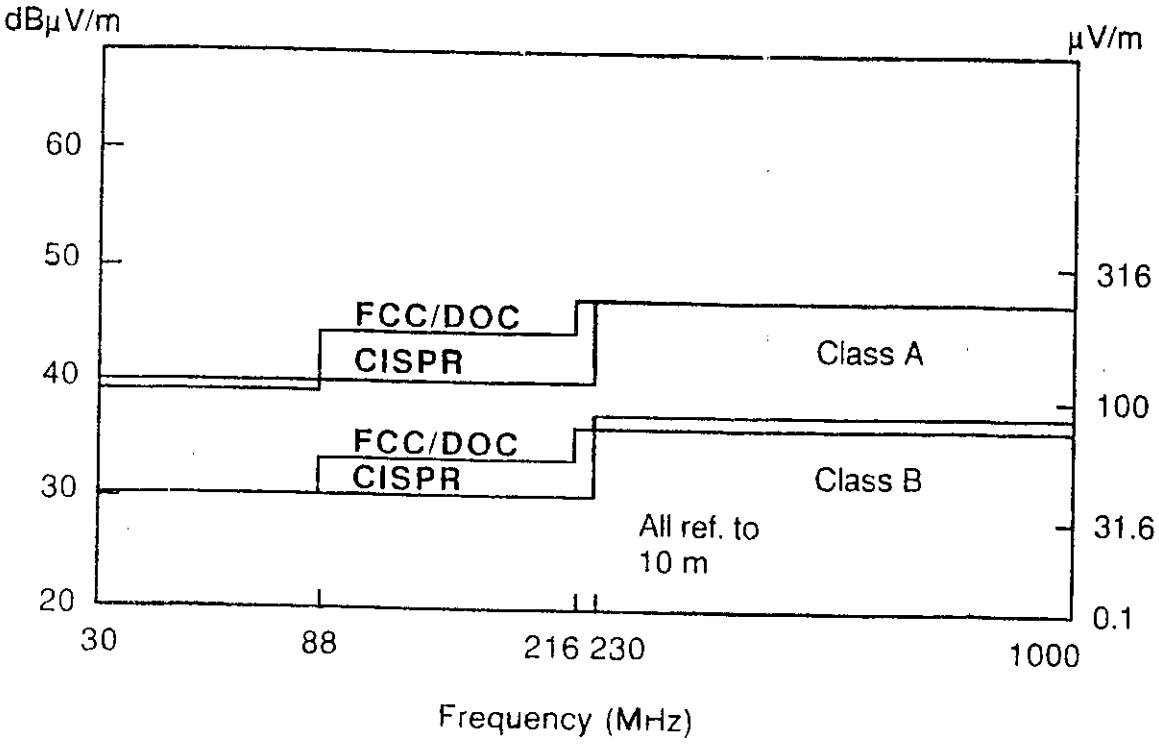

Figure 1.2: CISPR and FCC Radiated Emission Requirements

most cost effective means of dealing with this problem is to carefully design printed circuit boards in such a way as to prevent it.

1.2 Objectives

This thesis explores two critical areas of EMC design to gain an understanding of the electromagnetic interactions on PCBs. The goal is to establish general rules to assist designers in minimizing cross-talk and radiated emissions.

To accomplish this goal, the cross-talk between tracks on four of the most common PCB topologies will be examined. The aim is to be able to determine which PCB topology most effectively minimizes cross-talk. Techniques will be developed to further reduce this unwanted coupling.

The first step in controlling radiated emissions is to predict them. Various computer packages which use the method of moments (MOM) [4,5] already exist to predict radiated emissions from wire grid models. The principle problem with these packages is that due to lengthy execution times their usefulness designers is limited. Other computer-aided design (CAD) programs such as [6] also claim to accurately predict the radiated EMI but they consider the current loop area as the only important parameter. The assumption that the differential mode currents in a loop are the primary source of radiated emissions is shown in [7] and [8] to be questionable.

The other major goal of this thesis is to develop a simple method to accurately model the amount of radiated EMI from printed circuit boards. The model must be able to give more realistic estimates than [6] and should provide quicker results than if the PCBs were modeled with the MOM programs given in [4,5]. In this way, accurate and fast CAD packages could be created to aid designers in ascertaining whether their design will pass all the necessary regulatory tests.

1.3 Contributions

The new contributions to the understanding of electomagnetic compatibility related knowledge of printed circuit boards are described in this section. These new insights satisfy the desired objectives.

In the first chapter, the most common circuit board technologies were analyzed to determine the amount of crosstalk between their tracks. From this analysis, guidelines were established to aid designers in minimizing the crosstalk on PCB tracks.

The section on partial inductance links the crosstalk on printed circuit board tracks to the radiated emissions from PCB systems. It presents a simple method to reduce the self partial inductance of conductors.

A model was developed in the final chapter to predict the radiated emissions from real-life printed circuit boards using the self partial inductance of the ground. This fast and simple model can be implemented into a CAD package to predict the level of radiated EMI from an electronic system during the design phase.

Chapter 2

Prediction of Crosstalk on Different Printed Circuit Boards

2.1 Introduction

Printed Circuit Boards (PCBs) come in many different configurations, some with buried signal tracks, some with buried power planes. Even though they are extensively used throughout industry, no one has yet analyzed the relative merits and shortcomings of these different boards from an electromagnetic compatibility viewpoint using numerical methods. This chapter will examine the susceptibility to cross-talk of four of the most common board types. The four configurations are shown in Figs. 2.1–2.4.

2.2 Problem Definition

This chapter uses, whenever possible, real-life PCB geometries and parameters. All four configurations presented in Figs. 2.1–2.4 use parameters taken from standard

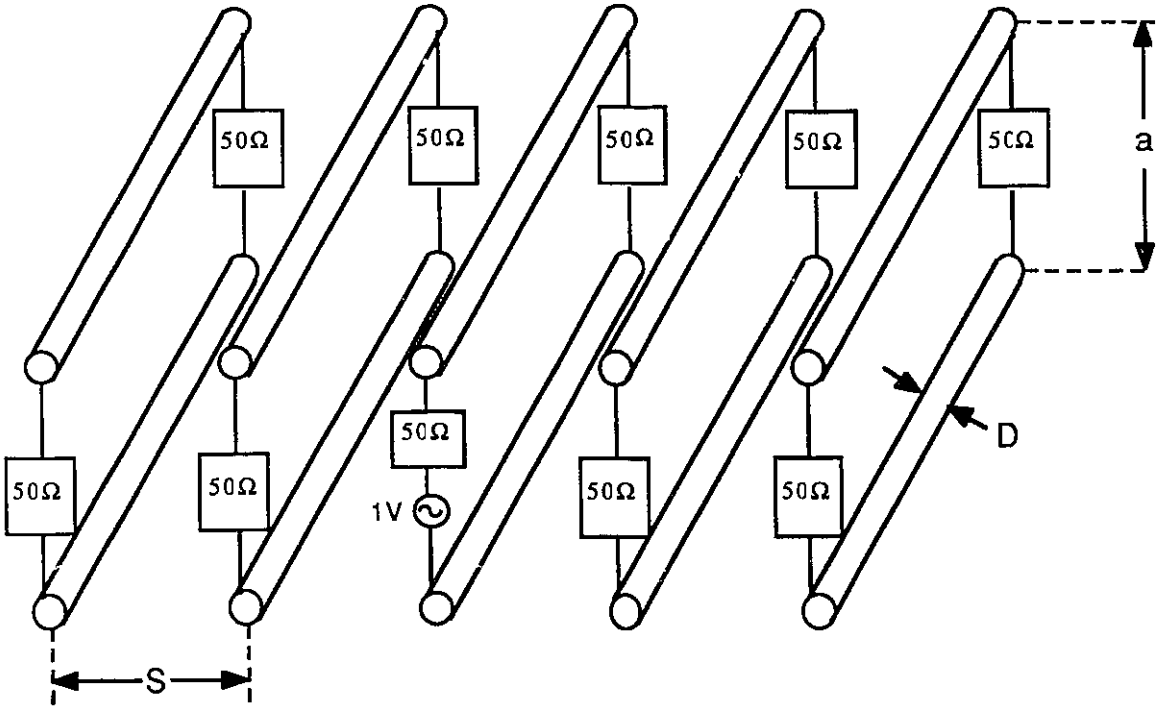

a=5.20E-4 m

Spacing Between Conductors (S):	3.05E-4 m
Conductor Width (W):	3.05E-4 m
Conductor Thickness:	1.70E-4 m
Conductor Length:	30 cm
Wire Diametre (D):	0.4E-4 m

Configuration 1

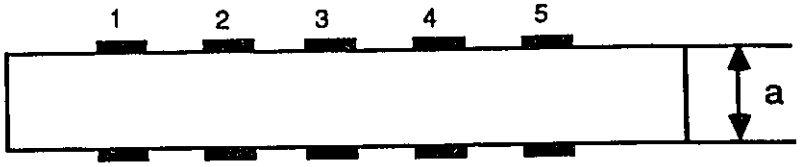

Figure 2.1: Four Common Printed Circuit Board Configurations -Configuration 1

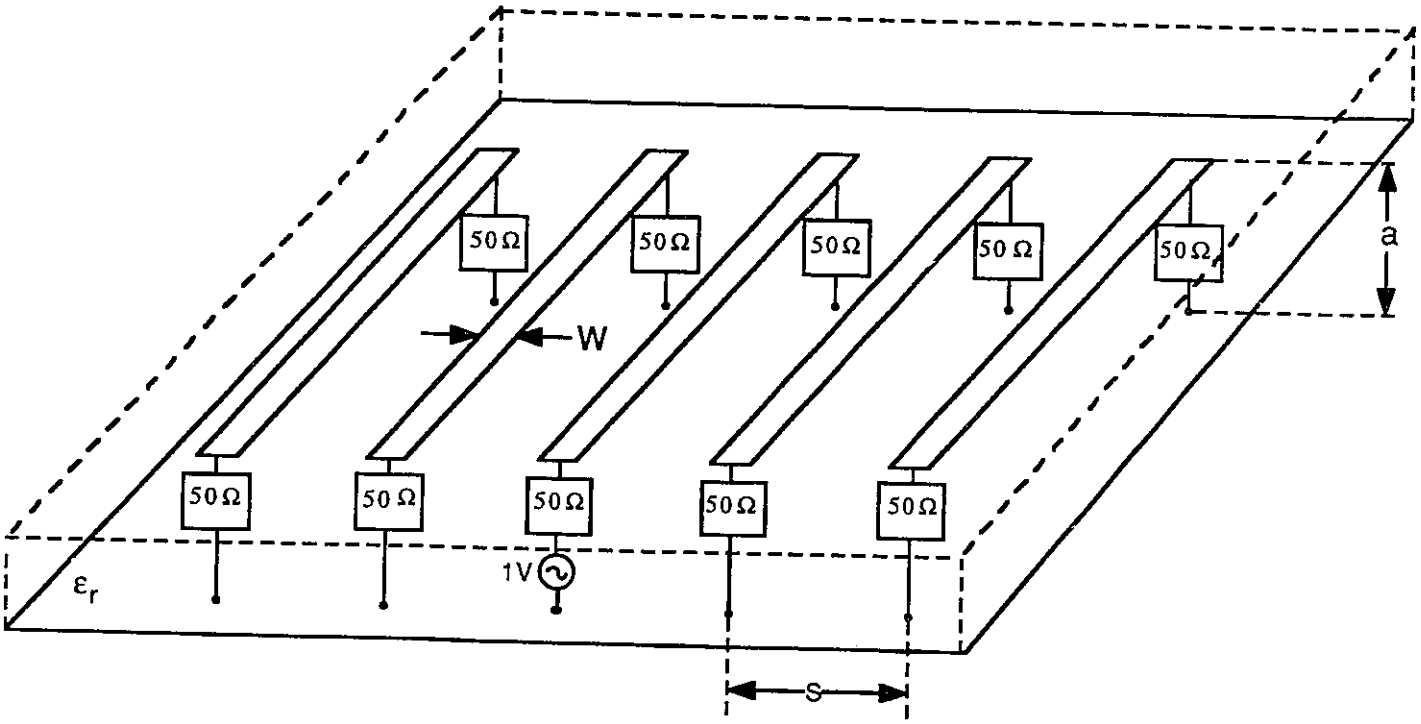

a=5.20E-4 m

Spacing Between Conductors (S):	3.05E-4 m
Conductor Width (W):	3.05E-4 m
Conductor Thickness:	1.70E-4 m
Conductor Length:	30 cm

Configuration 2
(Micro-strip)

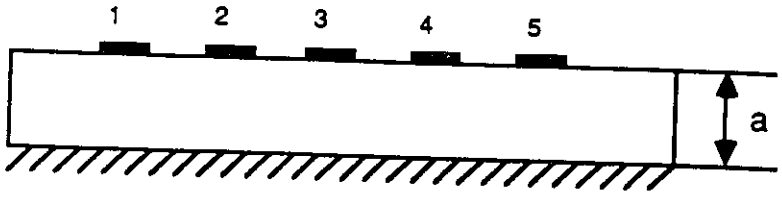

Figure 2.2: Four Common Printed Circuit Board Configurations -Configuration 2

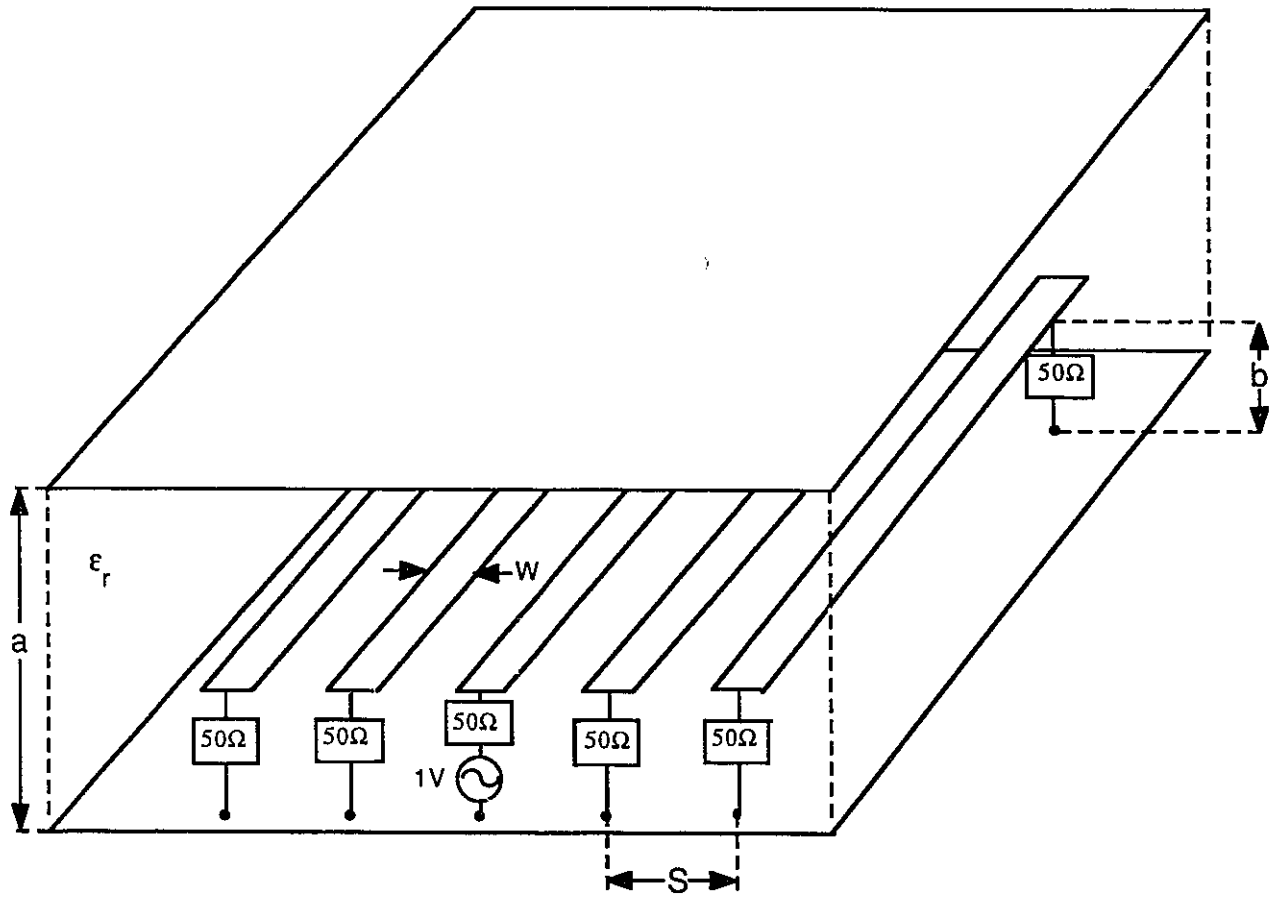

a=5.20E-4 m
b=2.60E-4 m

Spacing Between Conductors (S):	3.05E-4 m
Conductor Width (W):	3.05E-4 m
Conductor Thickness:	1.70E-4 m
Conductor Length:	30 cm

Configuration 3
(Strip-line)

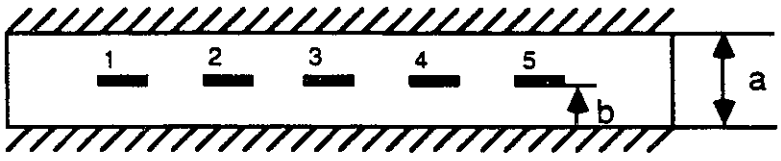

Figure 2.3: Four Common Printed Circuit Board Configurations -Configuration 3

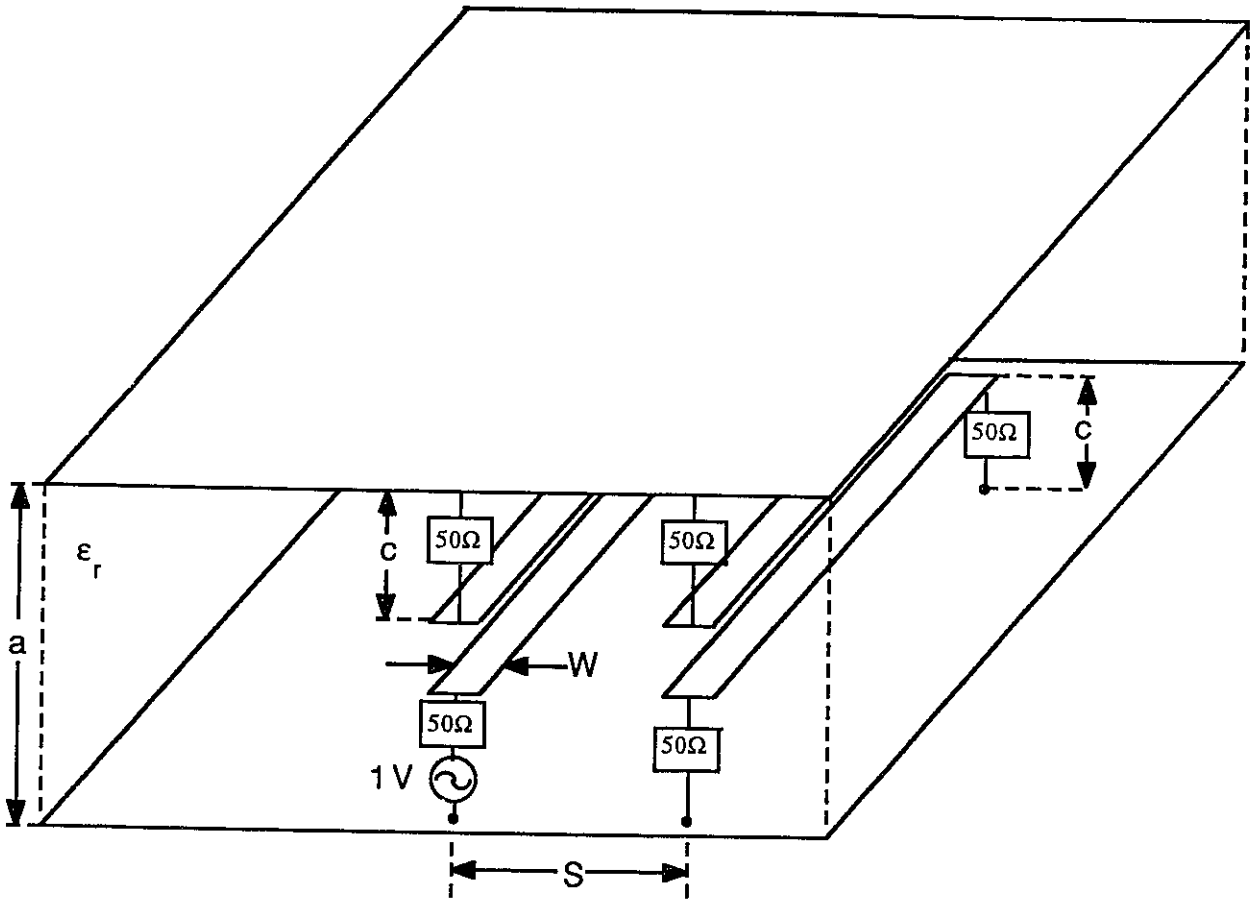

a=5.20E-4 m	Spacing Between Conductors (S):	3.05E-4 m
b=2.60E-4 m	Conductor Width (W):	3.05E-4 m
c=1.73E-4 m	Conductor Thickness:	1.70E-4 m
d=3.47E-4 m	Conductor Length:	30 cm

Configuration 4

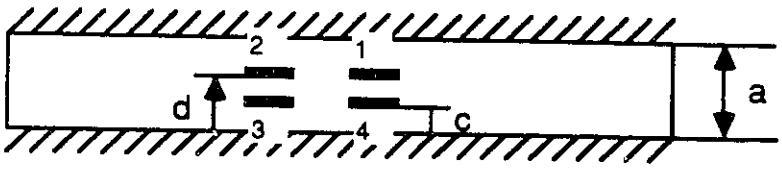

Figure 2.4: Four Common Printed Circuit Board Configurations -Configuration 4

PCBs made by general industry. All conductors are 30 cm long and are terminated at both ends with 50 Ω. In order to observe cross-talk at the various frequencies of operation, the centre conductor is excited with a voltage source of unit amplitude whose frequency varies from 10 MHz to 1 GHz. The ground planes are assumed to be perfectly conducting and the substrate has a dielectric constant equal to that of glass epoxy, i.e. $\varepsilon_r = 4.7$. In all cases, the separation between conductors is equal to the width of the conductors (i.e. S=W).

All the configurations were analyzed with a finite element method (FEM) program developed by Khan and Costache [9] with the exception of configuration 1 of Fig. 2.1. This latter case was analyzed using a common method of moments program, the *Numerical Electromagnetics Code* (NEC) [4], since the absence of a ground plane precludes using the FEM program. Since the NEC program requires conductors having circular cross-section, the rectangular conductors of Fig. 2.1 were approximated by circular conductors having the same cross-sectional area:

$$\text{Radius of equivalent round conductor} = \sqrt{\frac{A}{\pi}}$$

where A is the cross-sectional area of the rectangular conductor. Another shortcoming of the method of moments program is that the glass epoxy dielectric constant can not be included as it is when using the FEM program but, as will be shown, the results of the NEC analysis are meaningful.

The data supplied to the NEC program was well within the prescribed limitations. Studies have shown [4] that the segment length, Δ, relative to the wavelength, λ, must be within the limit $0.001\lambda < \Delta < 0.1\lambda$. It has also been experimentally shown that if $\Delta/\textit{wire radius} > 8$, then the error is less than 1%. Both these recommendations were followed whenever the NEC program was employed.

2.3 Results

Using the methods described in the previous section, the various topologies are analyzed. In order to make the results as clear as possible, the cross-talk is presented as the ratio of voltage on the receptor conductors to that on the driven conductor. Figures 2.5–2.9 show the results for both the near-end (NEXT) and far-end (FEXT) cross-talk.

A short explanation of Figs. 2.5–2.9 is necessary. Due to the symmetry of configurations 1–3, the cross-talk on conductor 2 is nearly identical to that on conductor 4. Likewise, the cross-talk on conductors 1 and 5 mirror each other. For this reason, only the cross-talk on conductors 1 and 2 is presented. Configuration 4 is not symmetrical and hence results for all conductors are shown. The same scale is used on all plots in order to facilitate comparisons. The resonances at each harmonic of 250 MHz is due to the quarter wavelength of the 30 cm long conductor.

Configuration 2 was modified by reducing the separation between the conductors and the ground plane by two-thirds in order to observe the effect of the proximity of the ground plane to the cross-talk. The results are presented in Fig. 2.10.

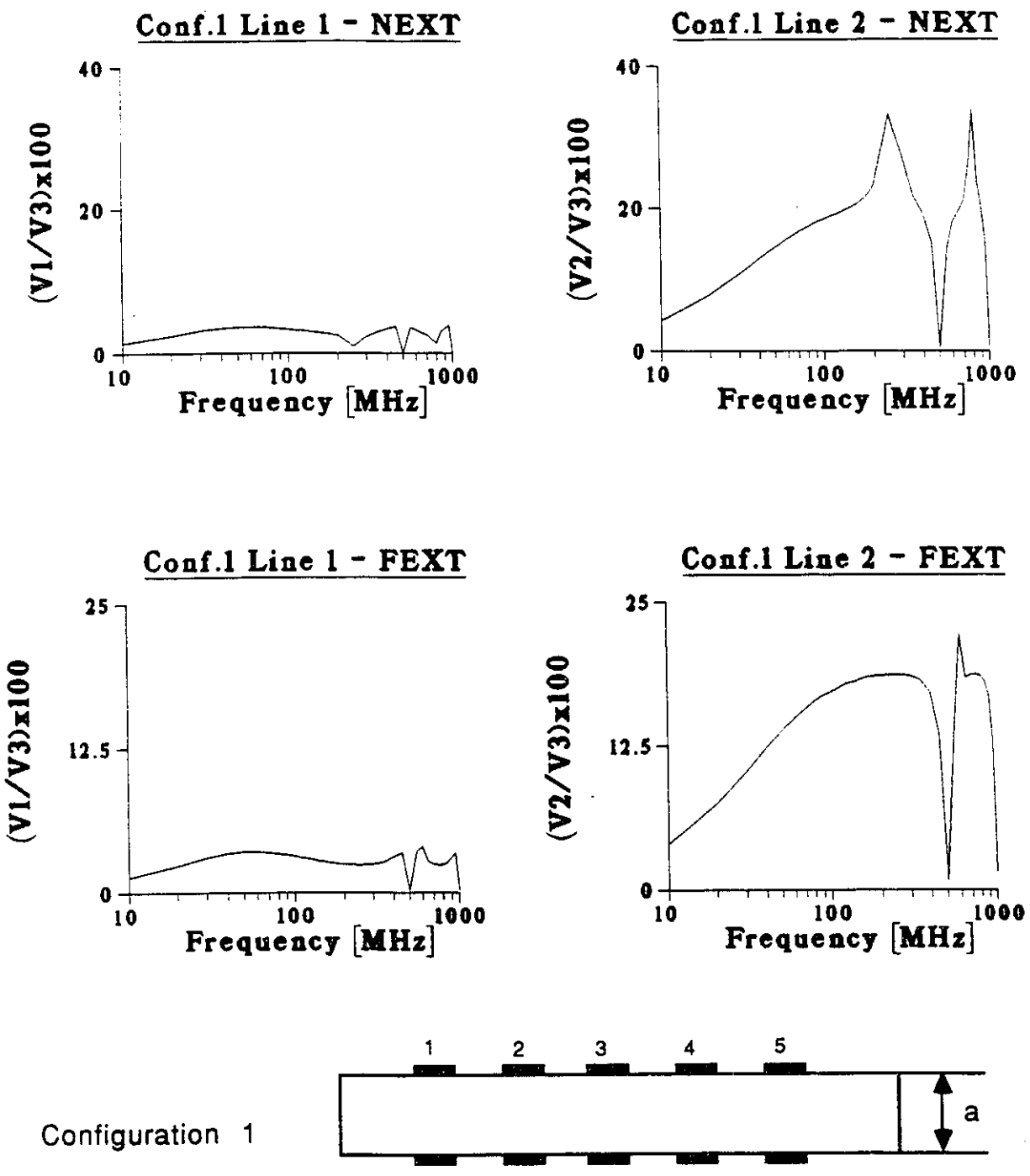

Figure 2.5: Cross-talk on Configuration 1.Calculated using MOM.

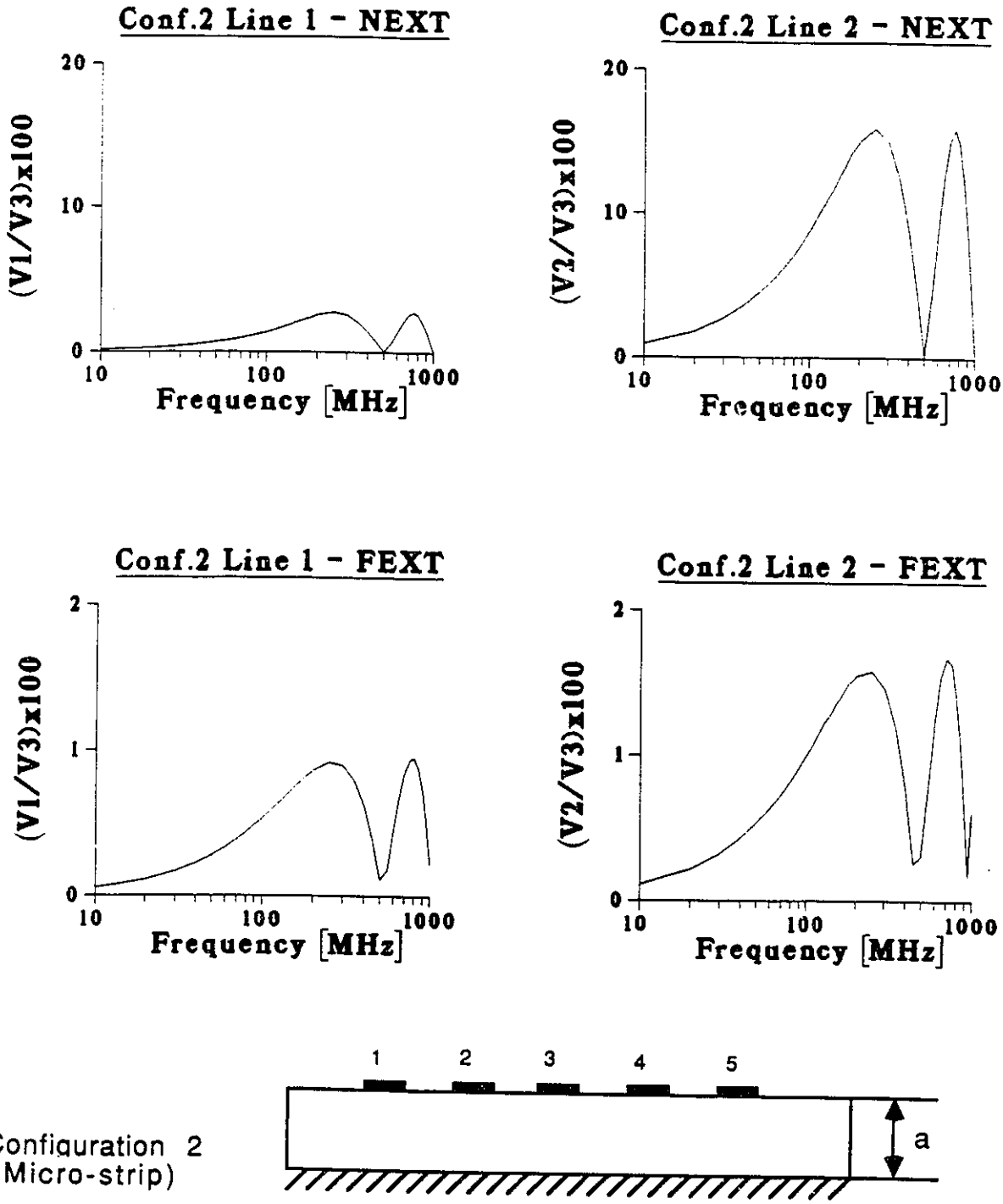

Figure 2.6: Cross-talk on Configuration 2.Calculated using FEM.

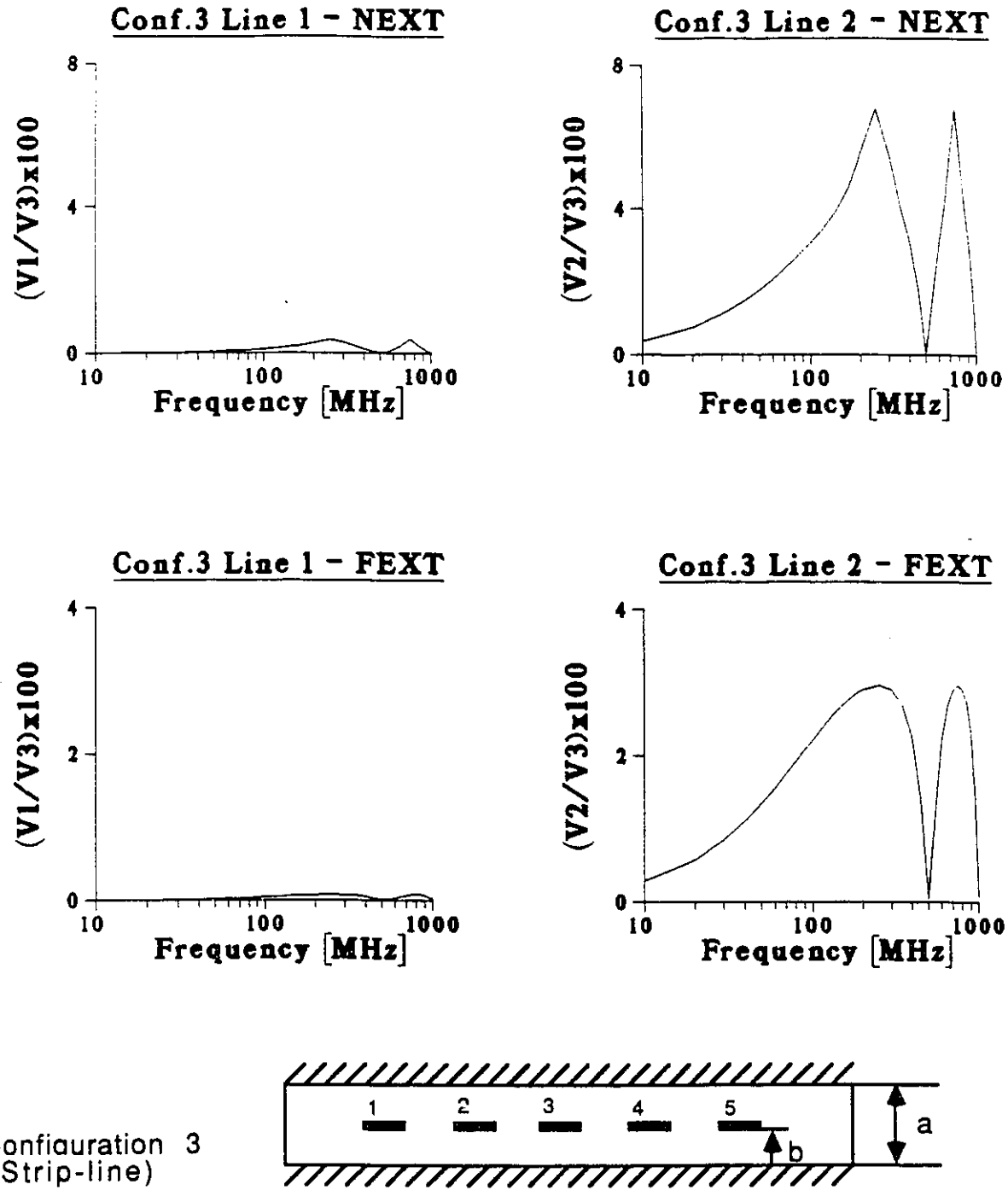

Figure 2.7: Cross-talk on Configuration 3.Calculated using FEM.

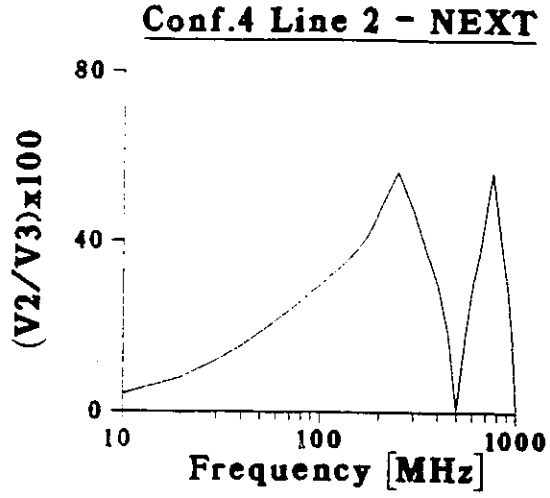

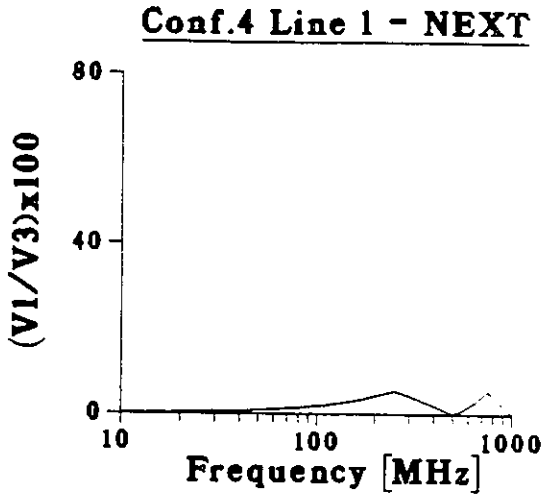

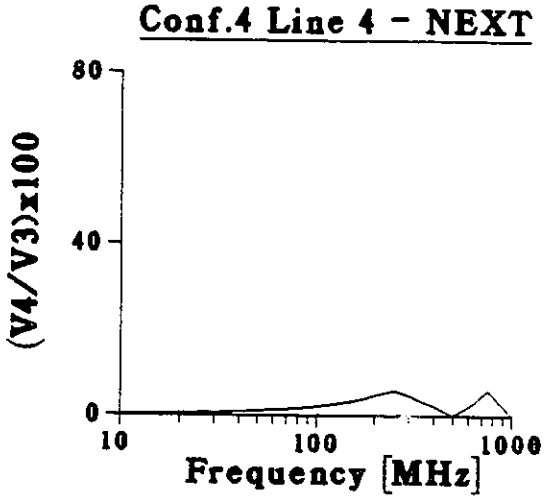

Configuration 4

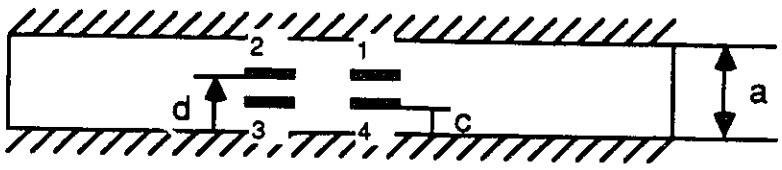

Figure 2.8: Near-End Cross-talk on Configuration 4.Calculated using FEM.

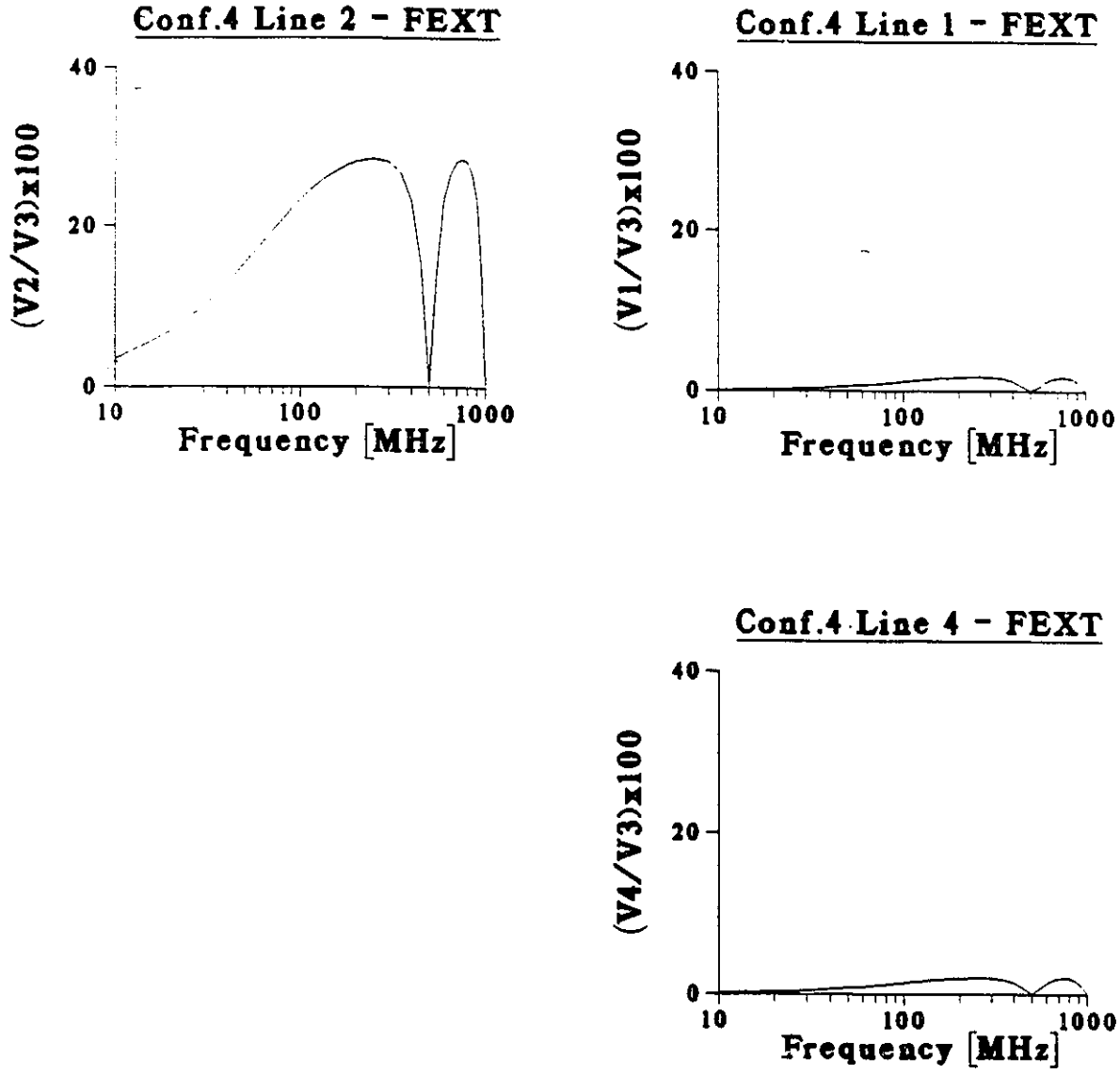

Configuration 4

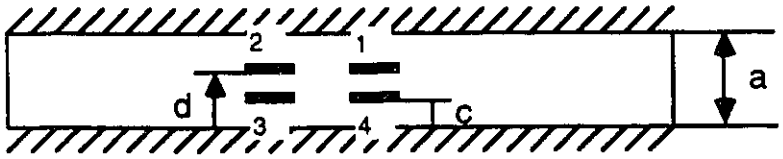

Figure 2.9: Far-End Cross-talk on Configuration 4.Calculated using FEM.

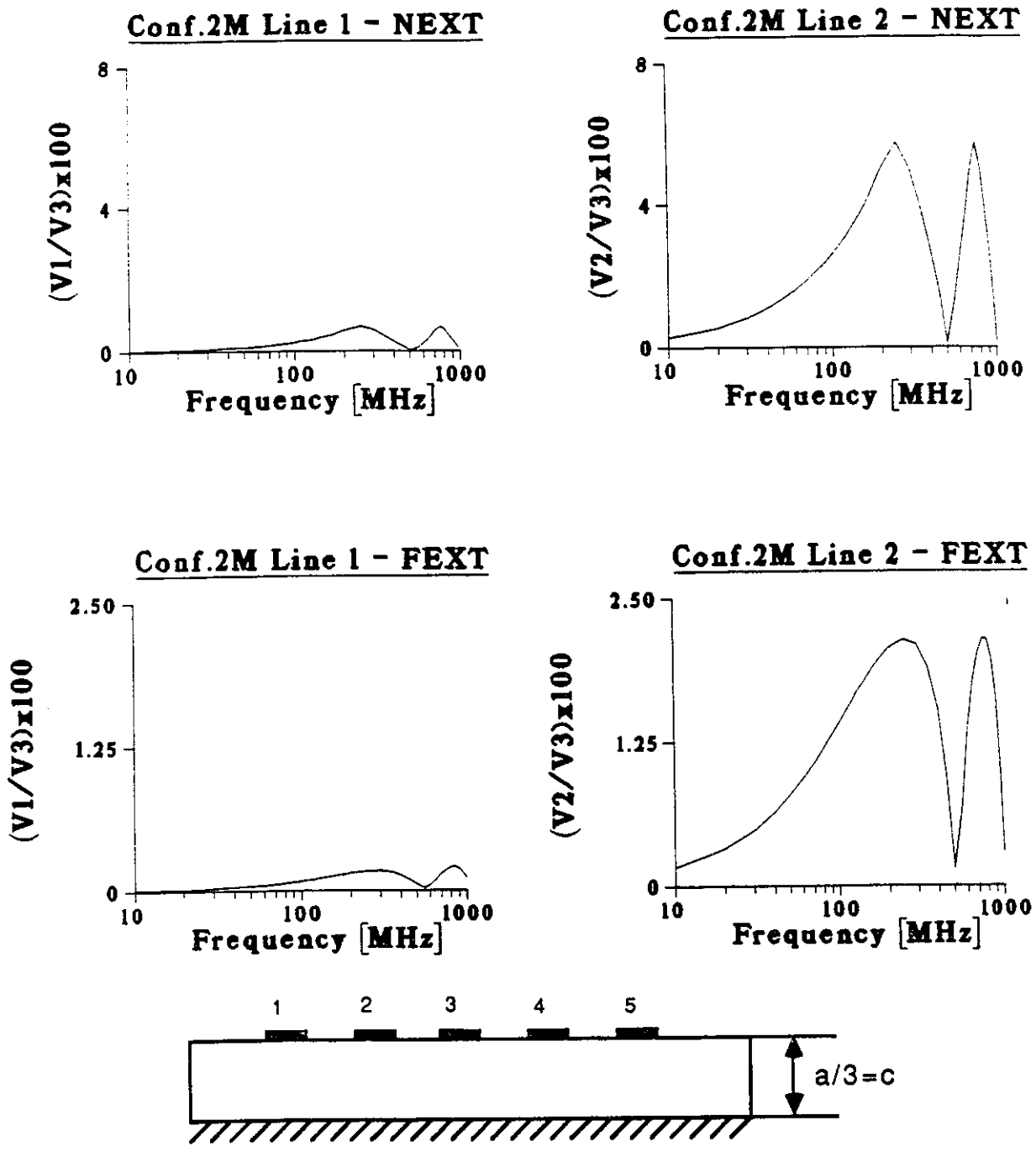

Figure 2.10: Cross-talk on Modified Configuration 2.
Calculated using FEM.
Configuration 2 is modified by reducing the separation between the conductors and the ground plane by two-thirds.

2.4 Observations and Discussions

Many interesting observations can be made from the results. As is generally assumed, much more EMI coupling occurs on the closest neighbours which leaves the further conductors relatively noise-free. Therefore circuit designers who are worried about cross-talk from a certain track, the clock signal for example, should only concern themselves with coupling to it's closest neighbouring conductors.

From the graphs in Figs. 2.5—2.9, the cross-talk is seen to be very frequency dependant yet general conclusions may still be reached regarding the cross-talk susceptibility of the different PCB topologies. Figures 2.11–2.12 show a comparison of the different PCB's cross-talk. The least amount of cross-talk occurs on configuration number 3, the strip-line. It is closely followed by the micro-strip set-up, number 2, which has the next lowest cross-talk. The remaining two configurations have by far the highest level of coupling.

Closer examination of the PCB shown in Fig. 2.4 reveals that it has the single greatest coupling between any two conductors. At 250 and 750 MHz, the driven conductor couples 56.3% of it's voltage onto the conductor directly above it. This suggests that this configuration should be avoided. A possible solution would be to stagger the conductors. The analysis shows that the susceptor conductor, if placed off on an angle with respect to the driven line such as conductor 1, results in cross-talk which is reduced by an order of magnitude.

An interesting effect occurs when the ground plane and conductors are brought in closer proximity to each other: the cross-talk voltages are greatly reduced. This can be observed from Fig. 2.13 which compares the cross-talk from Figs. 2.10 and 2.6. It is clear that Fig. 2.10 has less near-end cross-talk at virtually every frequency and

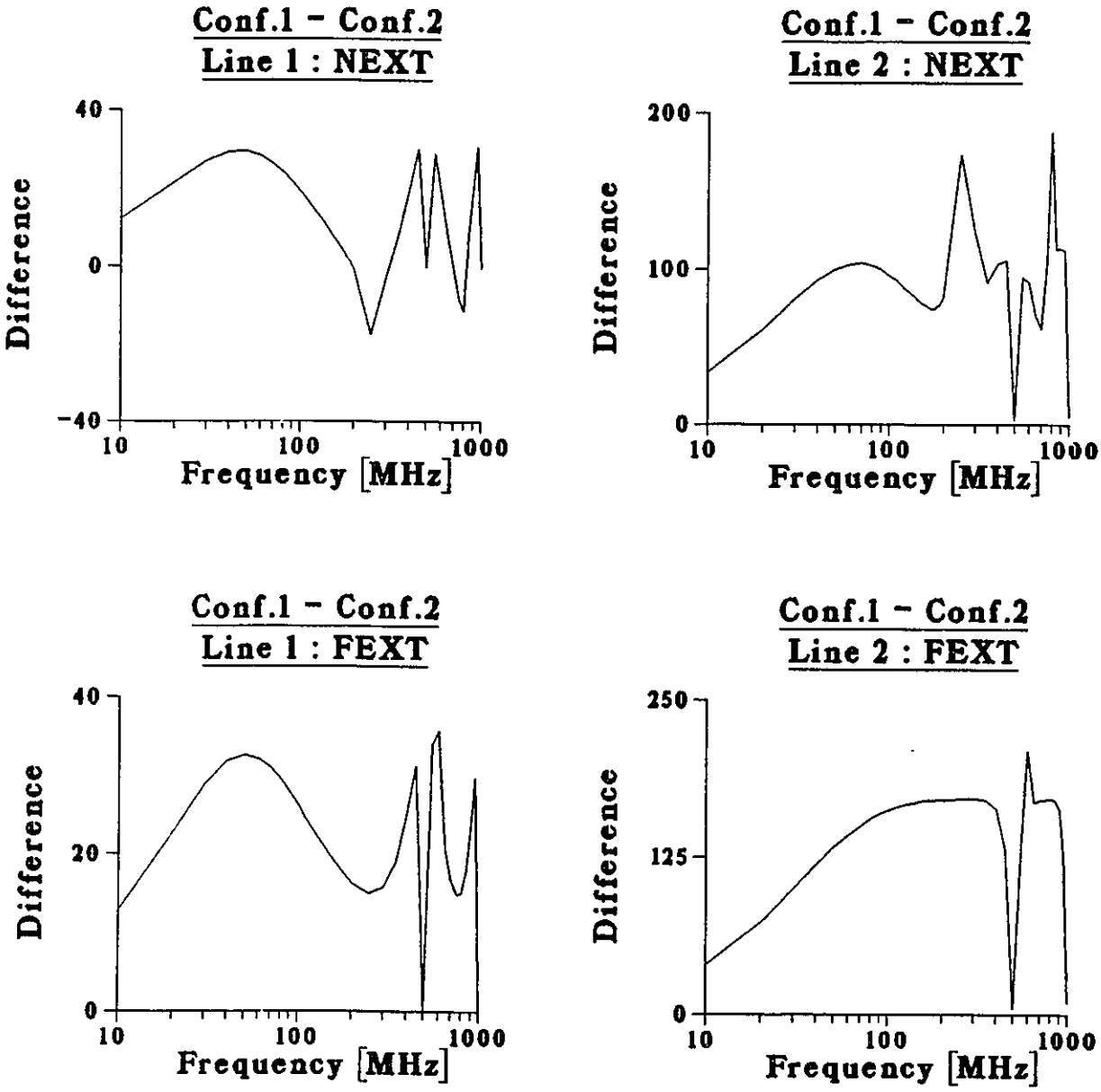

Figure 2.11: Comparison of Cross-talk between Configuration 1 and 2.
Configuration 1 values were calculated using MOM.
Configuration 2 values were calculated using FEM

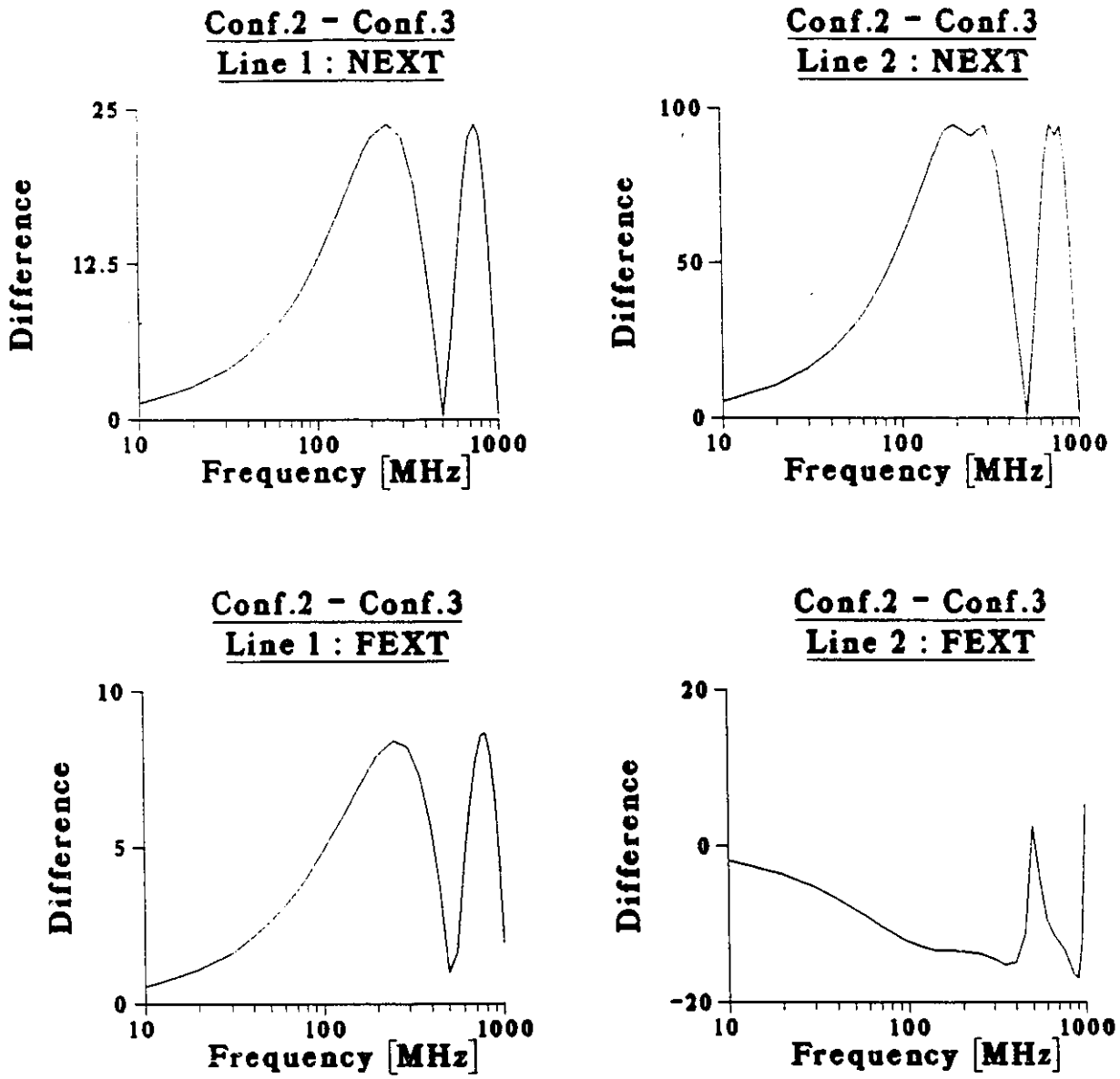

Figure 2.12: Comparison of Cross-talk between Configuration 2 and 3. All values were calculated using FEM.

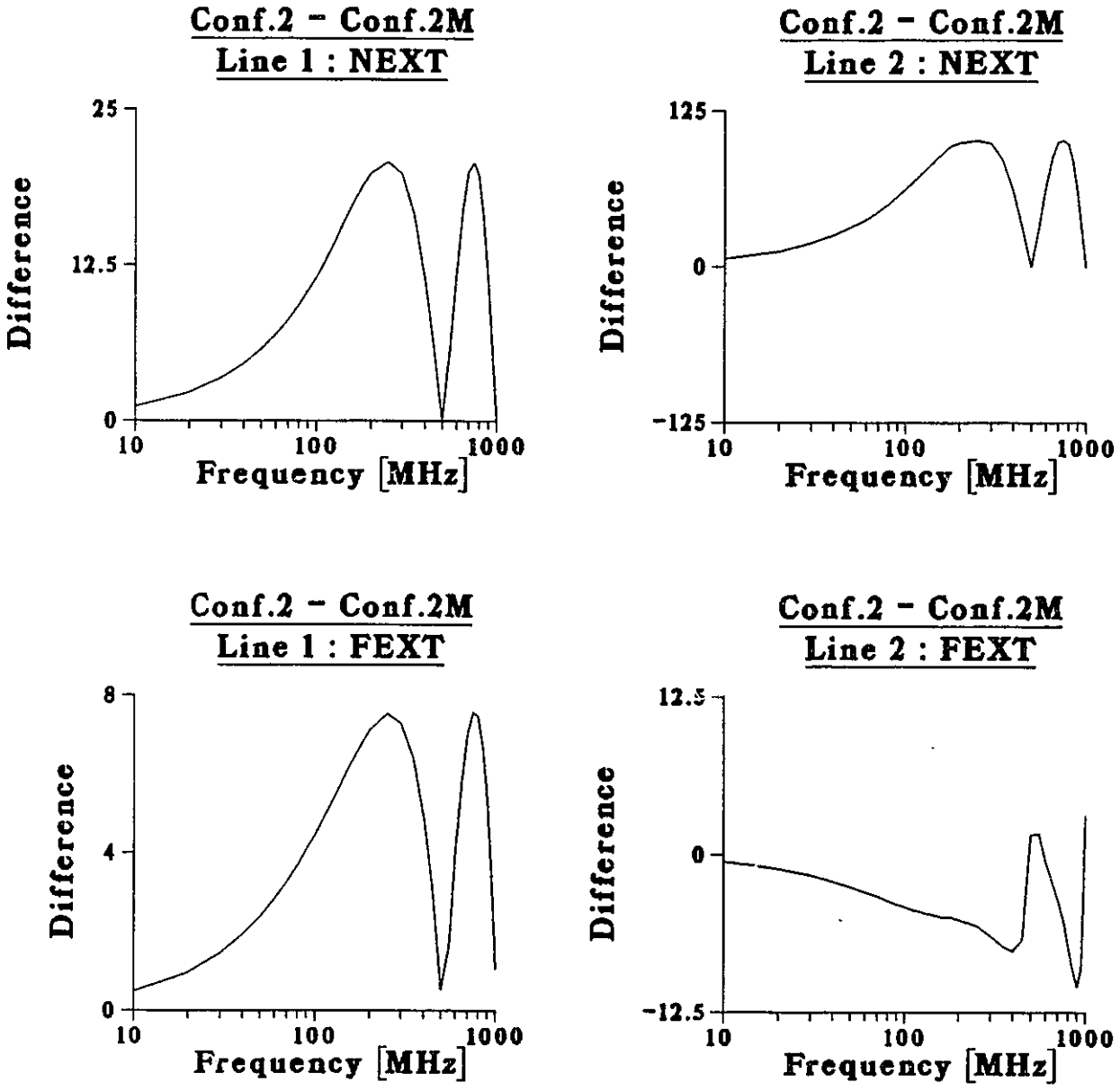

Figure 2.13: Comparison of Cross-talk between Configuration 2 and the modified version of Configuration 2.
All values were calculated using FEM.

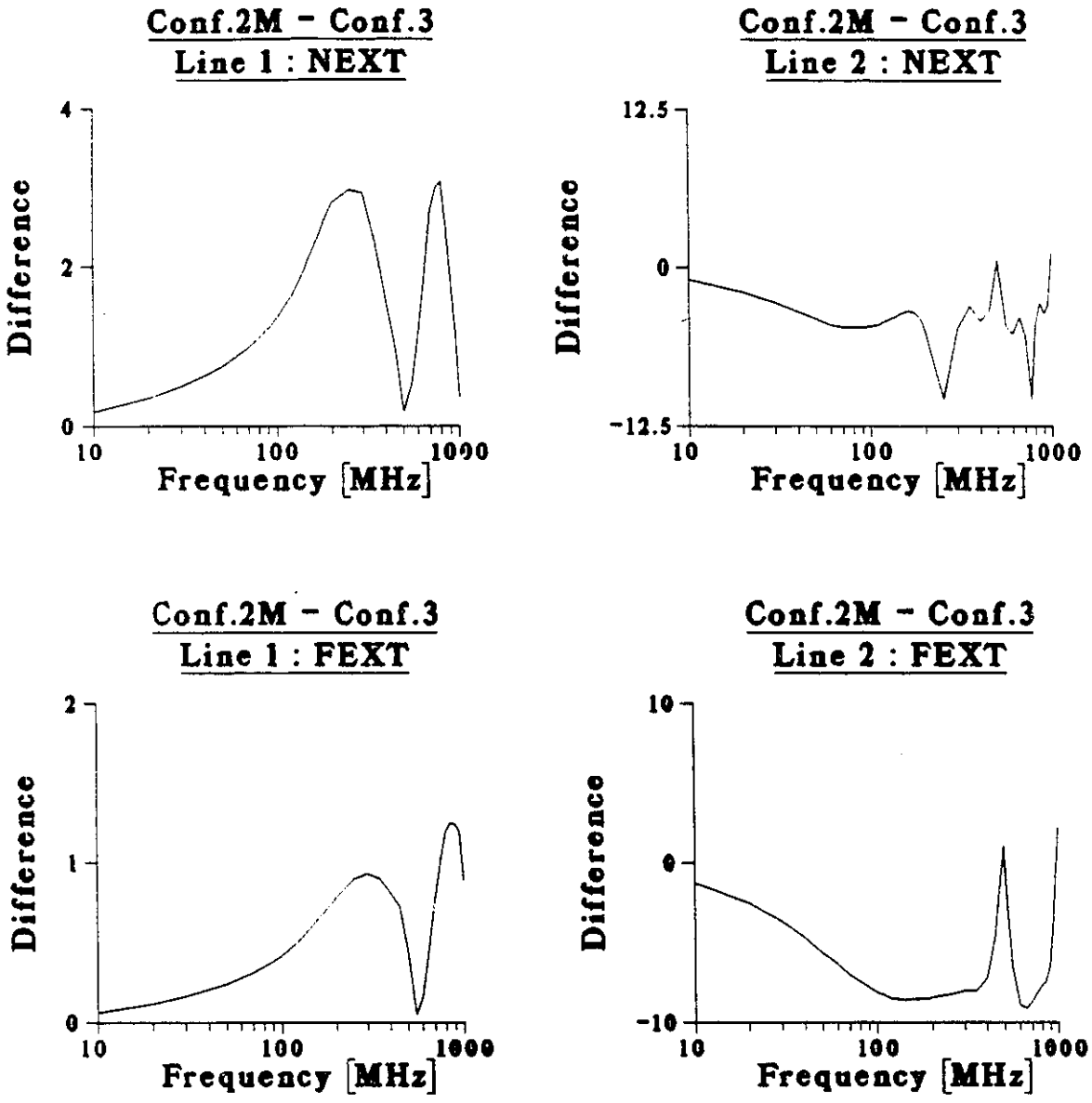

Figure 2.14: Comparison of Cross-talk between Configuration 3 and the modified version of Configuration 2.
All values were calculated using FEM.

less far-end cross-talk for the majority of cases.

To see how this modification affects the relative rankings of the different PCB's, Fig. 2.14 compares the cross-talk voltages of the modified second configuration with those of the third configuration. It is seen that the NEXT and the FEXT of configuraton 3 is now actually *larger* for the immediate neighbours[1]. Therefore, reducing the separation between the conductors and the ground plane greatly reduces the cross-talk. In practice, the separation must be chosen to take into account other factors such as the break-down voltage of the dielectric as well as mechanical, thermal and production requirements [10].

[1]For the further conductors configuration 3 is still a superior technology but as was discussed earlier, they are not important relative to the closest neighbours.

Chapter 3

Calculation of Partial Inductance

3.1 Introduction

The need to accurately calculate partial inductances of conductors is due to the fact that both the cross-talk and the radiated emissions are related to it. Paul [12] has shown that reducing the partial inductances of printed circuit tracks reduces the cross-talk and chapter 4 shows that the partial inductance of the ground conductor is a major factor in producing radiated EMI.

The various types of inductances will be briefly discussed below in order to properly define *partial inductance.*

Historicaly, inductance is only defined for a closed loop. Consider the rectangular loop in Fig. 3.1. The current I on the loop segments produce a magnetic flux density $\vec{B}$. The inductance of the loop is then defined as the total magnetic flux penetrating the surface S bounded by the loop per unit of the current,

$$\text{Inductance} = \frac{\int_S \vec{B} \cdot d\vec{S}}{I} \quad . \tag{3.1}$$

Also since the vector magnetic potential $\vec{A}$ is defined as $\vec{B} = \nabla \times \vec{A}$, Equ. (3.1) can

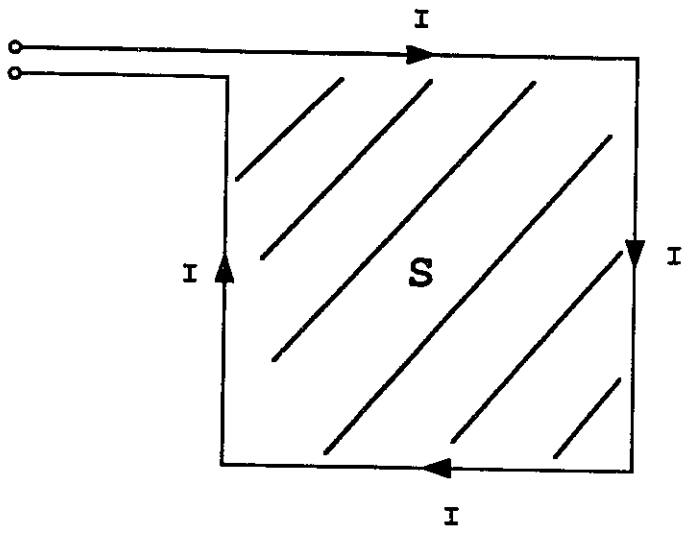

Figure 3.1: Rectangular loop supporting a current

be written as

$$\text{Inductance} = \frac{\oint_c \vec{A} \cdot \vec{dl}}{I} \tag{3.2}$$

where c is the contour of the loop.

The partial inductance can now be understood by considering the equivalent circuit of a rectangular loop which is shown in Fig. 3.2. Each segment in the circuit has an associated self partial inductance, $L_{p_{ii}}$, and all of these inductances are linked by mutual partial inductances, $L_{p_{ij}}$. These partial inductances can be defined as

$$L_{p_{ij}} = \frac{\int_{u_j} \vec{A}_{ij} \cdot \vec{du_i}}{I_j} \tag{3.3}$$

where $\vec{A}_{ij}$ is the magnetic vector potential along segment u_i due to the current I_j on segment u_j. When $i = j$, the resulting inductances are defined as *self partial inductances* and when $i \neq j$, the inductances are known as *mutual partial inductances.* The overall effect of the actions and interactions of these partial inductances is to

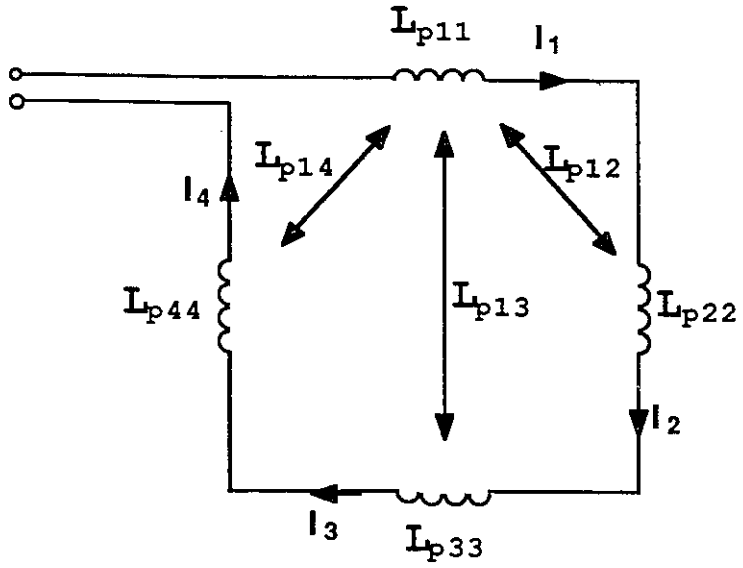

Figure 3.2: Partial inductances present on a rectangular loop

produce the inductance of the loop.

The internal inductance is due to the finite conductivity of the conductor. If a current is present in a wire which is not perfectly conducting, a magnetic flux will be produced inside the conductor. This magnetic field gives rise to an inductance internal to the conductor. As the frequency increases, there will be less of a field inside the conductor due to the skin effect and hence the internal inductance will decrease. Appendix 1 formulates the equation for the internal inductance of a rectangular conductor at low frequency and it also shows that the internal inductance of typical printed circuit tracks is usually negligible.

A good discussion on the definition of inductances, and especially the partial inductance, is presented in Ruehli[11] and Paul[12].

This chapter presents a method for calculating the self partial inductance of a rectangular wire. It will also show that the self partial inductance of a wire decreases in the presence of other wires as is expected from empirical observations [12].

For simplicity, the self partial inductance will be referred to in this document as simply the partial inductance.

3.2 Problem Formulation

Consider the various printed circuit board configurations shown in Fig. 3.3. To find the partial inductance of such rectangular cross-section conductor configurations, Poisson's equation,

$$\nabla^2 \vec{A} = -\mu_o \vec{J}, \tag{3.4}$$

must be solved inside the active conductor, i.e. the conductor which has a current in it, and Laplace's equation,

$$\nabla^2 \vec{A} = 0, \tag{3.5}$$

must be solved outside the active conductor. In the preceding equations, $\vec{A}$ is the vector magnetic potential, $\vec{J}$ is the current density and μ_o is the permeability of free space ($4\pi \times 10^{-7}$ H/m).

The finite element method (FEM) is used here to solve these equations. If the conductor is assumed infinitly long or by ignoring the end effects, the problem can be reduced to two dimensions. The mesh of 2D finite elements for one of the configurations to be analyzed is shown in Fig. 3.4. The top drawing in the figure is the mesh of the entire configuration but since the middle of the mesh is difficult to see, a blow-up is shown in the bottom drawing of the figure.

As was previously mentioned, the Poisson's equation must be solved inside the active conductor hence the following functional will be minimized inside the active conductor

$$F(A) = \int (\nabla A)^2 \, dx\, dy - 2 \int \mu_o J A \, dx\, dy \tag{3.6}$$

and the same equation less the last term, i.e.

$$F(A) = \int (\nabla A)^2 \, dx\, dy \, , \tag{3.7}$$

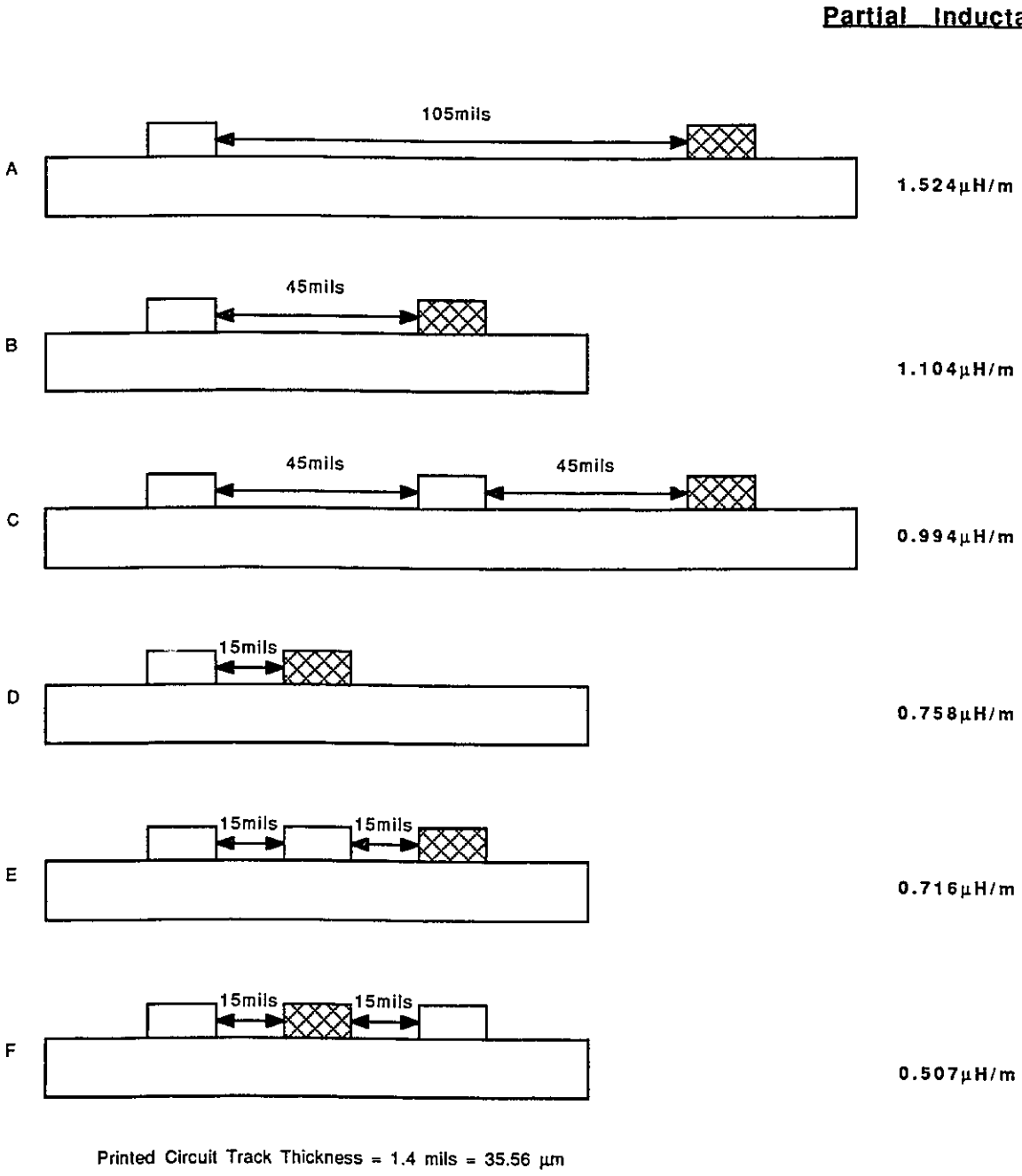

Figure 3.3: Different Rectangular Cross-Section Conductor Configurations

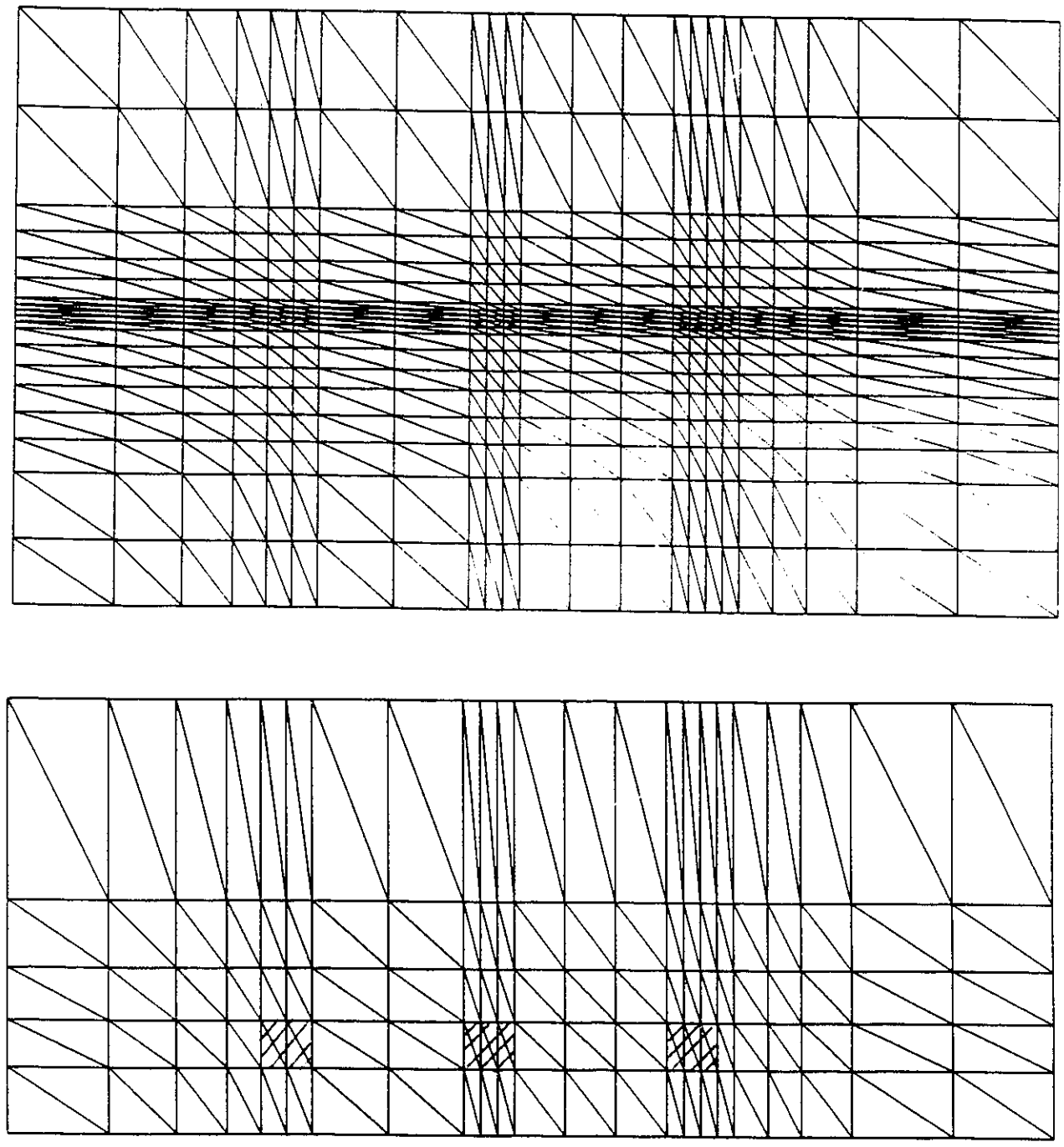

Figure 3.4: Finite Element Mesh Used to Determine Partial Inductance
Top Drawing: Entire Mesh
Bottom Drawing: Blow-up of the Middle of the Mesh

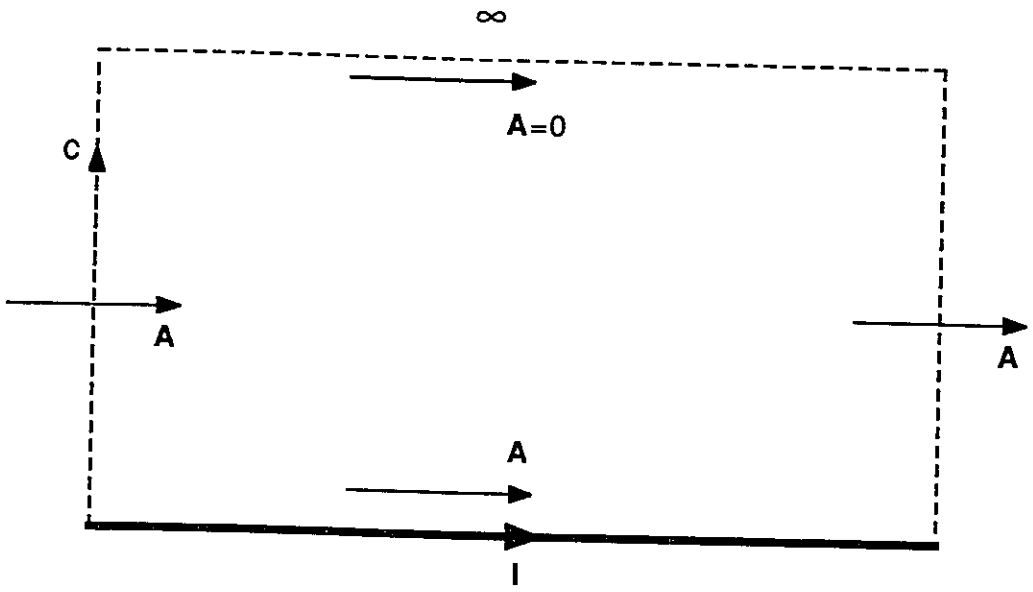

Figure 3.5: Contour of integration used to find partial inductance

will be minimized outside the active conductor.

Once the vector magnetic potential is known, the partial inductance L_p is found from Equ. (3.3). The formula is repeated below for clarity.

$$L_p = \frac{\int_c \vec{A} \cdot \vec{dl}}{I} \tag{3.8}$$

where I is the current inside the active rectangular conductor and c is the contour of integration shown in Fig. 3.5.

A uniformly distributed current of 1A is assumed inside the conductor. When the frequency is larger than 3.5 MHz, the skin depth (δ) is greater than 35.56 μm which is the thickness of the copper conductors that were studied. Hence the uniformly distributed approximation is somewhat compromised but it is still a necessary assumption in order to limit the number of finite elements that are needed.

The properties of the vector magnetic potential, $\vec{A}$, will help reduce the contour

integral in (3.8) to a line integral. First, $\vec{A}$ is assumed to decay to zero at infinity and second, since it is parallel to the conductor, the dot product between it and the contour will also be zero for the parts of the contour perpendicular to the conductor. Due to these two properties, the partial inductance is the magnitude of the magnetic vector potential at the surface of the conductor times the length of the conductor.

All the conductors were assumed to be infinite and to have a uniform current through their cross-sections. The Dirichlet condition, $\vec{A} = 0$, is enforced on all non-active conductors and Neumann boundaries, $\partial A/\partial n = 0$, are assumed at the limit of the finite element mesh. From Fig. 3.6, where the equipotential lines of A are drawn for configuration F, the Neumann boundary assumption is not true at all places but since the finite element mesh is so large with respect to the configuruation, the majority of the energy is contained in them and any contributions from infinite elements would be small.

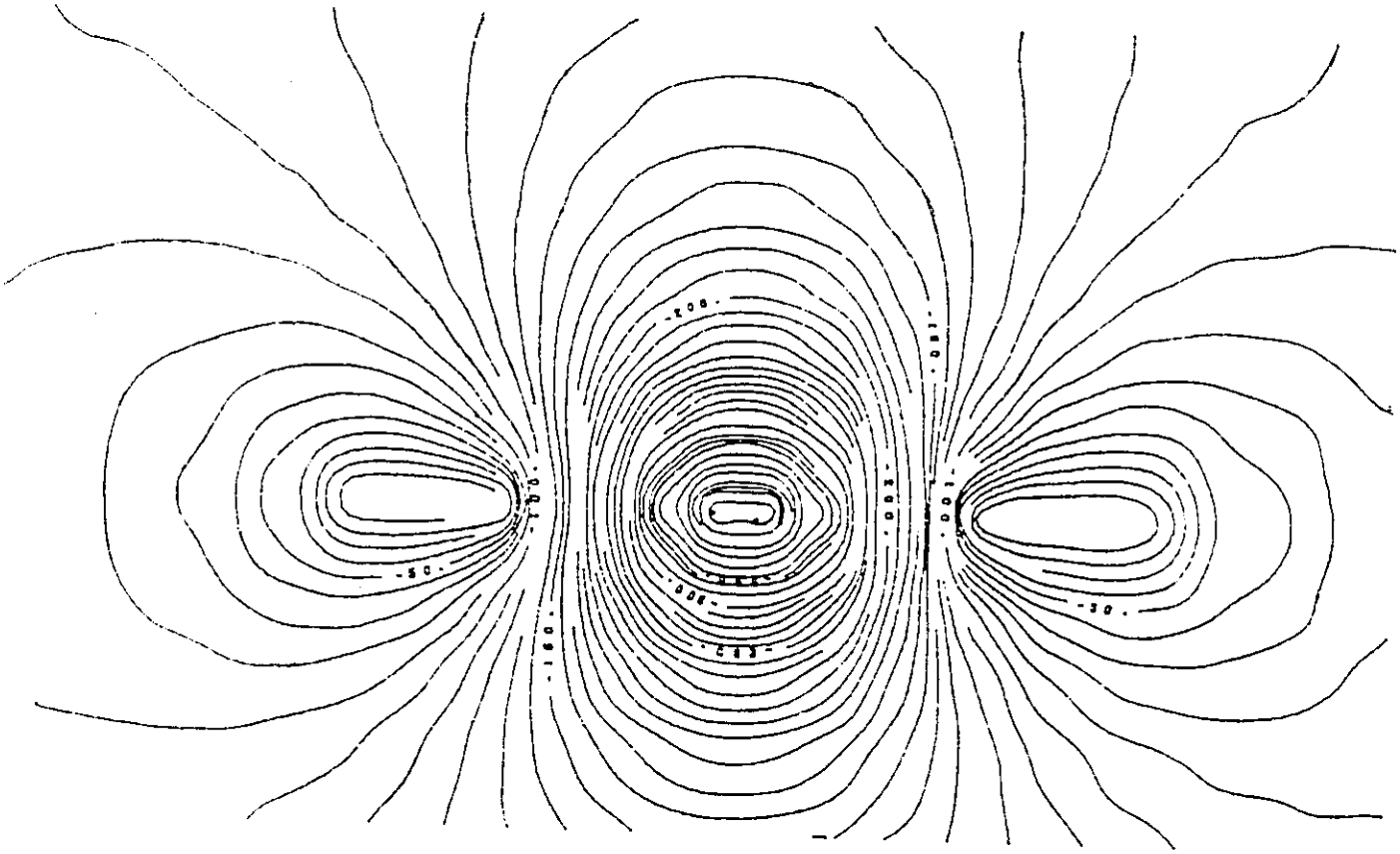

Figure 3.6: Equipotential lines of A from Configuration F

Configuration	Partial Inductance [μH/m]
A	1.5242
B	1.1040
C	0.99410
D	0.75817
E	0.71594
F	0.50704

Table 3.1: Comparison of the partial inductance for different structures

3.3 Results

Using the method just described, the value of the partial inductances for the configurations shown in Fig. 3.3 were found and are presented in Table 3.1. It can be seen that the value of the partial inductance decreases as the active conductors are placed in closer proximity with other conductors. For example, by comparing the results for configurations A, B and D, the partial inductance of the active conductor is seen to decrease as another conductor is brought closer and closer. These results confirm the long held belief by people working in the EMI field that partial inductances are reduced by the presence of other conductors [12].

3.4 Verification of Results

The validity of the results obtained in this chapter may be verified by comparing the value of the partial inductance predicted by an analytic expression for a conductor in isolation with the value obtained for configuration A.

The equation (3.9) below gives an analytic expression for the partial inductance of a rectangular conductor in isolation [11]. The formulation, which neglects the thickness of the conductor, is

$$\frac{L_p}{l} = \frac{\mu}{6\pi}\left[3\ln(u+\sqrt{u^2+1}) + u^2 + u^{-1} + 3u\ln(u^{-1}+\sqrt{u^{-2}+1}) - (u^{4/3}+u^{-2/3})^{3/2}\right] \tag{3.9}$$

where l is the length of the conductor and u is the ratio of l to the width (W) of the conductor, i.e. $u = l/W$.

Configuration A is used for comparison because it is the configuration which most closely resembles a conductor in isolation. However, since there is another conductor in the vicinity and since the thickness of the printed circuit track is being considered, a smaller partial inductance than the analytic prediction is expected.

If the dimensions of the tracks from the examples in this chapter are used in Equ. (3.9), namely l = 1m and W = 15 mils (= 381μm), the partial inductance is found to be 1.8132 μH/m. This value is slightly higher than the value of the partial inductance obtained for configuration A, L_p = 1.5242 μH/m, as was expected. This shows that the values of the partial inductance obtained for the different configurations are correct and hence that the method is valid.

3.5 Discussion

The partial inductances of several rectangular printed circuit track PCBs were determined and verified. It was seen that the partial inductance of a track *decreases* as other tracks are put in closer vicinity.

These conclusions have applications in two different aspects of electromagnetic compatibility: cross-talk and radiated emissions. Paul shows that a decrease in the value of the partial inductance reduces the cross-talk between printed circuit tracks [12]. The following chapter will show why the partial inductance is needed to predict the radiated emissions from printed circuit boards.

Chapter 4

Models to Determine Radiated Emission for Printed Circuit Boards

4.1 Introduction

The prediction of radiated emissions from printed circuit boards (PCBs) has long been a problem of major concern in the EMI field [13]–[17]. A new approach is presented in this chapter which uses the two following principles to accurately predict the electromagnetic radiation from PCBs:

1. Common-mode currents cause the majority of radiated emissions [7,8].

2. The voltage developed on the ground return path is the major source of the common-mode currents [12].

Due to the electrically small dimensions of standard PCBs, the return current of a signal is usually in close proximity to the signal itself and since the differential-mode

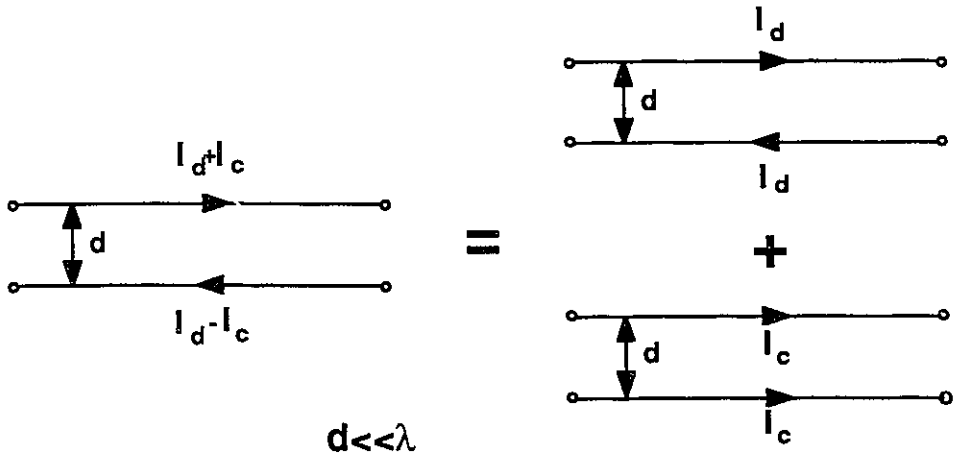

Figure 4.1: Differential and common mode currents on transmission lines

currents are 180° out of phase, they tend to produce emissions which partly cancel each other out (see Fig. 4.1). On the other hand, when common-mode currents are produced on signal lines, the currents are in phase and the radiated emissions tend to add.

The largest source of these common-mode currents is usually the voltage developed on the ground return path. Since most PCBs contain components which operate at frequecies in the Mega Hertz range, a considerable voltage drop, V_{gnd}, may occur on the ground due to the inductance of the ground, L_{gnd}. The ground voltage is also a factor of the skin-effect impedance of the ground, Z_{gnd}, and the ground current I_{gnd}:

$$V_{gnd} = (Z_{gnd} + j\omega L_{gnd}) \times I_{gnd} \,. \tag{4.1}$$

All PCBs are connected by cables to other components of the system such as the power supply, other PCBs, the monitor, etc... These cables will typically have

a ground reference which will be attached to the ground of the PCB. For example, a common inter-connection cable, the twisted pair, typically has one wire attached to the PCB ground in order to, among other things, control the radiated emissions due to differential-mode currents. Unfortunatly, this practice creates a common-mode current on the ground wire.

A simple demonstration that the common-mode current developed on attached cables is very important is shown in Fig. 4.2 which compares the radiated electric field from the circuit in Fig. 4.4 when the attached cables are present and absent. It is evident that the inter-connecting cables must be included in any model which attempts to predict electromagnetic radiation from real-life PCBs.

The standard parameter of interest for radiated EMI measurements is the radiated electric field [1,2,3] and hence all references made in this thesis to radiated emissions is understood to be radiated electric field.

Determining radiated emissions from complicated PCB circuits will therefore require a method of determining the impedance of the ground return path.

This chapter shows how the impedance can be calculated for a rectangular cross-section printed circuit track and then using this result, along with the partial inductance results from the previous chapter, the radiated emissions from a printed circuit board can be predicted with the aid of the Numerical Electromagnetics Code (NEC) [4].

NEC has been proven to be reliable hence it is extensivly used by the EMC community in place of experimental measurements([8,18,19]). Therefore, the accuracy of the new method is verified using NEC.

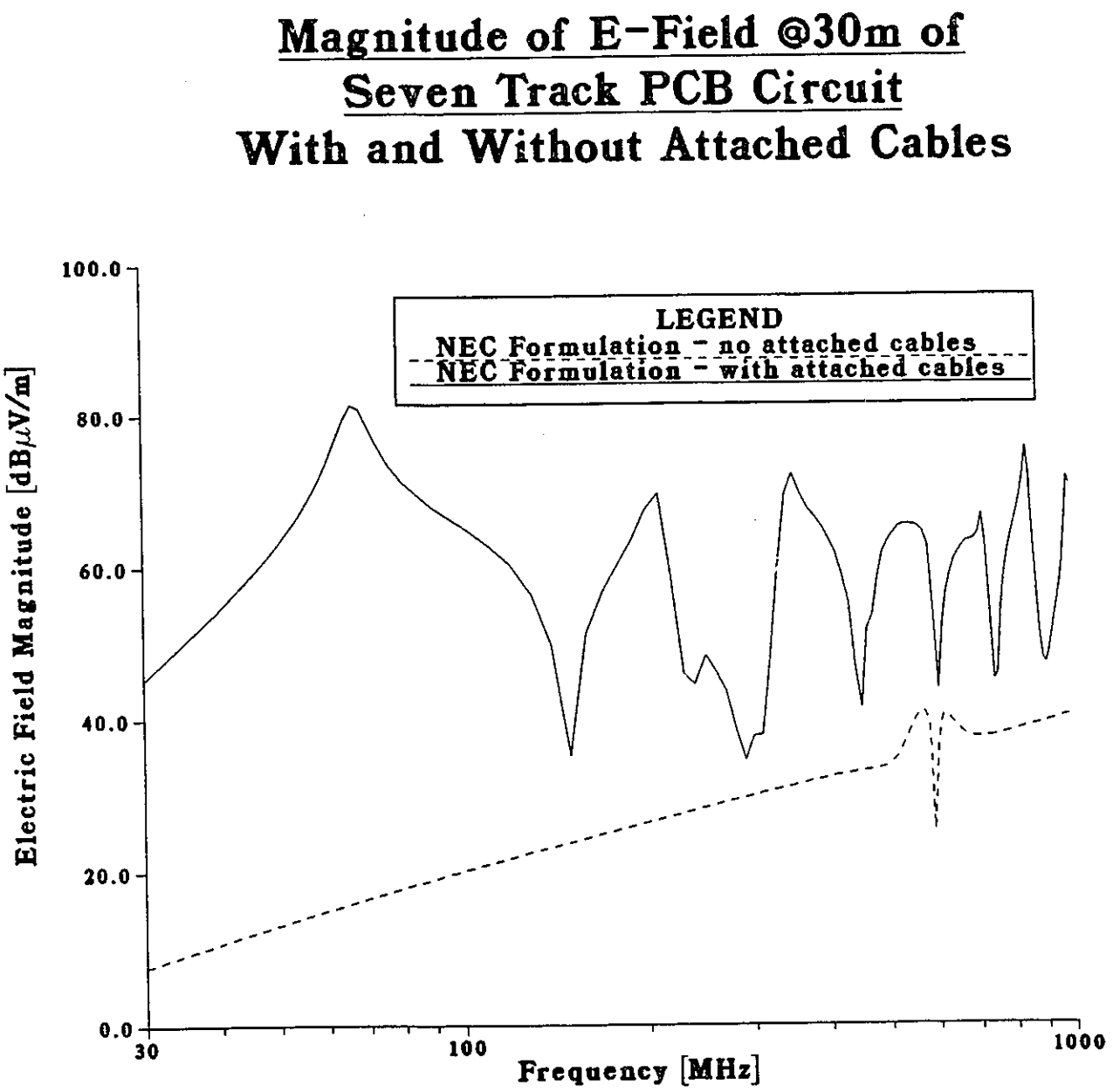

Figure 4.2: Comparison of radiated emissions from a typical circuit with and without attached cables.
All results were obtained using NEC.

In order to test the validity of this approach, the new method was applied to some much simpler circuits first. This original analysis is given in Appendix B. The results proved to be very encouraging and therefore an analysis of more realisticly complicated PCB circuits was undertaken. The following chapter presents this work.

Line	Length [m]	# of Segs.	Segment Length [m]
1	25.0E-2	10	2.5E-2
2	25.0E-2	10	2.5E-2
3	25.0E-2	10	2.5E-2
4	25.0E-2	10	2.5E-2
5	25.0E-2	10	2.5E-2
6	25.0E-2	10	2.5E-2
7	25.0E-2	10	2.5E-2
8	3.048E-3	1	3.048E-3
9	5.0E-4	1	5.0E-4
10	5.0E-4	1	5.0E-4
11	3.048E-3	1	3.048E-3
12	5.0E-4	1	5.0E-4
13	5.0E-4	1	5.0E-4
14	1.524E-3	1	1.524E-3
15	1.524E-3	1	1.524E-3
16	1.0E+0	34	2.94E-2
17	1.0E+0	34	2.94E-2

Table 4.1: Segementation data of the wire grid model shown in Fig. 4.4

4.2 Synthesis of Problem

The printed circuit board, as well as the circuit to be analyzed, is identical to that used by Clayton Paul in [12]. Figure 4.3 shows the actual dimensions of the PCB, Fig. 4.4 gives the wire grid model of the circuit and Table 4.1 presents the wire segmentation data required by NEC of the circuit. The circuit uses the second and fourth printed circuit tracks as signal lines, the sixth one as the ground return track and the other tracks are left "floating", i.e. not connected to a voltage reference. As was discussed earlier, the cables attached to the ground return are the main cause of radiated electromagnetic interference (EMI) and hence must be included. A ground plane is present because FCC and CISPR compliance measurement procedures call for the equipment under test to be placed above one [1], [3].

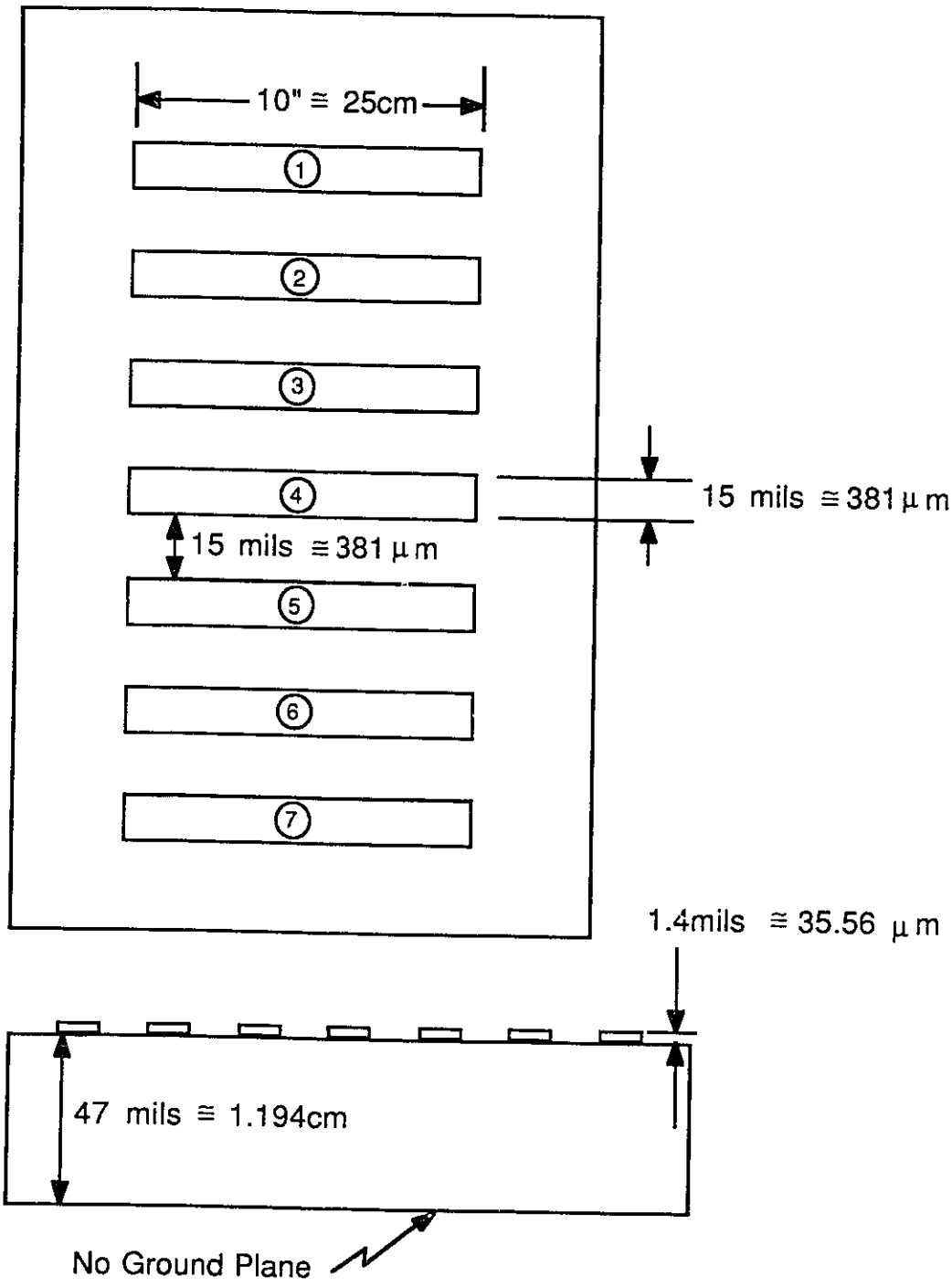

Figure 4.3: Seven track printed circuit board to be studied

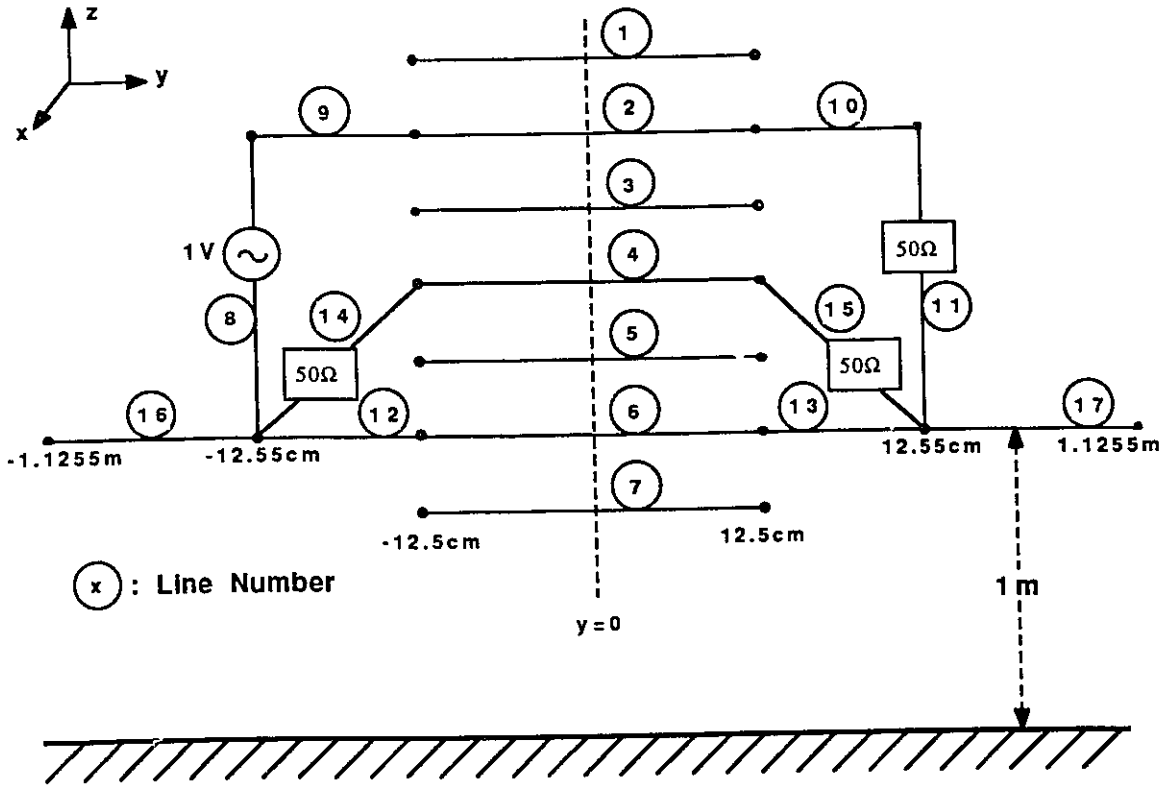

Figure 4.4: NEC wire grid model for the circuit to be analyzed

4.3 Determining Impedance of Ground Track

In this section the formulation for calculating the impedance of a rectangular ground track is presented.

The first quantity that must be determined is the magnetic field H. To accomplish this, Ampère's law is applied to the conductor shown in Fig. 4.5. The contour of integration is around the circumference of the conductor and if the width is much greater than the height ($L \gg 2a$), the result is:

$$H(s,x) \cdot 2L = I(s).$$

Evaluating this equation at $x = \pm a$ results in:

$$H(s,\pm a) = \frac{I(s)}{2L}. \tag{4.2}$$

The diffusion equation for a conductive media is given by:

$$\frac{\partial^2 H}{\partial x^2} - \mu\sigma\frac{\partial H}{\partial t} = 0.$$

In this case, the initial condition is that there is no H-field at zero time, i.e. $H(0,x) = 0$. Hence, taking the Laplace transform of the diffusion equation and applying the initial conditions gives:

$$\frac{\partial^2 H(s,\pm a)}{\partial x^2} - s\mu\sigma H(s,\pm a) = 0. \tag{4.3}$$

Solving this second order, linear homogenous differential equation results in:

$$H(s,x) = 2C_1 \sinh\sqrt{s\mu\sigma}\, x. \tag{4.4}$$

and enforcing the boundary condition given in (4.2) gives:

$$H(s,x) = \frac{I(s)}{2L}\frac{\sinh\sqrt{s\mu\sigma}\, x}{\sinh\sqrt{s\mu\sigma}\, a}. \tag{4.5}$$

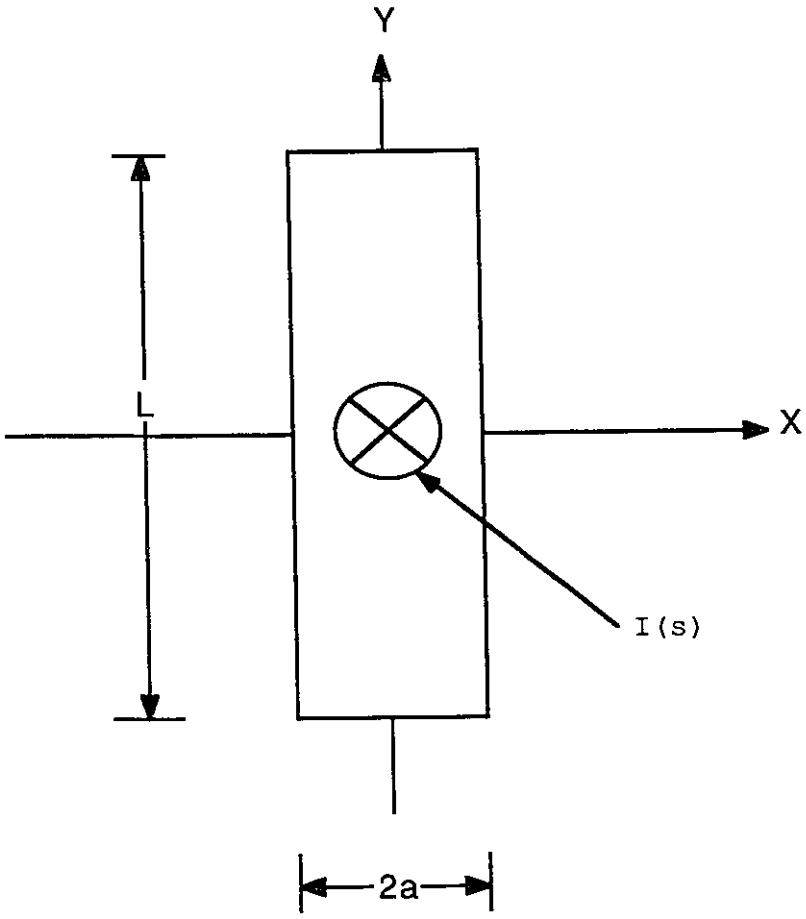

Figure 4.5: Schematic representation of ground track conductor

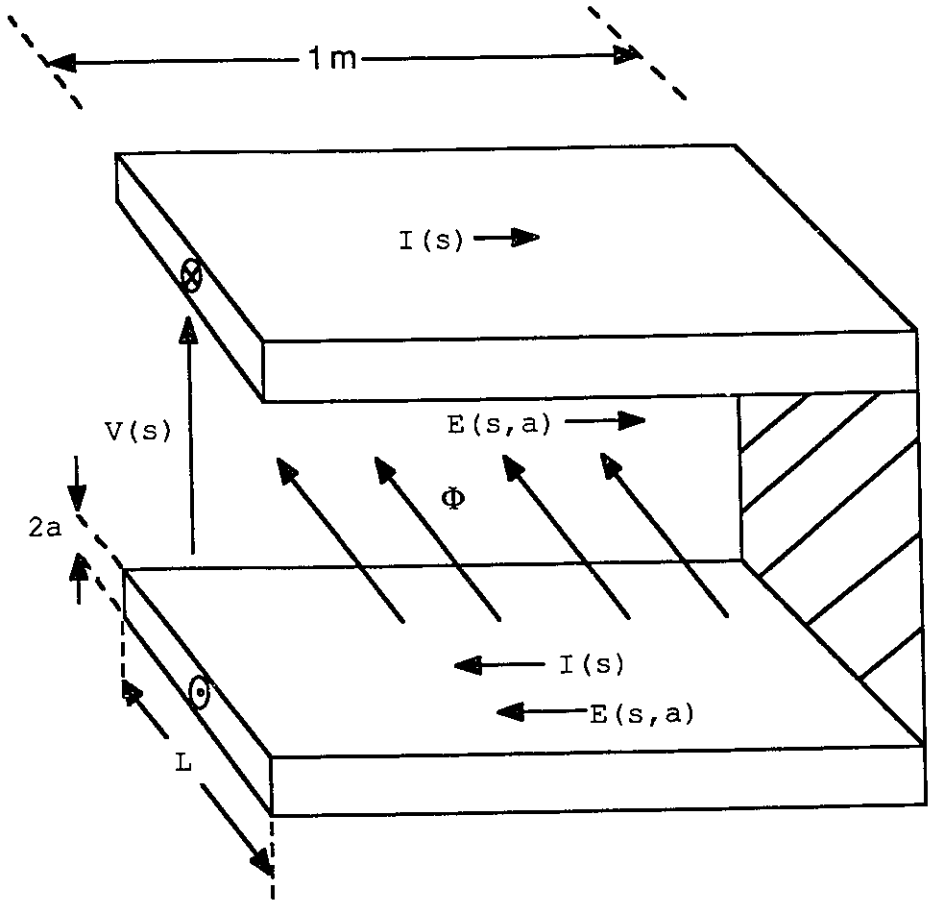

Figure 4.6: Determining equivalent impedance of printed circuit track

If the substitution $\tau = \mu\sigma a^2$ is made, the final solution to the magnetic field is obtained:

$$H(s,x) = \frac{I(s)}{2L} \frac{\sinh\left(\frac{x}{a}\sqrt{s\tau}\right)}{\sinh\sqrt{s\tau}} \quad [A/\mathrm{m}]. \tag{4.6}$$

Now to find the equivalent impedance of the printed circuit track, we consider the structure shown in Fig. 4.6. The circuit consists of two 1 meter long parallel plates. There is an applied voltage source at one end and a short circuit termination at the other. A current I is induced on the plates and a flux ϕ results inside the region between the plates. An equivalent circuit of this parallel plate structure is shown in Fig. 4.7.

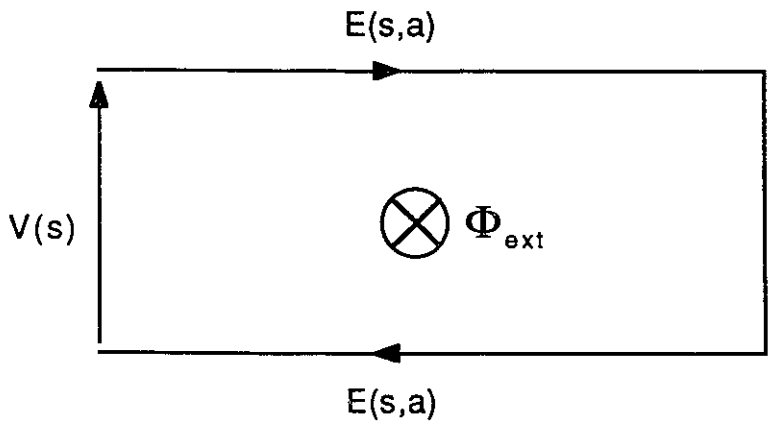

Figure 4.7: Equivalent circuit of parallel plates

The electromagnetic induction law,

$$\oint_C \vec{E} \cdot d\vec{l} = -\frac{d}{dt}\int_S \vec{B} \cdot \vec{n}\, dA, \tag{4.7}$$

can now be applied to this problem which results in:

$$-V(t) + 2E(t,a) \cdot 1 = L_{ext}\frac{dI(t)}{dt} \tag{4.8}$$

and taking the Laplace transform of (4.8) gives

$$-V(s) + 2E(s,a) = sL_{ext}I(s). \tag{4.9}$$

In Eqs. (4.8) and (4.9), $E(s,a)$ is the E-field evaluated at the surface of the plate and L_{ext} is the external inductance.

In order to solve the impedance of the rectangular signal track, the next step will be to calculate the electric field from the magnetic field found in (4.6). The relation between these two fields at steady state is given by Ampère's law:

$$\sigma\vec{E} = \vec{\nabla} \times \vec{H} \tag{4.10}$$

which is valid for a good conductor where the displacement current can be neglected.

Substituting (4.6) into (4.10) results in an electric field given by:

$$\vec{E}(s,x) = \frac{I(s)}{2L\sigma}\frac{\sqrt{s\tau}}{a}\frac{\cosh\left(\frac{x}{a}\sqrt{s\tau}\right)}{\sinh\sqrt{s\tau}} \quad \text{for} \mid x \mid \leq a\,. \tag{4.11}$$

Evaluating Equ. (4.11) at $x = a$ gives

$$\vec{E}(s,a) = \frac{I(s)}{2L\sigma}\frac{\sqrt{s\tau}}{a}\coth\sqrt{s\tau} \tag{4.12}$$

and then this equation can be substituted into Equ. (4.9) to find:

$$V(s) = I(s)\left[sL_{ext} + \frac{\sqrt{s\tau}}{L\sigma a}\coth\sqrt{s\tau}\right] \tag{4.13}$$

Therefore the expression for the impedance of the printed circuit tracks in Fig. 4.6 is found to be

$$Z(s) = \frac{V(s)}{I(s)} = sL_{ext} + \frac{\sqrt{s\tau}}{L\sigma a}\coth\sqrt{s\tau}.$$

This result was obtained for a two parallel track circuit hence the impedance of a *single* track is

$$Z(s) = sL_p + \frac{\sqrt{s\tau}}{2L\sigma a}\coth\sqrt{s\tau} \tag{4.14}$$

where the inductance of the circuit has been replaced by the partial inductance of the track, L_p[1].

Examining Equ. (4.14), it can be seen that it is composed of two parts; the first part is due to the external inductance of the track and the second part comes from the finite conductivity of the track. The validity of the second part of the equation is verified in Appendix A.

The impedance of the ground current return track, Z_{gnd}, can now be found by using the partial inductance of the rectangular conductor found in Chapter 3. Appendix A

[1]The total inductance of a conductor which does not form a loop is the value of it's partial inductance [11]. For a more complete discussion on partial inductances, see Chapter 3.

shows that the internal inductance of the conductor is included in the second term of Equ. (4.14).

The steady state value of the impedance is obtained by changing Eqn. (4.14) from the Laplace to the Fourier domain, i.e. $s \rightarrow j\omega$,

$$Z_{gnd}(\omega) = j\omega L_p + \frac{\sqrt{j\omega\tau}}{2L\sigma a} \coth \sqrt{j\omega\tau} \quad [\Omega/\mathrm{m}]. \tag{4.15}$$

The method to find the partial inductance, as well as the value of the partial inductance for this configuration, has been given in the preceding chapter.

It is interesting to note that the partial inductance is the dominant factor in Equ. (4.15) for most printed circuit tracks at all frequencies of interest.

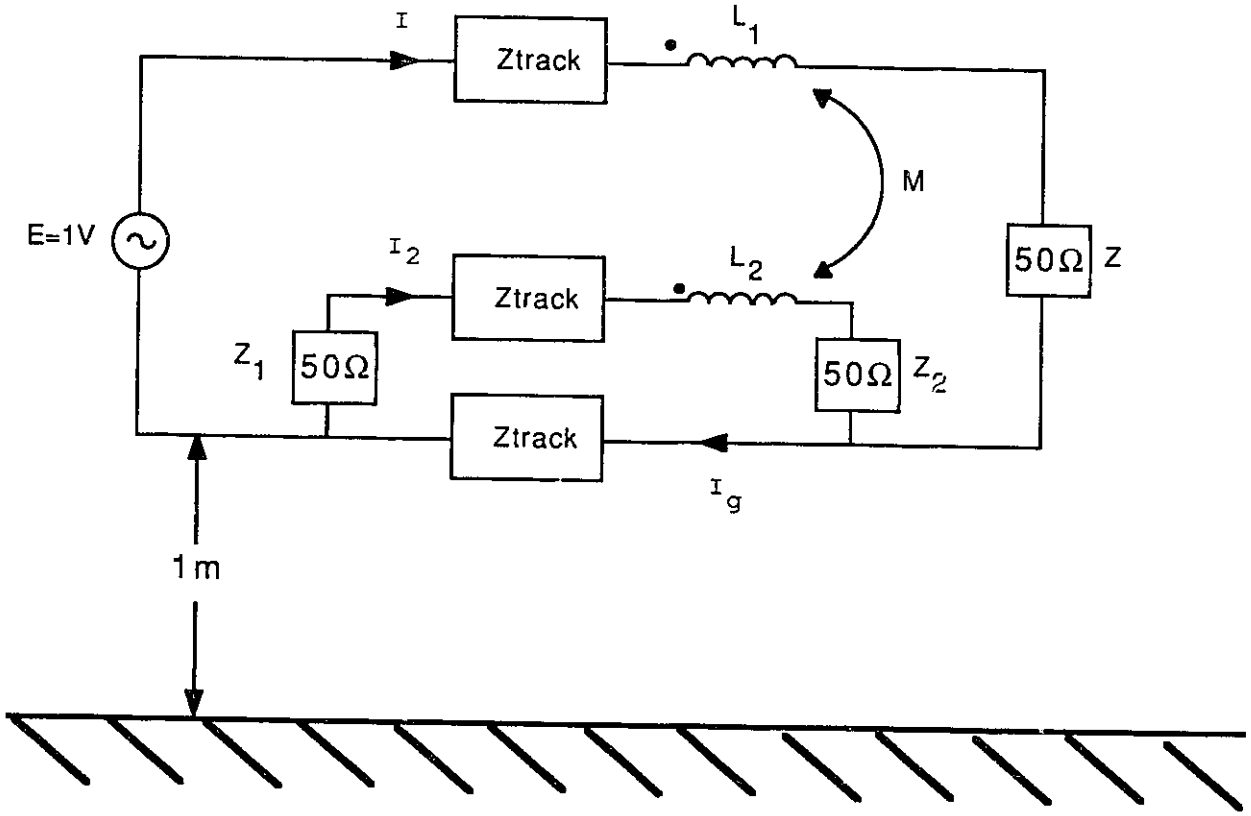

Figure 4.8: Seven track circuit with lumped impedances

4.4 Calculation of Ground Current

Figure 4.8 shows the circuit described in the preceding section along with the impedances due to the skin effect. The floating printed circuit tracks are still present but are not included in the figure. Also shown are the inductances due to the loops and the mutual coupling which results from them. This circuit model will be used to determine the ground current.

Using basic circuit theory, the ground current is found to be:

$$I_G = \frac{EA}{BC + j\omega MA + (A + B)\, Z_{track}} \tag{4.16}$$

where

$$\begin{aligned} A &= Z_{track} + Z_1 + Z_2 + j\omega(L_2 - M) \\ B &= Z_{track} + Z + j\omega(L_1 - M) \\ C &= Z_{track} + Z_1 + Z_2 + j\omega L_2 \end{aligned}$$

and Z_{track} is the impedance of a printed circuit board track as derived in Equ. (4.15).

The loop inductances, L_1 and L_2, are found by using the formula for small rectangular loops formed by round wires [20]:

$$L = \frac{\mu}{\pi}\left(width\cosh^{-1}\frac{length}{d} + length\cosh^{-1}\frac{width}{d}\right) \tag{4.17}$$

where *length* and *width* are the length and width of the loop, respectively and d is the diameter of the wire. Since Equ. (4.17) is for round wires, an approximation must be made when dealing with rectangular tracks in order to find an equivalent diameter. A reasonable estimate is obtained by keeping the areas of the rectangular and circular wires the same, i.e. $d = 2\sqrt{A_\square/\pi}$ where $A_\square$ is the area of the rectangular conductor.

To find the mutual inductance M, the following formula can be used [21]:

$$M = \frac{\mu_o}{2\pi}\ln\left(1 + \frac{4h^2}{d_{12}}\right) \tag{4.18}$$

where h is the height of the conductors above ground and d_{12} is the separation between the conductors.

In the preceding calculations, the assumption was made that the lines were smaller than the quarter-wavelength. Since the lines are 25 cm long, the assumption is valid for all frequencies below $\sim$ 300 MHz. Above this frequency, the current becomes non-uniform along the wire but as will be seen in the following section, the results remain meaningfull.

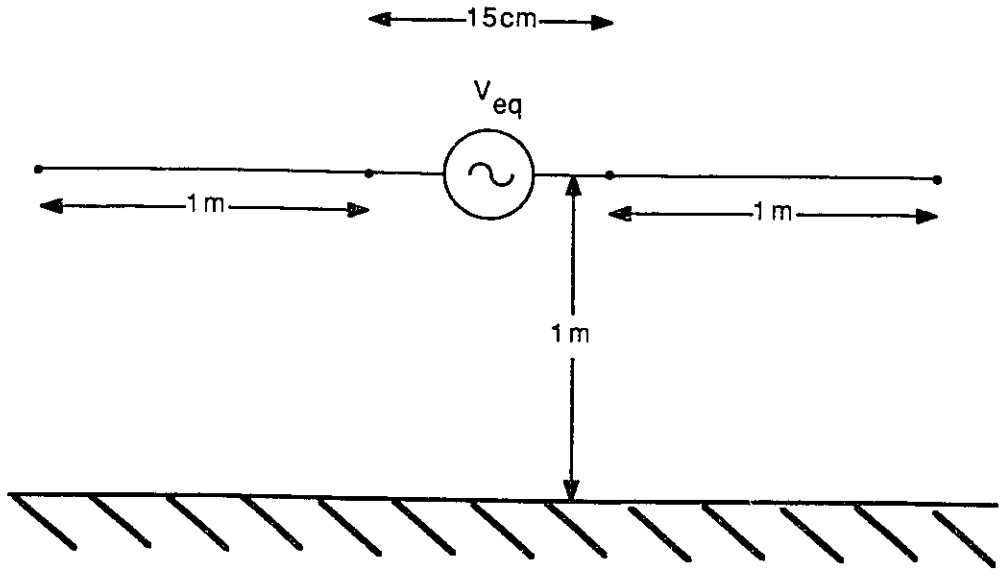

Figure 4.9: Simplified model of circuit shown in Fig. 4.4 used to predict radiated emissions

4.5 Prediction of Radiated Emissions

All the necessary preparatory development has been completed and it is now possible to predict the radiated emissions. The circuit originally shown in Fig. 4.4 can be reduced to a much simpler one by replacing all the elements between the attached cables by an equivalent voltage source (see Fig. 4.9). The equivalent voltage source is the voltage drop that occurs on the ground return track. This voltage drop is found by taking the product of the impedance of the ground track, Equ. (4.15), with the ground return current, Equ. (4.16), :

$$V_{eq} = (Z_{gnd} \times \text{length of track}) \times I_{gnd} \quad [V]. \tag{4.19}$$

All other elements of the PCB circuit can now be neglected.

As mentioned previously, the partial inductance is the dominant factor in the ground impedance of a printed circuit track and it is therefore the major reason that a voltage is developed on the ground return path.

Method	CPU Time [sec]
NEC Only	41418.69
Ground Impedance Simplification	8083.59

Table 4.2: Comparison between CPU times of the two methods on a DEC VAXstation II

Using the equivalent voltage source V_{eq}, the radiated emissions from the circuit shown in Fig. 4.9 can be found using NEC. The advantage to this simplification is that the input file is now much smaller and hence will take much less time to run. A comparison of CPU times on a DEC VAXstation II is shown in Table 4.2. The ground impedance method is seen to be more than five times faster and hence requires more than five times fewer calculations. This will result in less round-off errors than if the entire circuit is analyzed.

The magnitude of the radiated electric field, calculated at distances of 30 m and 3 m are presented in Figs. 4.10 and 4.11, respectively[2]. It can be seen that the results obtained from the new ground impedance method are in close agreement with the results from the NEC analysis of the complete configuration for EMI/EMC applications. The descrepancies may be due to the NEC round-off errors mentioned earlier or they may be caused by the low-frequency approximation for the ground current (see Section 5.3).

Implementation of this method into a CAD package will therefore significantly reduce the time required to obtain the expected radiated interference from a PCB without sacrificing much, if any, accuracy.

Another configuration will be analyzed to show the effect of the "floating" printed

[2]Three and thirty metre measurements are standard distances specified by the FCC[1].

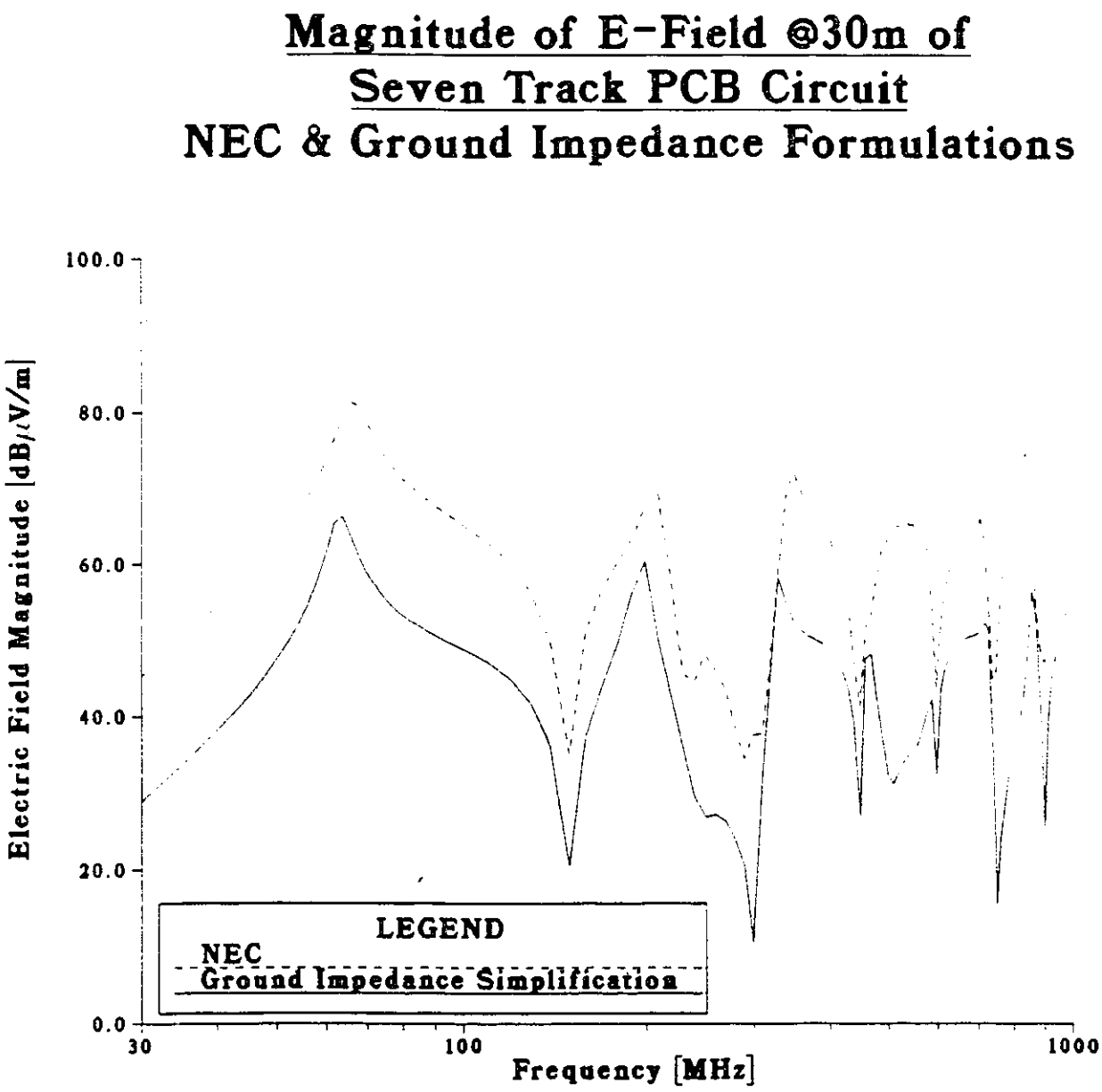

Figure 4.10: Comparison of 30m radiated electric field from seven track circuit

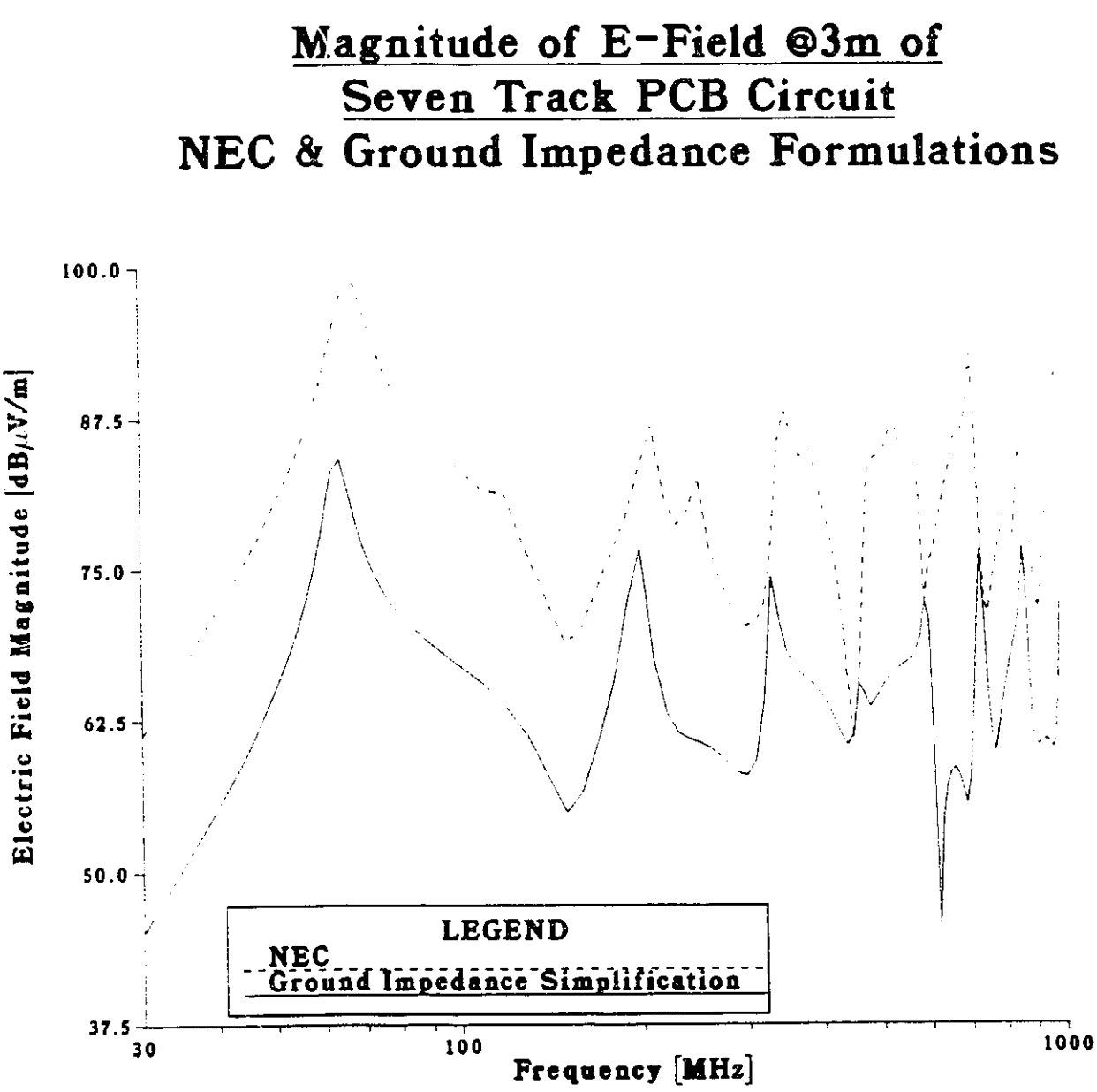

Figure 4.11: Comparison of 3m radiated electric field from seven track circuit

circuit tracks. Figure 4.12 shows a printed circuit board with only the three active tracks remaining from Fig. 4.3. This configuration has the same geometry as the one shown in Fig. 3.3(C) therefore the partial inductance of the ground return track is the same, i.e. $L_p = 0.99410\mu$H/m. The same method of analysis is used for this three track circuit as was used for the previous seven track circuit and the resulting radiated electric fields are shown in Figs. 4.13 and 4.14.

Comparing the results shows that the three track PCB has on the average 3.1dB more radiated emissions than the seven track PCB. This proves that the presence of extra ground lands serves to *decrease* the radiated emissions from a PCB.

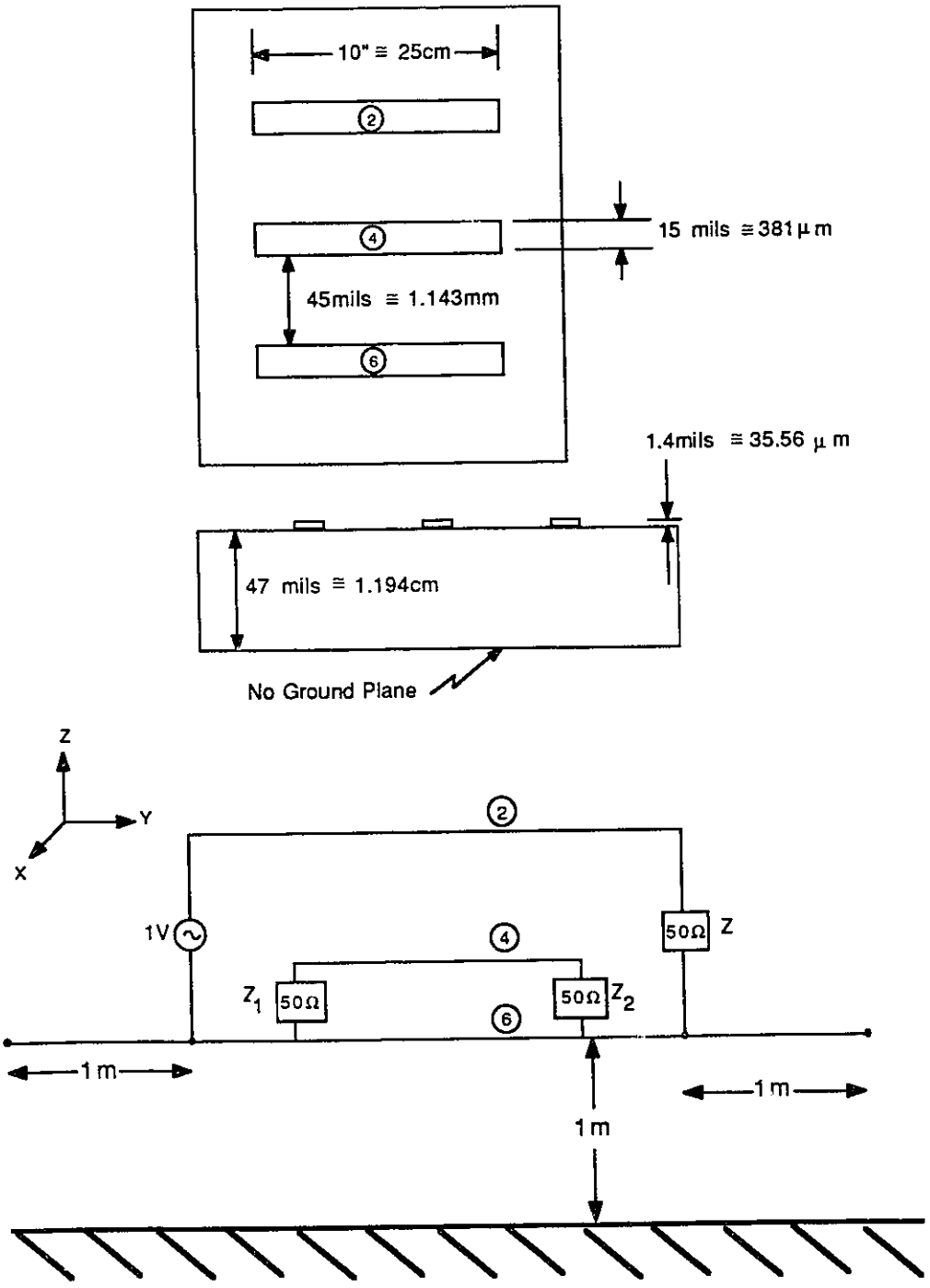

Figure 4.12: Three track printed circuit board

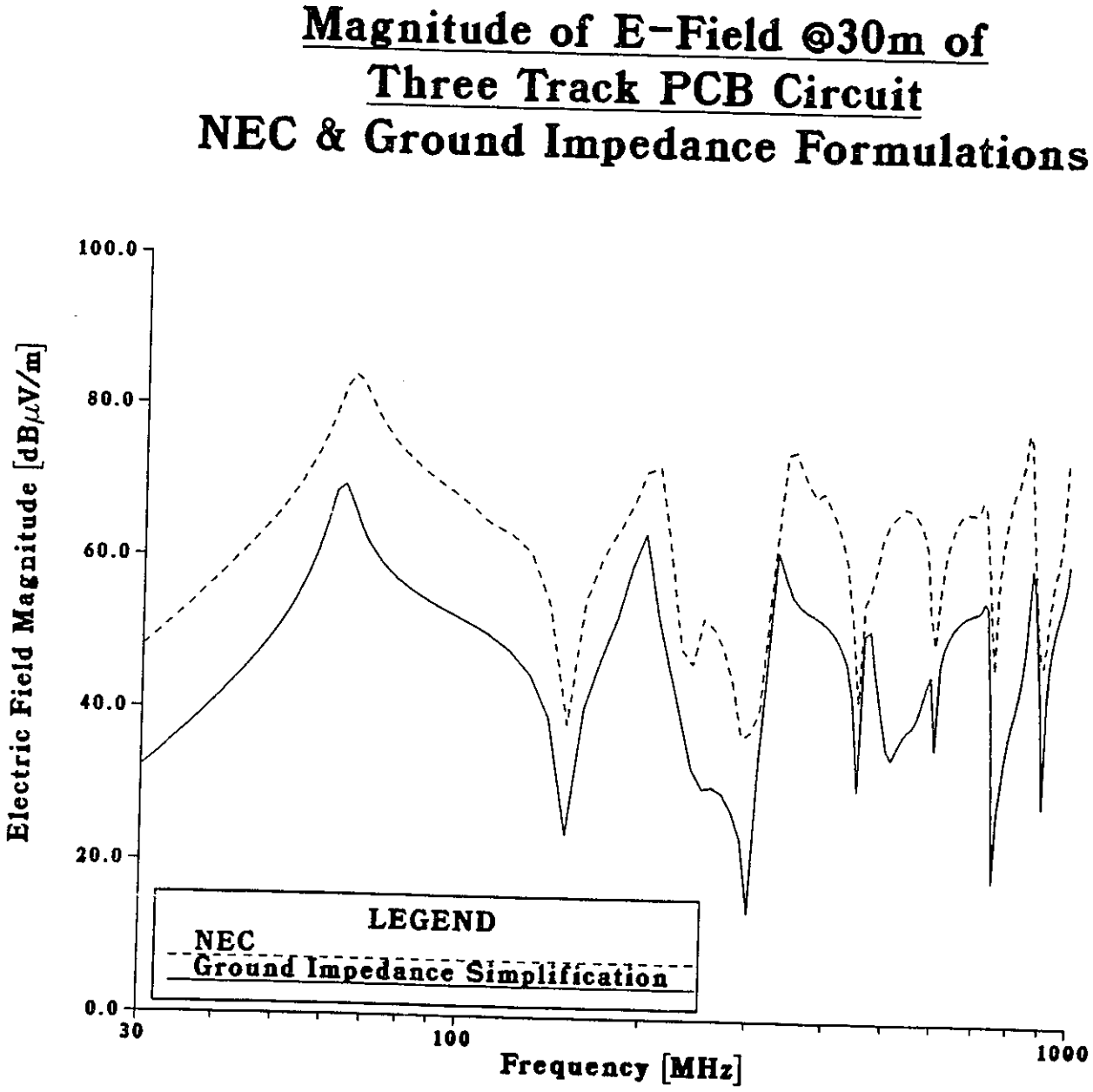

Figure 4.13: Comparison of 30m radiated electric field from three track circuit

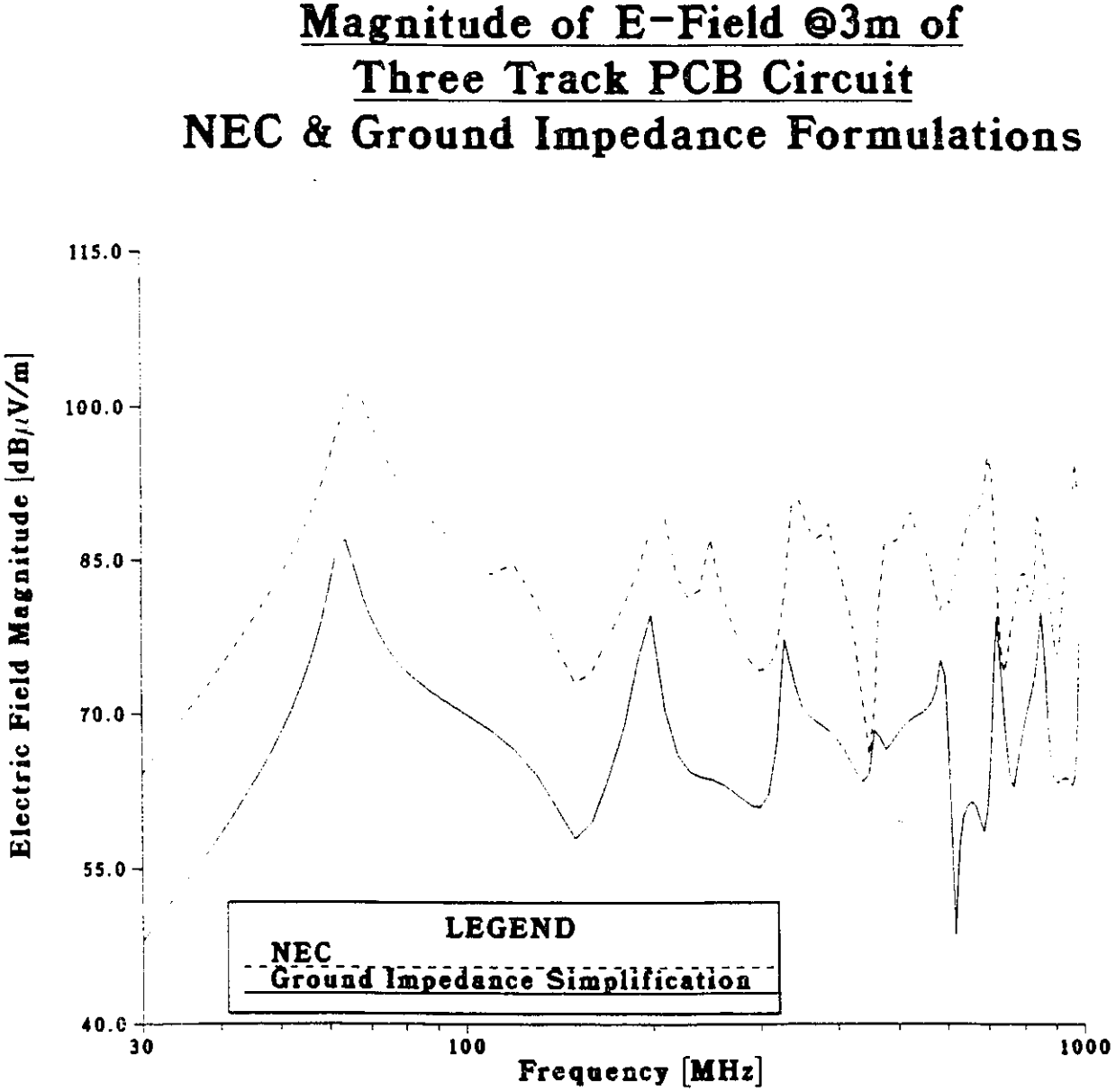

Figure 4.14: Comparison of 3m radiated electric field from three track circuit

Chapter 5

Conclusions

The overall objective of this thesis was to explore and understand various properties of printed circuit boards and then using these findings, establish guidelines that designers could use to minimize cross-talk and radiated EMI.

An overview of all the conclusions and guidelines developed in this thesis are presented in this concluding chapter.

5.1 Cross-Talk

The first topic explored was the cross-talk on various printed circuit board topologies. It was shown that there are certain ways of designing PCBs which are better than others from the cross-talk point of view. For example, more cross-talk was seen to occur when the printed circuit tracks are stacked one on top of the other, as was done in configurations 1 and 4 of Chapter 2, as opposed to when they are side by side. These results suggest that when dealing with applications where controlling cross-talk is essential, there should always be some horizontal distance between the printed circuit tracks. This can be achieved by

1. Using technologies such as configurations 2 and 3 of Chapter 2 (See Figs. 2.2 and 2.3) or,

2. Staggering the conductors by at least two conductor widths so that they are never directly one above the other.

The results of the analysis show that, in general, the four types of printed circuit boards may be ranked in order of increasing cross-talk as follows:

1. Configuration 3 (Strip-line)

2. Configuration 2 (Micro-strip)

3. Configuration 1

4. Configuration 4.

Cross-talk proved to be much more prevalent on the immediate neighbours of the driven line. Hence, the signal tracks connected to cross-talk sensitive components should be separated from printed circuit tracks, such as those carrying the clock signal, which are constantly active. This may be accomplished by placing grounded tracks on both sides of the active track.

Ground planes were seen to be very important in minimizing cross-talk. The addition of ground lands reduces the cross-talk between signal tracks significantly.

Conductor to ground plane separation was also examined by modifying Configuration 2 (Fig. 2.10). The analysis showed that as the separation is diminished, the cross-talk is also diminished. The separation is therefore a critical factor in the amount of cross-talk which will be coupled onto the susceptor lines. Unfortunatly,

other electrical and mechanical considerations limit the minimum size of the separation.

5.2 Partial Inductance

The chapter on partial inductances was mainly a necessary background preparation for the problem of predicting radiated emissions. Regardless of that, some interesting observations can still be made.

The partial inductance of a conductor was shown to *decreases* as other conductors were put in closer vicinity. This can be observed by comparing the values of the partial inductance obtained from configurations A, B and D (see Fig. 3.3 and Table 3.1).

Minimizing the partial inductance of a printed circuit track was shown by Paul to also reduce the cross-talk between tracks [12] hence these findings are also important for researchers who are studying cross-talk.

5.3 Predicting Radiated Emissions

A new technique was developed to quickly and accurately predict the radiated emissions from multi-track printed circuit boards. The theoretical basis of the technique relies on two theories: the voltage drop on the ground return path is the main source of common-mode current on attached cables and that the common-mode currents are themselves the dominant source of radiated EMI.

Using these two basic theories, the technique reduces a complicated circuit to a centre-driven dipole. The model can then be used to predict radiated emissions from printed circuit boards.

To test the model, the radiated electric field from two different circuits is predicted. The element which differentiated the two circuits was the number of tracks on the PCB. The first circuit had floating tracks on both sides of every active track. The second circuit did not have the floating tracks. The analysis shows that the ground impedance simplification method gave good results for these two complicated PCB circuits in a much shorter time than if the entire circuit was modeled with NEC.

The partial inductance was observed to be the dominant component of the ground impedance and hence the majority of radiated EMI is due directly to it. This was justified by comparing the radiated emissions from the two circuits. The seven track PCB whose ground return had a smaller partial inductance produced *less* radiated emissions than the PCB consisting of only three tracks. From these results, it may be concluded that *including as much land area as possible on a PCB will minimize the radiated emissions.*

Appendix A

Verification of Equation (4.14)

A.1 Introduction

In Chapter 4, a formula was derived to calculate the impedance of a printed circuit track, Equ. (4.14). This appendix shows that the result is correct by evaluating the equation at low frequency and comparing it with the analytic expectation.

The impedance of a conductor at low frequency, i.e. when the skin depth is much larger than the conductor, is due to the dc resistance and the internal inductance. Considering the rectangular conductor shown in Fig. A.1, the dc resistance is given by

$$R_{\mathrm{dc}} = \frac{1}{\sigma} \times \frac{1}{2al} \ [\Omega/\mathrm{m}] \tag{A.1}$$

where σ is the conductivity of the material. Hence it's total low frequency impedance is

$$Z_{\mathrm{lf}} = R_{\mathrm{dc}} + j\omega L_{int} \tag{A.2}$$

where L_{int} is the internal inductance.

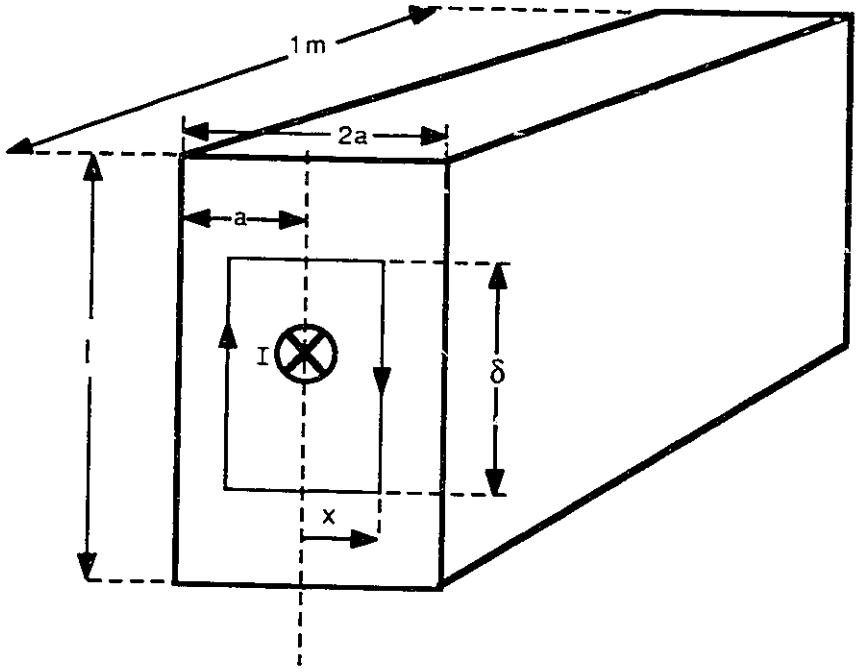

Figure A.1: Conductor with rectangular cross-section

The following sections determine the analytic expression for the internal inductance and then show Equ. (4.14) is correct.

A.2 Calculation of Internal Inductance for a Rectangular Conductor

To calculate the internal inductance of a rectangular conductor, Ampère's law is applied to the conductor shown in Fig. A.1.

$$\oint \vec{H} \cdot d\vec{l} = I_{total} \tag{A.3}$$

where $\vec{H}$ is the magnetic field and I_{total} is the total current inside the contour of integration.

When performing the integration, the contribution for the contour parallel to the x-axis will be zero since the dot product between the two vectors is zero. Assuming the current is uniformly distributed,

$$I_{\text{total}} = \frac{I}{2al} \cdot 2x \cdot \delta$$

and therefore,

$$H(x) \cdot 2\delta = \frac{I}{2al} \cdot 2x \cdot \delta$$

$$H(x) = \frac{I}{2al} x \quad [A/\text{m}] \tag{A.4}$$

Now the magnetic energy formula,

$$W_M = \frac{1}{2} \int_V \mu H^2 \, dV, \tag{A.5}$$

is applied to the problem where the volume of integration, V, is a unit length volume *inside* the conductor since the internal inductance is the only value being sought. (If the total inductance was required, the volume of integration would be infinite.)

Hence, the magnetic energy, W_M, is found by solving

$$W_M = \frac{\mu}{2} \int_0^1 \int_0^l \int_{-a}^a H^2 \, dx \, dy \, dz \; . \tag{A.6}$$

Due to the properties of fields inside rectangular structures, the magnetic field is constant in the y and z directions and hence the integration need only be performed from $x = -a$ to $+a$.

$$W_M = \frac{\mu}{2} \int_{-a}^a H^2 \, dx \cdot l \cdot 1 \; . \tag{A.7}$$

Substituting the expression for the magnetic field given by Equ. (A.4) into Equ. (A.7),

$$\begin{aligned} W_M &= \frac{\mu l}{2} \cdot 2 \int_0^a \left(\frac{I}{2al} \right)^2 x^2 \, dx \\ &= \mu l \frac{I^2}{4a^2 l^2} \frac{a^3}{3} \\ &= \frac{\mu I^2}{12} \frac{a}{l} \; . \end{aligned} \tag{A.8}$$

Since the magnetic energy is also defined by

$$W_M = \frac{L I^2}{2} \tag{A.9}$$

where L is the inductance, the value of the internal inductance for a rectangular conductor is found by equating the two expressions, Equs. (A.8) and (A.9), for the magnetic energy:

$$L_i = \frac{\mu a}{6l} \; . \tag{A.10}$$

As an interesting aside, the partial inductance can be shown to be negligible for most printed circuit applications. In the problem using the configuration shown in chapter 4, $a = 17.5\,\mu$m and $l = 1$ m hence the internal inductance of this rectangular conductor is

$$L_i = 3.66\,\text{pH} \; .$$

This value is very small compared to the partial inductances which were found in chapter 3 to be on the order of a *thousand* pico Henries. The internal inductance would only become significant if a material with a higher resistivity were used or if the conductor dimensions were much larger.

A.3 Verification of Results

Recalling that the second term of Equ. (4.14 is

$$Z_{\text{skin}} = \frac{\sqrt{j\omega\tau}}{2l\sigma a} \coth\sqrt{j\omega\tau}\,,$$

the low frequency approximation will have to determine the following limit

$$\lim_{x\to 0} \coth x = \lim_{x\to 0} \frac{e^x + e^{-x}}{e^x - e^{-x}}\,. \tag{A.11}$$

Using the expansion $e^x = 1 + x + \frac{x^2}{2!} + \frac{x^3}{3!} + ...$ and keeping only the first four terms, the result for the limit in Equ. (A.11) is found

$$\lim_{x\to 0} \coth x \cong \frac{1 + x^2/3}{x}\,. \tag{A.12}$$

Substituting the result of Equ. (A.12) into the expression for Z_{skin}, the expression for the low frequency skin impedance is found to be

$$\begin{aligned} \lim_{x\to 0} Z_{\text{skin}} &= \frac{1}{2a l\sigma} + j\omega\frac{\mu a}{6l} \\ &= R_{\text{dc}} + j\omega L_{int} \end{aligned} \tag{A.13}$$

where L_{int} is the internal inductance derived in section A.2 and R_{dc} is the dc resistance found in Equ. (A.1). Therefore, the low frequency impedance is as predicted in Equ. (A.2).

A.4 Conclusion

The expression for the impedance of a rectangular track derived in Chapter 4 was verified by comparing it to the analytic formulation for the impedance at low frequencies. The result shows that at Equ. (4.14) is correct since it includes the effect of all impedances.

Appendix B

A Model to Predict Radiated Emissions From Simple Electronic Circuits

B.1 Introduction

This appendix establishes the validity of the technique used in Chapters Three and Four to determine the radiated emissions from realistic printed circuit boards. It uses an analytic formula to determine the partial inductance of the ground return path instead of the finite element results derived in Chapter 3.

B.2 The Model

A printed circuit board can be thought of as a collection of sources driving loads connected by transmission lines. Some of these circuits will have cables attached to them to carry signals to other PCBs. An example is a circuit where there is only one system clock, but many different boards use it. The clock signal must therefore be

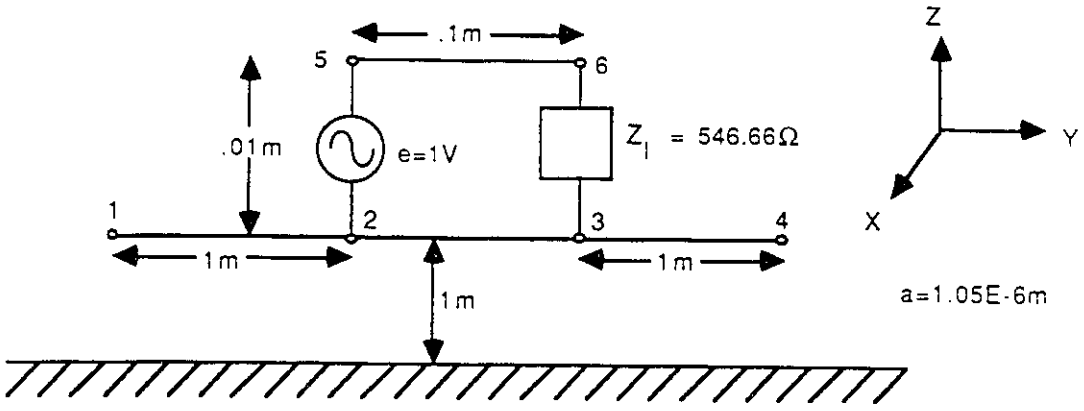

Figure B.1: Printed circuit board model

sent using cables, backplanes or some other such means to every board that requires it. Figure B.1 shows a simplified model of a system where one track on a PCB is replaced by a single transmission line carrying the signal. The connecting cables are represented by conductors (1–2) and (3–4). A ground plane is present because FCC and CISPR compliance measurement procedures call for the equipment under test to be placed above one [1], [3].

The attached cables are very important for the accurate prediction of emissions. If they are not included, large under-estimations of the radiated emissions could occur. It has been shown by Hubing and Kaufman[8] that the majority of electromagnetic radiation is due to the common-mode currents developed on connecting cables. The common explanation for the source of this current is that high frequency voltages are developed between the ends of the ground return path due to the *partial inductance* of the path as well as the resistance. The graph in Fig. B.2 compares the electric field at 30 meters radiated from the circuit shown in Fig. B.1 to that of the same circuit, but

with no attached cables. There is a difference of several orders of magnitude between the two results which shows that the connections to an electronic circuit must be analyzed along with the circuit itself.

By using the approach suggested by Paul in [12], the loop described by nodes 2–3–6–5 in Fig. B.1 will be replaced by an equivalent voltage which is a function of the voltage drop across the ground return 2–3. In order to accomplish this, it is required to first bring the load to the source using the transmission line equation,

$$Z_{it} = Z_o \left(\frac{Z_l + jZ_o \tan \beta l}{Z_o + jZ_l \tan \beta l} \right) \tag{B.1}$$

where Z_o is the characteristic impedance of the transmission line; for two parallel wires, it is given by [22],

$$Z_o = \frac{1}{\pi} \sqrt{\frac{\mu_o}{\varepsilon_o}} \ln \left[\frac{S}{2a} + \sqrt{\left(\frac{S}{2a}\right)^2 - 1} \right] \tag{B.2}$$

which can be reduced, if $S/2a \gg 1$, to

$$Z_o \cong 120 \ln(S/a). \tag{B.3}$$

The variables are defined as follows: $\beta = 2\pi/\lambda$, $S =$ wire separation, $l =$ line length, and $a =$ wire radius.

Figure B.3 shows the resulting configuration, and hence the current I_{gnd}, between points 2 and 3, can now easily be found:

$$I_{gnd} = \frac{e}{Z_{it}}. \tag{B.4}$$

In order to find the impedance of the ground return path 2–3, the partial inductance, as well as the resistance, of the wire must be determined. The partial

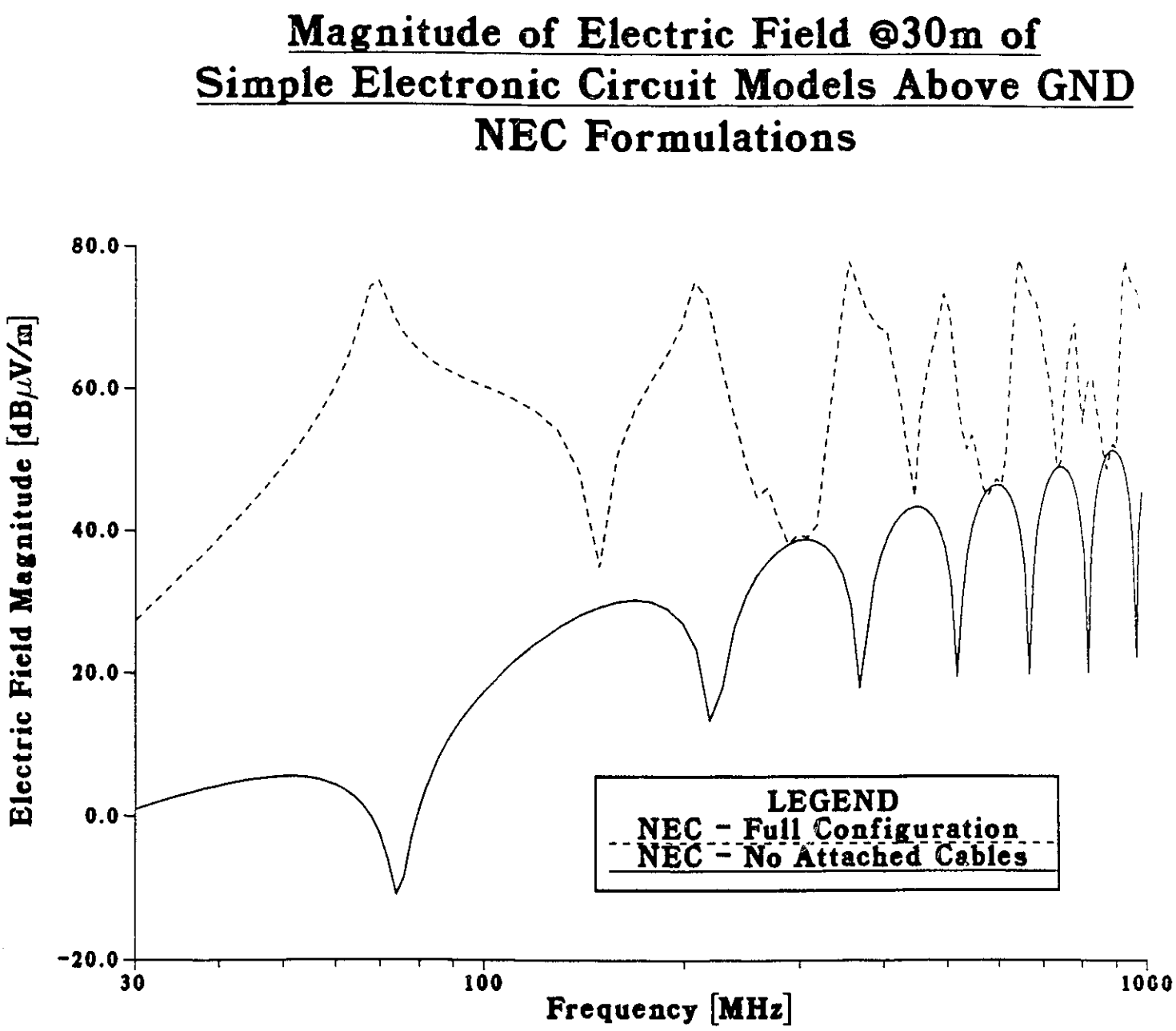

Figure B.2: Comparison of 30m radiated electric field

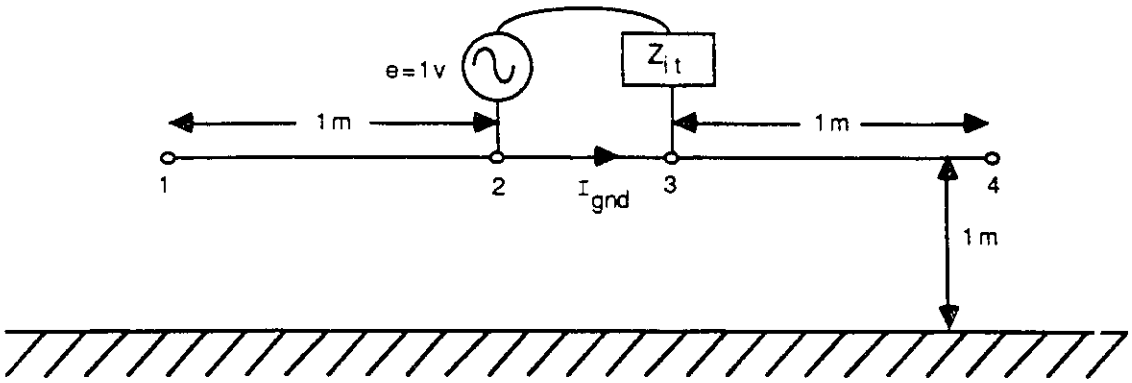

Figure B.3: Determination of ground current

inductance is found by using the following equation:

$$L_p = \frac{\mu_o}{4\pi} \ln \left[\frac{\sqrt{L^2 + a^2} + L}{\sqrt{L^2 + a^2} - L} \right] \tag{B.5}$$

where L is half the wire length [23] and the resistance is calculated using [24]:

$$R = \frac{1}{\pi a} \sqrt{\frac{\pi f \mu_c}{\sigma_c}} \tag{B.6}$$

where σ_c and μ_c are the conductivity and permeability of the conductor, respectively. Since the partial inductance is generally much larger than the internal inductance, the effect of the internal inductance of the wire is neglected.

It is now possible to find the equivalent voltage source of the loop 2–3–6–5 in Fig. B.1 by basic circuit theory:

$$E_{equ} = (R + j\omega L_p)\, I_{gnd}. \tag{B.7}$$

To evaluate the radiated field, the current into the terminating cables is now calculated. First the equivalent impedance of the open-circuited transmission lines above ground is found using (B.1) where the characteristic impedance is now given by [22]

$$Z_o = \frac{1}{2\pi} \sqrt{\frac{\mu_o}{\varepsilon_o}} \ln \left[\frac{h}{a} + \sqrt{\left(\frac{h}{a}\right)^2 - 1} \right] \tag{B.8}$$

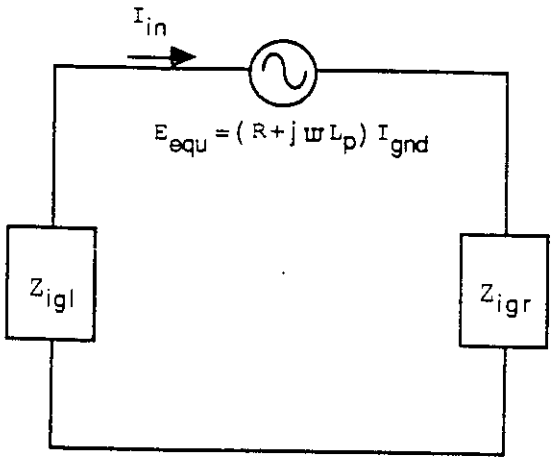

Figure B.4: Determination of input current

which can be reduced, if $h/a \gg 1$, to

$$Z_o \cong 60 \ln(2h/a) \tag{B.9}$$

where h is the height of the line above ground.

The equivalent circuit is shown in Fig. B.4 and the current in the loop is simply

$$I_{in} = E_{equ}/(Z_{igl} + Z_{igr}). \tag{B.10}$$

This input current is compared to the currents obtained using NEC and the results are shown in Fig. B.5. There is a good correspondance between the currents resulting from the two different methods and hence radiation predictions, which are a function of the current, should also correspond well.

The calculated input current is now used to predict the radiated emissions from the simplified model of our circuit, Fig. B.6, which is a centre-driven dipole. The electric field is found from [24] to be, in the far-field case,

$$E(\theta) \cong j\eta I_{in} \frac{e^{-j\beta r}}{2\pi r} \left[\frac{\cos\left(\frac{\beta l}{2}\cos\theta\right) - \cos\left(\frac{\beta l}{2}\right)}{\sin\theta} \right] \tag{B.11}$$

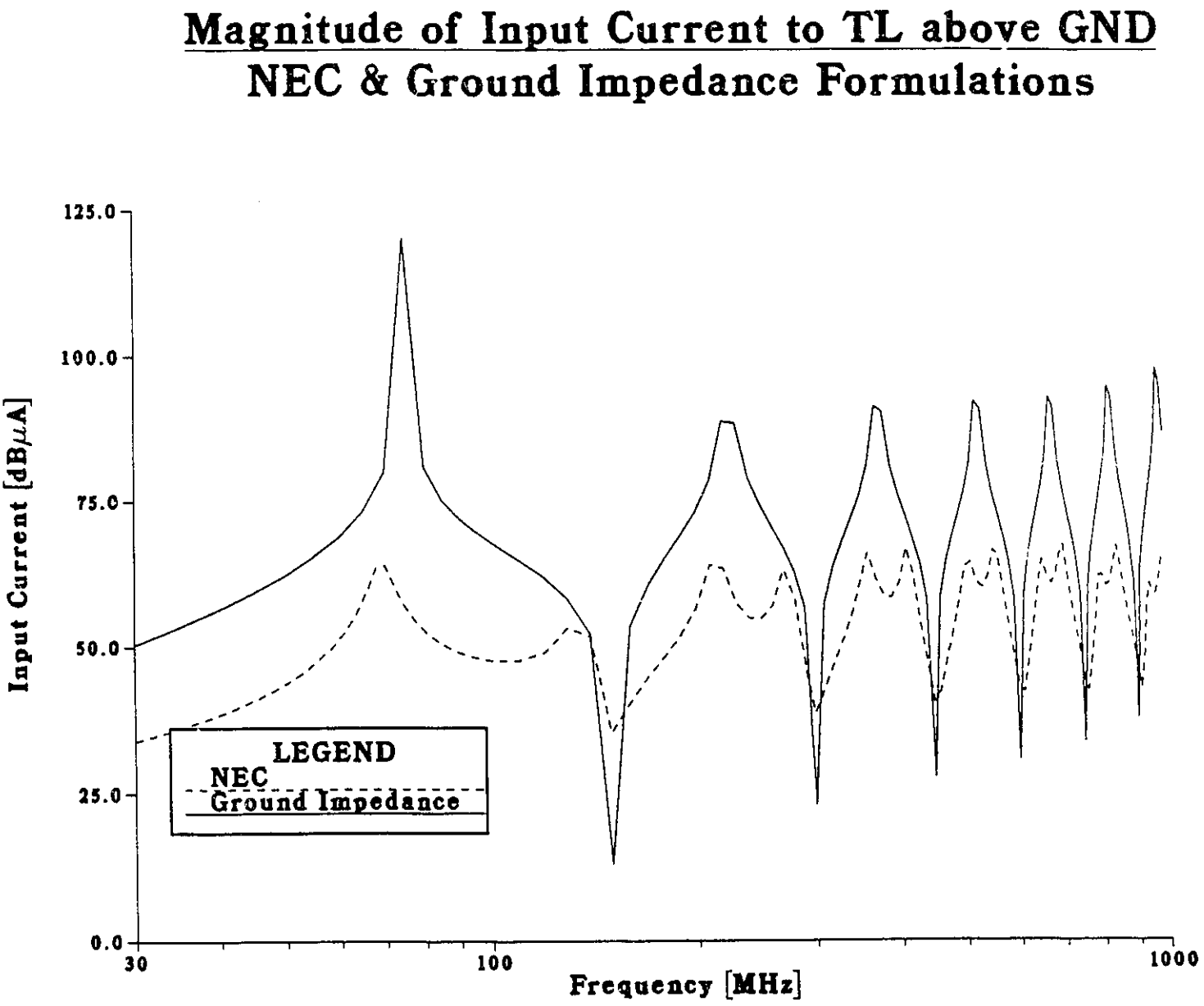

Figure B.5: Comparison of input currents

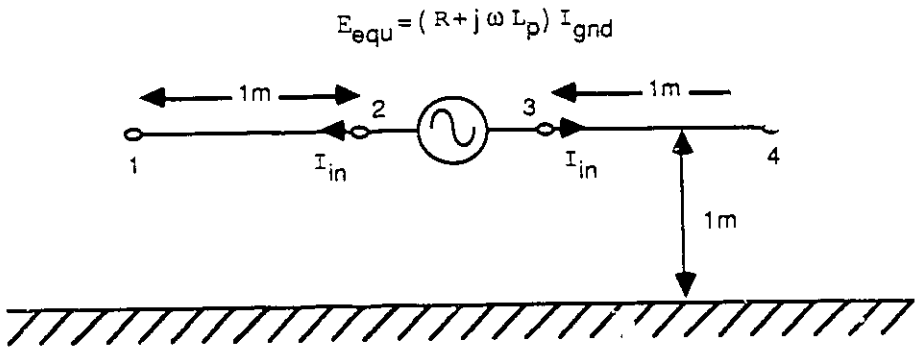

Figure B.6: Determination of radiated field

where η is the intrinsic impedance in free space ($\sqrt{\mu_o/\varepsilon_o}$), θ is the angle from the Y-axis and l is the length of the wire.

For the case of $\theta = \pi/2$, (B.11) reduces to

$$E(\theta = \pi/2) \cong j\eta I_{in} \frac{e^{-j\beta r}}{2\pi r} \left(1 - \cos\left(\frac{\beta l}{2}\right)\right). \tag{B.12}$$

Due to the presence of the ground plane, there is both direct and reflected radiation hence (B.12) must be calculated for both these cases.

$$E(\vartheta = \pi/2)_{Direct} \cong j\eta I_{in} \frac{e^{-j\beta r_1}}{2\pi r_1} \left(1 - \cos\left(\frac{\beta l}{2}\right)\right)$$

$$E(\theta = \pi/2)_{Reflected} \cong j\eta I_{in} \frac{e^{-j\beta r_2}}{2\pi r_2} \left(1 - \cos\left(\frac{\beta l}{2}\right)\right) \times RC$$

Where RC is the *R*eflection *C*oefficient of the ground plane. In this example, a perfect ground is assumed which means a resulting reflection coefficient of -1.

Therefore the total electric field is

$$E(\theta = \pi/2)_{Total} \cong \frac{j\eta I_{in}}{2\pi} \left(1 - \cos\frac{\beta l}{2}\right) \left(\frac{e^{-j\beta r_1}}{r_1} - \frac{e^{-j\beta r_2}}{r_2}\right) \tag{B.13}$$

where r_1 and r_2 are the distances that the direct and the reflected emissions must travel to the point of observation respectively.

Method	CPU Time [*sec*]
NEC	106810.48
Ground Impedance	3.63

Table B.1: Comparison between CPU times of the two methods on a DEC VAXstation II

B.3 Results

The calculated electric field can now be compared to that found with NEC. The results are shown in Fig. B.7 for radiation at 30 meters and in Fig. B.8 for 3 meters. The pattern of the results obtained from the ground impedance formulation, based on Eqs. (B.13) and (B.10), resemble those found by NEC to a large enough degree that a PCB designer would have a very reasonable estimate of how much radiation to expect. It is seen that there are larger differences between the curves for the 3 meter case than for the 30 meter one. This is due to the far-field approximation used in Equ. (B.11) which no longer applies for the lower frequencies at the 3 meter observation point.

The large advantage of the ground impedance formulation, besides it's simplicity, is seen from a comparison of the CPU times as shown in Table B.1. All programs were run on a DEC VAXstation II.

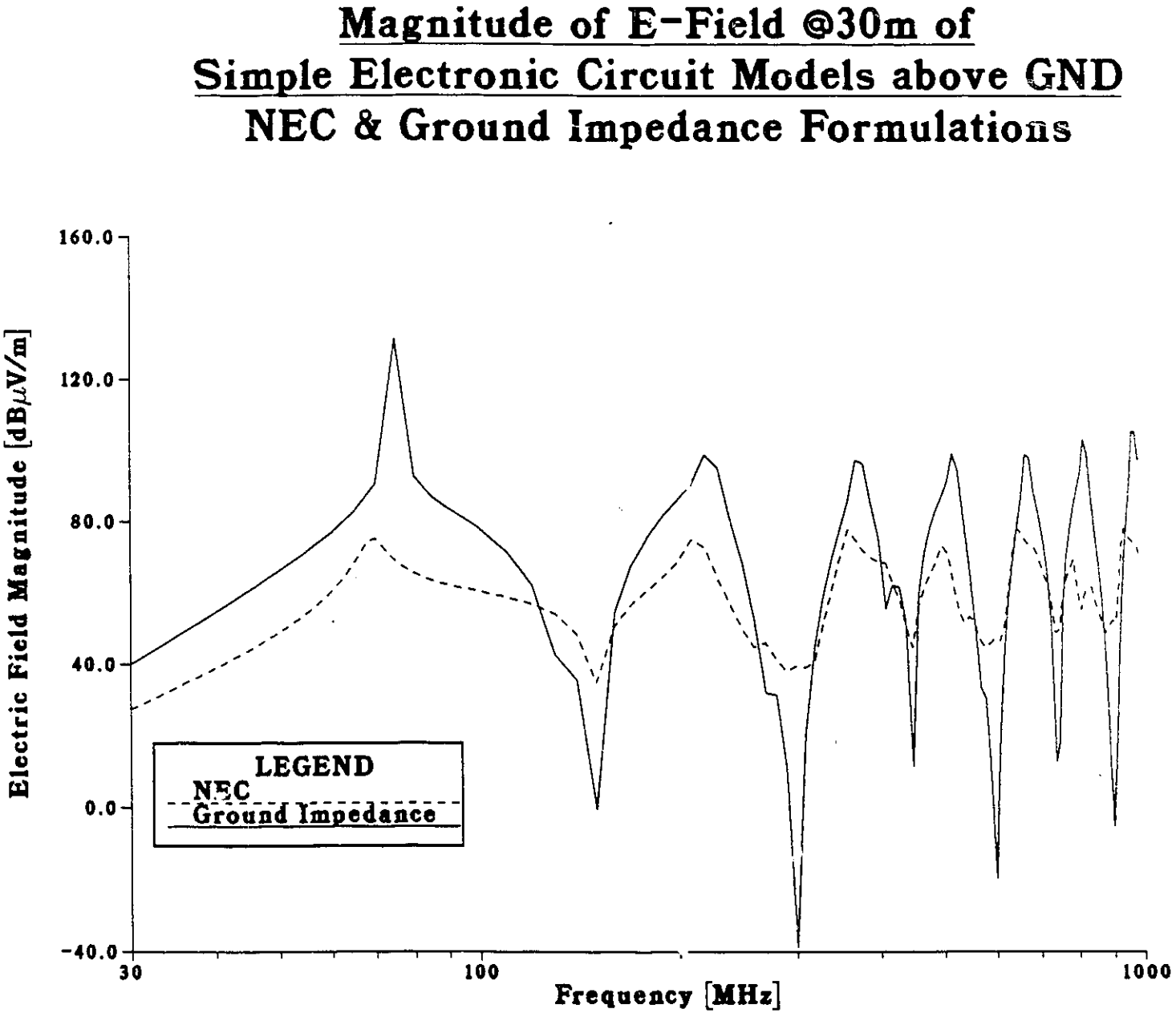

Figure B.7: Comparison of 30m radiated electric field

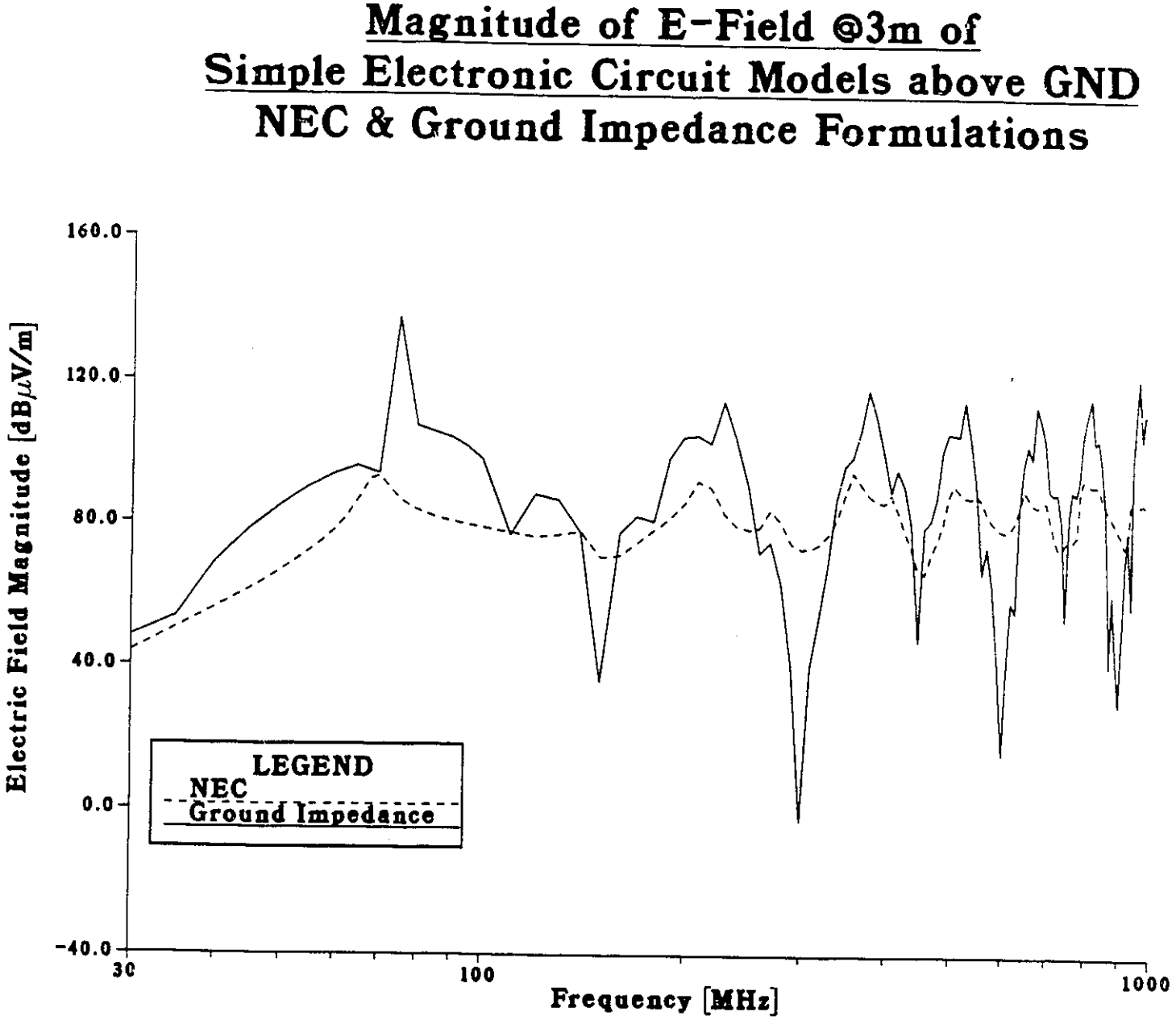

Figure B.8: Comparison of 3m radiated electric field

B.4 Summary and Conclusions

Attached signal cables were shown to be the primary source of radiated emissions from simple models of PCBs. It was then demonstrated that a reasonable estimate of these emissions can be obtained by determining the partial inductance of the ground return path in a simple circuit. Some accuracy is sacrificed for the sake of a large increase in the speed of computation.

The partial inductance, L_p, is the only parameter that the designer has control of and hence every effort should be made to minimize it.

Due to these encouraging results, more ambitious and realistic circuits were studied in Chapters three and four. A paper was also submitted for publication which details these findings [25].

Appendix C

Program Listings

C.1 Program Created to Calculate Partial Inductance in Chapter 3

In order to find the self partial inductance of the active lines shown in Fig. 3.3, the following program was developed.

The program requires an input file containing the geometry of the problem. The program used to generate the mesh of finite elements for the different configurations is given in Section C.2.

```
      PROGRAM Poisson

C     Program calculates the vector magnetic potential for a configuration
C     specified by the input file.
C     Using the vector magnetic potential, the partial inductance is
C     found by taking the value of the v.m.p. on the conductor surface.

      IMPLICIT NONE

      INTEGER*4 i1, i2, i3, i, j, npois, dum
      INTEGER*4 noptl, ndir, notr, nn, itr, l, lc, k
      INTEGER*4 iv(874,3), eps(874)
      REAL*8  pot(480), x(480), y(480), s(480,480), b(480)
```

```
      REAL*8  aro, ar, vmiuo, pi
      REAL*8  q, x1, x2, x3, y1, y2, y3
      REAL*8  a1, a2, vol, d1, d2, f(3,3), si(3)
      REAL*8  det, ar1, ar2, cbi, pois(874)
      REAL*8  xi, yi, xi2, yi2
c-----
C Functions
      q(x1,y1, x2,y2, x3,y3) = x1*y2 - x2*y1 + x2*y3 - x3*y2 +
     &                         x3*y1 - x1*y3
      a1(x1,y1, x2,y2, x3,y3, d1) = d1*(2.d0*x1*y1 + 2.d0*x3*y3 + x1*y2
     &                            +     2.d0*x2*y2 +    x1*y3 + x2*y1
     &                            +        x2*y3 +    x3*y1 + x3*y2)/12.d0
      a2(y1,y2,y3, d2) = d2*( y1**2 + y2**2 + y3**2
     &                       +y1*y2 + y1*y3 + y2*y3)/6.d0
      vol(y1,y2,y3,d1) = d1*(y1+y2+y3)/3.d0

      open(unit=1, file='node.out',  status='old')
      open(unit=2, file='pois.out',  status='new')
      open(unit=4, file='pois.work', status='new')

C Constants
      pi = dacos(-1.d0)
      vmiuo = 36.d0*pi*1.D9
      npois = 1     !npois=1 means that Poisson's Eqn will be solved
C noptl - total number of points
C notr  - total number of triangles
C ndir  - total number of points with dirichlet values
      noptl = 480
      ndir  = 14
      notr  = 874
      nn = noptl - ndir
C*****************************************************
C  Read iv's and coordinates; initialize epsilon & pois
C*****************************************************
      read(1,*)  !two lines needed for "drawing" routine
      read(1,*)
      DO 1 i = 1, notr
        read(1,*) dum, iv(i,1), iv(i,2), iv(i,3)
C  For ground conductor at right
        IF (i .ge. 397 .and. i .le. 402) THEN
          pois(i) = 1.d0
        ELSE
          pois(i) = 0.d0
```

```
        END IF
        eps(i) = 1.d0
1     CONTINUE
      DO 2 i = 1, noptl
        read(1,*) dum, x(i), y(i)
        x(i) = x(i) * 25.4D-6
        y(i) = y(i) * 25.4D-6
        pot(i) = 0.d0
2     CONTINUE

C*******************************************************
C Initialize S and B matrices
C*******************************************************
      do 6 i = 1, noptl
        b(i) = 0.d0
        do 6 j = 1, noptl
          s(i,j) = 0.d0
6     continue

      do 16 itr = 1,notr
        i1 = iv(itr,1)
        i2 = iv(itr,2)
        i3 = iv(itr,3)

        det = q( x(i1),y(i1), x(i2),y(i2), x(i3),y(i3) )
        if(det .eq. 0.d0) then
          write(*,'('' Determinant = 0.!'')')
          write(2,'('' Determinant = 0.!'')')
          goto 100
        end if
        f(1,1) = (x(i2) * y(i3) - x(i3) * y(i2)) / det
        f(1,2) = (x(i3) * y(i1) - x(i1) * y(i3)) / det
        f(1,3) = (x(i1) * y(i2) - x(i2) * y(i1)) / det

        f(2,1) = (y(i2) - y(i3)) / det
        f(2,2) = (y(i3) - y(i1)) / det
        f(2,3) = (y(i1) - y(i2)) / det

        f(3,1) = (x(i3) - x(i2)) / det
        f(3,2) = (x(i1) - x(i3)) / det
        f(3,3) = (x(i2) - x(i1)) / det

        ar = dabs(det)/2.d0*eps(itr)
```

```
        if(npois .eq. 0) goto 400
        ar1 = vol(x(i1), x(i2), x(i3), ar)
        ar2 = vol(y(i1), y(i2), y(i3), ar)

400     continue
        aro = ar
        do 23 i = 1, 3
          l = iv(itr, i) - ndir
          if(iv(itr,i) .le. ndir) goto 23

          do 24 k = 1, 3
            si(k) = ar*( f(2,k)*f(2,i) + f(3,k)*f(3,i) )
24        continue
          do 14 k = 1, 3
            if(iv(itr,k) .le. ndir) goto 15
            lc = iv(itr,k) - ndir
            s(l, lc) = s(l, lc) + si(k)
15          b(l) = b(l) - pot(iv(itr,k)) * si(k)
14        continue
          if(npois .eq. 1 .and. pois(itr) .ne. 0.d0) then
            pois(itr) = 4.D-7*pi/ 1.35683D-8   !Uo * J
            cbi = -pois(itr) * (ar*f(1,i) + ar1*f(2,i) + ar2*f(3,i))
            b(l) = b(l) + cbi
          end if
23      continue
16    continue

C  Invert matrix
      call sist(s,b,nn,noptl)

C  Write values of vector magnetic potential: pot(i)
      do 20 k = 1, nn
        i = ndir + k
        pot(i) = b(k)
20    continue
      do 21 i = 1, noptl
        write(2, 162) x(i), y(i), pot(i)*1d9, i
        write(*, 162) x(i), y(i), pot(i)*1d9, i
162     format( 3(2x, 1pd12.4), 5x, i3)
21    continue
c-----
C Add more points for DPICT
      do 22 xi = 75, 90, .5
```

```
        do 22 yi = 87, 88.4, .2
          xi2 = xi * 25.4D-6
          yi2 = yi * 25.4D-6
          write(2, 162) xi2, yi2, 0.d0, 999
22    continue
      do 223 xi = 105, 120., .5
        do 223 yi = 87, 88.4, .2
          xi2 = xi * 25.4D-6
          yi2 = yi * 25.4D-6
          write(2, 162) xi2, yi2, 0.d0, 999
223   continue
c-----
      goto 99
100   write(*, '('' ***Singular Matrix***'', i4)') itr
      write(2, '('' ***Singular Matrix***'', i4)') itr
99    continue

      STOP
      END

C*******************************************************
C*******************************************************

      SUBROUTINE sist(a,b,n,noptl)

      IMPLICIT NONE

      INTEGER*4 i,j,k,l,m,n,kp1,noptl,nm1
      REAL*8 ba, d, h

      real*8 a(noptl,noptl), b(noptl)

      nm1 = n-1
      d = 1.d0
      do 7 k = 1,nm1
        write(4, '(x,i3)') k
        write(*, '(x,i3)') k
        ba=a(k,k)
        j = k
        kp1 = k+1

        do 1 i = kp1, n
          if(dabs(ba) .ge. dabs(a(i,k))) goto 1
```

```
          ba = a(i,k)
          j = i
1       continue
        write(1, '(x, ''ba='',1pd12.4)') ba
        write(*, '(x, ''ba='',1pd12.4)') ba
c        d = d*ba
        if(j .le. k) goto 3
c        if(dabs(d) .eq. 0.d0) goto 9
        if(dabs(ba) .eq. 0.d0) goto 9

        do 2 i = k,n
          h = a(k,i)
          a(k,i) = a(j,i)/ba
          a(j,i) = h
2       continue
        h = b(k)
        b(k) = b(j) /ba
        b(j) = h
        goto 5

3       do 4 i = kp1,n
4         a(k,i) = a(k,i) / ba
        b(k) = b(k)/ba
5       do 7 i = kp1,n
          do 6 j = kp1,n
6         a(i,j) = a(i,j) - a(i,k)*a(k,j)
7       b(i) = b(i) - a(i,k)*b(k)
        write(4, '(x, ''a(n,n)='',1pd12.4)') a(n,n)
        write(*, '(x, ''a(n,n)='',1pd12.4)') a(n,n)
c      d = d*a(n,n)
c      if(dabs(d) .eq. 0.d0) goto 9
      if(dabs(a(n,n)) .eq. 0.d0) goto 9
      b(n) = b(n)/a(n,n)

      do 8 i = 1,nm1
        k = n-i
        kp1 = k+1
        do 8 j = kp1,n
8       b(k) = b(k) - a(k,j)*b(j)

      return
9     write(*, '('' Singular Solution'')')
      write(2, '('' Singular Solution'')')
```

```
return
end
```

C.2 Program Used to Create Finite Element Mesh for Chapter 3

The finite element mesh for the configurations shown in Fig. 3.3 was generated using the following program.

```
      PROGRAM Node
      IMPLICIT NONE

      REAL    tri, xpos(24), ypos(20), x(1000), y(1000)
      REAL    x1(22), y1(22), x2(16), y2(16)
      INTEGER iv1(1000), iv2(1000), iv3(1000)
      INTEGER iv1a,iv1b,iv2a,iv2b,iv3a,iv3b, start, stop
      INTEGER iv2_1(40), iv2_2(40), iv2_3(40)
      INTEGER xk, yk, i
C--Position of mesh
      DATA xpos/0., 30., 50., 65., 75., 82.5, 90., 97.5, 105., 110.,
     &         115., 120., 125., 130., 135., 140., 145., 150., 155.,
     &         165., 175., 190., 220., 250./
      DATA ypos/0., 20., 40., 50., 58., 66., 72., 78., 83., 85., 87.,
     &         88.4, 90., 92., 98., 104., 112., 120., 150., 180./

C--Positions of conductor nodes
      DATA x1/75., 82.5, 90., 90., 82.5, 75., 135., 140., 145., 150.,
     &       150., 145., 140., 135., 105., 110., 115., 120., 120.,
     &       115., 110., 105./
      DATA y1/3*88.4, 3*87., 4*88.4, 4*87., 4*88.4, 4*87./

C--Positions of nodes between conductors
      DATA x2/97.5, 125., 130., 155., 165., 175., 190., 220., 250.,
     &       0., 30., 50., 65., 97.5, 125., 130./
      DATA y2/9*88.4, 7*87./

      DATA iv2_1/1, 195, 2, 196, 3, 197, 219, 198, 15, 199, 16, 200,
     &         17, 201, 18, 202, 220, 203, 221, 204, 7, 205, 8, 206,
     &         9, 207, 10, 208, 222, 209, 223, 210, 224, 211, 225, 212,
     &         226, 213, 227, 214/
      DATA iv2_2/6, 1, 5, 2, 4, 3, 232, 219, 22, 15, 21, 16, 20, 17, 19,
     &         18, 233, 220, 234, 221, 14, 7, 13, 8, 12, 9, 11, 10,
     &         235, 222, 236, 223, 237, 224, 238, 225, 239,226,240,227/
      DATA iv2_3/245, 6, 246, 5, 247, 4, 248, 232, 249, 22, 250, 21,
     &         251, 20, 252, 19, 253, 233, 254, 234, 255, 14, 256, 13,
```

```
     &         257, 12, 258, 11, 259, 235, 240, 236, 261, 237, 262, 238,
     &         263, 239, 264, 240/

      OPEN(2, file='node.out', status='new')
c----------------------
      iv1a = 23
      iv2a = 48
      iv3a = 47
      iv1b = 23
      iv2b = 24
      iv3b = 48
      start = 3
      stop  = 328
      CALL normal(iv1a,iv1b, iv2a,iv2b, iv3a,iv3b, start, stop, iv1,
     &            iv2, iv3)
c----------------------
      iv1a = 194
      iv2a = 1
      iv3a = 218
      iv1b = 194
      iv2b = 195
      iv3b = 1
      start = 331
      stop  = 360
      CALL strange(iv1a,iv2a,iv3a, iv1b,iv2b,iv3b, start,stop, iv2_1,
     &             iv1, iv2, iv3)
c----------------------
      iv1a = 209
      iv2a = 223
      iv3a = 222
      iv1b = 209
      iv2b = 210
      iv3b = 223
      start = 361
      stop  = 374
      CALL normal(iv1a,iv1b, iv2a,iv2b, iv3a,iv3b, start, stop, iv1,
     &            iv2, iv3)
c----------------------
      iv1a = 218
      iv2a = 6
      iv3a = 231
      iv1b = 218
      iv2b = 1
```

```
      iv3b = 6
      start = 377
      stop  = 406
      CALL strange(iv1a,iv2a,iv3a, iv1b,iv2b,iv3b, start,stop, iv2_2,
     &             iv1, iv2, iv3)
c----------------------
      iv1a = 222
      iv2a = 236
      iv3a = 235
      iv1b = 222
      iv2b = 223
      iv3b = 236
      start = 407
      stop  = 420
      CALL normal(iv1a,iv1b, iv2a,iv2b, iv3a,iv3b, start, stop, iv1,
     &            iv2, iv3)
c----------------------
      iv1a = 231
      iv2a = 245
      iv3a = 244
      iv1b = 231
      iv2b = 6
      iv3b = 245
      start = 423
      stop  = 452
      CALL strange(iv1a,iv2a,iv3a, iv1b,iv2b,iv3b, start,stop, iv2_3,
     &             iv1, iv2, iv3)
c----------------------
      iv1a = 235
      iv2a = 260
      iv3a = 259
      iv1b = 235
      iv2b = 236
      iv3b = 260
      start = 453
      stop  = 874
c      write(2, 222) (start-2),iv1a,iv2a,iv3a, (start-1),iv1b,iv2b,iv3b
      CALL normal(iv1a,iv1b, iv2a,iv2b, iv3a,iv3b, start, stop, iv1,
     &            iv2, iv3)
c----------------------
222   FORMAT( x, i3, 2x, 3(i3,2x), /, x, i3, 2x, 3(i3,2x) )
C*********************************************************************
      DO 5 i = 1, 22
```

```
        x(i) = x1(i)
        y(i) = y1(i)
5     CONTINUE
c-----------------------
      xk = 1
      yk = 20
      DO 6 i = 23, 218
        IF (xk .le. 24) THEN
          x(i) = xpos(xk)
          xk = xk + 1
        ELSE                    !new row
          x(i) = xpos(1)
          xk = 2
          yk = yk - 1
        END IF
        y(i) = ypos(yk)
6     CONTINUE
c-----------------------
      xk = 1
      yk = 1
      DO 7 i = 219, 234
        x(i) = x2(xk)
        y(i) = y2(yk)
        xk = xk + 1
        yk = yk + 1
7     CONTINUE
c-----------------------
      xk = 19
      yk = 11
      DO 8 i = 235, 480
        IF (xk .le. 24) THEN
          x(i) = xpos(xk)
          xk = xk + 1
        ELSE                    !new row
          x(i) = xpos(1)
          xk = 2
          yk = yk - 1
        END IF
        y(i) = ypos(yk)
8     CONTINUE
c-----------------------
      write(2, '(55(''-''),/,''480 874'')')
      DO 10 i = 1, 874
```

```
10      WRITE(2, '(x,i3,x,3(i3,2x))') i,iv1(i),iv2(i),iv3(i)
      DO 9 i = 1, 480
9       WRITE(2, '(x,i3,x,2(f6.1,x))') i, x(i), y(i)
c-----------------------
c-----------------------
      STOP
      END


C*********************************************************************
      SUBROUTINE normal(iv1a,iv1b, iv2a,iv2b, iv3a,iv3b, start, stop,
     &                  iv1, iv2, iv3)

      IMPLICIT NONE
      REAL tri
      INTEGER iv1a,iv1b,iv2a,iv2b,iv3a,iv3b, start, stop
      INTEGER iv1(1000), iv2(1000), iv3(1000)

      iv1(start-2) = iv1a
      iv2(start-2) = iv2a
      iv3(start-2) = iv3a
      iv1(start-1) = iv1b
      iv2(start-1) = iv2b
      iv3(start-1) = iv3b
      DO 1 tri = start, stop
        IF( ((tri-1)/46) .EQ. AINT((tri-1)/46) ) THEN       !begin. of row
c          write(2, '('' begining of row / 47'')')
          iv1(tri) = iv1(tri-1) + 2
          iv2(tri) = iv2(tri-2) + 2
          iv3(tri) = iv3(tri-1) + 1
        ELSE IF( ((tri-2)/46) .EQ. AINT((tri-2)/46) ) THEN !begin. of row
c          write(2, '('' begining of row / 48'')')
          iv1(tri) = iv1(tri-1)
          iv2(tri) = iv2(tri-2) + 2
          iv3(tri) = iv3(tri-1) + 1
        ELSE IF( (tri/2) .EQ. AINT(tri/2) ) THEN    !even number triangle
          iv1(tri) = iv1(tri-1)
          iv2(tri) = iv2(tri-2) + 1
          iv3(tri) = iv3(tri-1) + 1
        ELSE                                        !odd number triangle
          iv1(tri) = iv1(tri-1) + 1
          iv2(tri) = iv2(tri-2) + 1
          iv3(tri) = iv3(tri-1)
```

```
        END IF
c        WRITE(2, '(x,f4.0,x,3(i3,2x))') tri,iv1(tri),iv2(tri),iv3(tri)
1     CONTINUE

      RETURN
      END

C*********************************************************************
      SUBROUTINE strange(iv1a,iv2a,iv3a, iv1b,iv2b,iv3b, start,stop,
     &                   iv2_1, iv1, iv2, iv3)
      IMPLICIT NONE
      REAL tri
      INTEGER iv1a,iv1b,iv2a,iv2b,iv3a,iv3b, start, stop
      INTEGER iv1(1000), iv2(1000), iv3(1000), iv2_1(50), i

      iv1(start-2) = iv1a
      iv2(start-2) = iv2a
      iv3(start-2) = iv3a
      iv1(start-1) = iv1b
      iv2(start-1) = iv2b
      iv3(start-1) = iv3b
      i = 3
      DO 2 tri= start, stop
        iv2(tri) = iv2_1(i)
        IF( (tri/2) .EQ. AINT(tri/2) ) THEN   !even number triangle
          iv1(tri) = iv1(tri-1)
          iv3(tri) = iv2(tri-1)
        ELSE                                  !odd number triangle
          iv1(tri) = iv2(tri-1)
          iv3(tri) = iv3(tri-1)
        END IF
        i = i + 1
c        WRITE(2, '(x,f4.0,x,3(i3,2x))') tri,iv1(tri),iv2(tri),iv3(tri)
2     CONTINUE

      RETURN
      END
```

C.3 Sample of Input File for NEC

This input file was used to generate the NEC electric field results presented in Figure 4.11.

```
CM Program:           Radiation
CM Purpose:           Find the electric field from the circuit in Paul's paper.
CM                    From 30MHz to 100MHz
CM Configuration:     7 Transmission lines. (6) is ground return.
CE
GW 11   10        0.     -.125  1.003810        0.      .125  1.003810   74.1E-6
GW  2   10        0.     -.125  1.003048        0.      .125  1.003048   74.1E-6
GW 33   10        0.     -.125  1.002286        0.      .125  1.002286   74.1E-6
GW  4   10        0.     -.125  1.001524        0.      .125  1.001524   74.1E-6
GW 55   10        0.     -.125  1.000762        0.      .125  1.000762   74.1E-6
GW  6   10        0.      .125        1.        0.     -.125        1.   74.1E-6
GW 77   10        0.     -.125  0.999238        0.      .125  0.999238   74.1E-6
GW  1    1        0.     -.1255       1.        0.    -.1255  1.003048   74.1E-6
GW  3    1        0.     -.1255  1.003048        0.     -.125  1.003048   74.1E-6
GW  5    1        0.      .125  1.003048        0.     .1255  1.003048   74.1E-6
GW  7    1        0.     .1255  1.003048        0.     .1255        1.   74.1E-6
GW  8    1        0.     .1255        1.        0.      .125        1.   74.1E-6
GW  9    1        0.     -.125        1.        0.    -.1255        1.   74.1E-6
GW 10    1        0.     -.125        1.        0.     -.125  1.001524   74.1E-6
GW 14    1        0.      .125  1.001524        0.     .1255        1.   74.1E-6
GE
FR  0   35    0    0        30         2
LD  0    7    1    1      50.0
LD  0   10    1    1      50.0
LD  0   14    1    1      50.0
EX  0    1    1   00  1.00E+00         0         0         0         0         0
PT -1    4    1
NE  0    1    1    1        0.        0.        4.         0         0         0
XQ  0
MX
CM Program:           Radiation
CM Purpose:           Find the radiation from the circuit in Paul's paper.
CM                    From 100MHz to 1GHz
CM Configuration:     7 Transmission lines. (6) is ground return.
CE
GW 11   10        0.     -.125  1.003810        0.      .125  1.003810   74.1E-6
```

```
GW  2   10      0.     -.125  1.003048      0.      .125  1.003048  74.1E-6
GW 33   10      0.     -.125  1.002286      0.      .125  1.002286  74.1E-6
GW  4   10      0.     -.125  1.001524      0.      .125  1.001524  74.1E-6
GW 55   10      0.     -.125  1.000762      0.      .125  1.000762  74.1E-6
GW  6   10      0.      .125        1.      0.     -.125        1.  74.1E-6
GW 77   10      0.     -.125  0.999238      0.      .125  0.999238  74.1E-6
GW  1    1      0.     -.1255       1.      0.     -.1255 1.003048  74.1E-6
GW  3    1      0.     -.1255 1.003048      0.     -.125  1.003048  74.1E-6
GW  5    1      0.      .125  1.003048      0.      .1255 1.003048  74.1E-6
GW  7    1      0.      .1255 1.003048      0.      .1255       1.  74.1E-6
GW  8    1      0.      .1255       1.      0.      .125        1.  74.1E-6
GW  9    1      0.     -.125        1.      0.     -.1255       1.  74.1E-6
GW 10    1      0.     -.125        1.      0.     -.125  1.001524  74.1E-6
GW 14    1      0.      .125  1.001524      0.      .1255       1.  74.1E-6
GE
FR  0   91   0   0      100       10
LD  0    7   1   1     50.0
LD  0   10   1   1     50.0
LD  0   14   1   1     50.0
EX  0    1   1  00 1.00E+00        0       0       0       0       0
PT -1    4   1
NE  0    1   1   1       0.       0.      4.       0       0       0
XQ  0
EN
```

C.4 Program Created to Calculate the Radiated Emissions From Fig. B.1

The radiated emissions from the circuit shown in Fig. B.1 are predicted using this program. The curves labelled "Ground Impedance" in Figs. B.7 and B.8 show the results of the program for 30 meter and 3 meter distances, respectively.

```
      PROGRAM Etotal

C  Program calculates the radiated E-field at 3 and 30 metres from a
C  wire loop with 2 attached wires.
C  The loop is driven with a 1V supply and loaded with 546.66 Ohms.

      REAL*4    c, ehta, pi, rterm, iterm
```

```
      real*8    root, da, dvlt
      COMPLEX*8 vj, e, zl, zit, zi1, zi2, ct, ct1

      open(unit=2, file='jul289.out', status='new')
      open(unit=3, file='jul289.Eequ', status='new')

15    write(*, '(50(''*''), /, '' 3 or 30 meter range? [3,30]'')')
      read(*, *) ans
      if (ans .ne. 3. .and. ans .ne. 30.) goto 15

c--Physical constants
      pi = acos(-1.)
      c = sqrt((4e-7*pi*8.8542e-12)**-1.)
      ehta = sqrt(4.e-7*pi/8.8542e-12)
      uo = 4*pi*1e-7

C-- F is frequency in Hz
      fi = 30.e+06
      ff = 100.e+06
      n = 14
      df = (ff-fi)/n

      s = .01
      a = 1.05e-06
      h = 1.

C  Zot charact. impedance of T.L.
C  Zog charact. impedance of T.L. above GND plane
      zot = 120. * alog(s/a)       !2 wire T.L.
      zog = 60. * alog(2. * h/a)   !T.L. above ground

C  Vlt is length of T.L.
C  Vlc1, Vlc2 are lengths of wires above GND
      vlt = .1
      vlc1 = 1.
      vlc2 = 1.

C  Zl is T.L. load
      zl = CMPLX(546.766, 0.)

C  Calculate partial inductance for CIRCULAR signal track
      da   = 1.05d-06
      dvlt = 0.1d0
```

```
      root = dsqrt( (dvlt/2.d0)**2 + da**2 )
      vlp  = 1d-07 * dlog( (root + dvlt/2) / (root - dvlt/2) )

C  Calculate equivalent voltage driving the antenna
      vj = CMPLX(0., 1.)
      e = CMPLX(1., 0.)
      DO 6 i = 1,n
        f = fi + (i-1)*df
        om = 2.*pi*f
        beta = om / c

C  Determine Ground Current
c 1 Bringing load back to source
        zit = zot* (zl*cos(beta*vlt) + vj*zot*sin(beta*vlt)) /
     &             (zot*cos(beta*vlt) + vj*zl*sin(beta*vlt))

c 2 Resistance of circular wire
        res = 1/(2*pi*a) * SQRT(pi * f * uo /5.8e7) * vlt

c 3 Equivalent voltage source
        e = (res + vj*om*vlp) / zit

c 4 Equivalent circuit
        zi1 = -vj * zog * cos(beta*vlc1)/sin(beta*vlc1)
        zi2 = -vj * zog * cos(beta*vlc2)/sin(beta*vlc2)

c  ct1: ground Current
        ct1 = e/(zi1+zi2)

C  Calculate Radiated Electric Field
        if(ans. eq. 3.) then                          !3m E-field
          iterm = sin(3*beta)/3 - sin(5*beta)/5
          rterm =-cos(3*beta)/3 + cos(5*beta)/5
        else                                          !30m E-field
          iterm = sin(30*beta)/30 - sin(32*beta)/32
          rterm =-cos(30*beta)/30 + cos(32*beta)/32
        end if

        Etot = ehta * ct1 * (1 - cos(beta)) / (2*pi) *
     &         CMPLX(rterm, iterm)

        write(2, 30) f/1.e+06, ABS(Etot)
30      format(f7.0, 3x, 1pe12.4)
```

```
6     continue

      STOP
      END
```

Bibliography

[1] *U.S. Code of Federal Regulations*, Title 47, part 15, subpart J.

[2] *Canadian Radio Act*, based on CSA C108.8, July, 1983.

[3] C.I.S.P.R. Specification for Radio Interference Measuring Apparatus and Measurement Methods, C.I.S.P.R Pub. 16, 1977, appendix F.

[4] G.J.Burke and A.J. Poggio, *Numerical Electromagnetics Code (NEC) - Method of Moments*, Naval Electronic Systems Command, Naval Ocean Systems Center, San Diego, CA 92152.

[5] J.H. Richmond, *Radiation and Scattering by Thin-Wire Structures in the Complex Frequency Domain*, Langley Research Center, National Aeronautics and Space Administration Contractor Report NASA CR-2396, Washington, D.C., May, 1974.

[6] F. Leitl, "EMI-CAD: A New Approach to Efficient EMC PC-Board Design", *Proceedings*, International Conference on Electromagnetics in Aerospace Applications, Torino, Italy, September, 1989.

[7] C.R. Paul, "A Comparison of the Contributions of Common-Mode and Differential-Mode Currents in Radiated Emissions", *IEEE Trans. Electromagnetic Compatibility*, EMC-31 No. 2, May, 1989.

[8] Todd H. Hubing and J. Frank Kaufman, "Modeling the Electromagnetic Radiation from Electrically Small Table-Top Products", *IEEE Trans. Electromagnetic Compatibility*, EMC-31 No. 1, February, 1989.

[9] R.Khan and G.Costache, "Finite Element Method Applied to Modeling Crosstalk Problems on Printed Circuit Boards", *IEEE Trans. Electromagnetic Compatibility*, EMC-31 No. 1, February, 1989.

[10] Albert J. Blodgett, Jr., "Microelectronic Packaging", *Sci. Amer.*, pp 86-97, July, 1983.

[11] A.E. Ruehli, "Inductance Calculations in a Complex Integrated Circuit Environment", *IBM J. Res. Develop.*, Vol. 16, No. 5, September, 1972.

[12] Clayton R. Paul, "Modeling Electronic Interference Properties of Printed Circuit Boards", *IBM J. Res. Develop.*, Vol. 33, No. 1, January, 1989.

[13] H.W. Ott, "Controlling EMI by Proper Printed Wiring Board Layout", *Proceedings*, 1985 International Symposium and Technical Exhibition on Electromagnetic Compatibility, Zurich, March, 1985.

[14] V. Ungvichian and R. Perez-Rodriquez, "Prediction of Electromagnetic Radiation of a Multilayer Board", *Electronics Letters*, Vol. 23, No. 14, July, 1987.

[15] R.F. German, "Use of a Ground Grid to Reduce Printed Circuit Board Radiation", *Proceedings*, 1985 International Symposium and Technical Exhibition on Electromagnetic Compatibility, Zurich, March, 1985.

[16] R. Raut, "On the Computation of Electromagnetic Field Components from a Practical Printed Circuit Board", *Proceedings*, IEEE International Symposium on EMC, 1986.

[17] D.R. Bush, "Radiated Emissions of Printed Circuit Board Clock", *Proceedings*, IEEE International Symposium on EMC, 1985.

[18] Todd H. Hubing, "The effect of Cable Terminations on EMI Measurements", *Proceedings*, IEEE Symposium on EMC, 1989.

[19] Chester L. Smith, "EMC and the 20-meter Band", *Proceedings*, IEEE Symposium on EMC, 1989.

[20] Warren L. Stutzman and Gary A. Thiele, *Antenna Theory and Design*, John Wiley & Sons, Inc., 1981.

[21] Dawn A. Koopman and Clayton R. Paul, "Basic EMC Technology Advancement For C^3 Systems - Modeling Crosstalk In Balanced Twisted Pairs", RADC-TR-82-286, Vol. IVd, Rome Air Development Center, Griffiss Air Force Base, NY, August, 1984.

[22] Bernhard Keiser, *Principles of Electromagnetic Compatibility*, Artech House, 1979.

[23] David K. Cheng, *Field and Wave Electromagnetics*, Addison-Wesley, 1983.

[24] C.A. Balanis, *Antenna Theory - Analysis and Design*, Harper & Row, 1982.

[25] Marko Radojičić and George Costache, "Simple Models to Predict Radiated Emissions From Electronic Circuits", Submitted for publication in *EMC Technology*, August, 1989.

[26] H.W. Ott, *Noise Reduction Techniques in Electronic Systems*, John Wiley and Sons, New York 1976.

[27] Erwin Kreyszig, *Advanced Engineering Mathematics*, 5th Ed., John Wiley and Sons, New York 1983.